Analysis of many-body methods for quantum dots

Simen Kvaal

Centre of Mathematics for Applications
and
Department of Physics
University of Oslo

November 2008

Dissertation presented for the degree of
Philosophae Doctor (PhD)

Happy is he who gets to know the reasons for things.

— *Virgil, Georgics book II*

Preface

Writing a PhD thesis is no walk in the sun. But I don't think it should be either, because you learn a lot more that way, and at times when doing research is a struggle uphill, the reward of attaining new understanding and connecting a few more dots is profoundly rewarding. The feeling of illumination is *priceless*. So, looking back, it has been an experience I wouldn't want to be without. It would not be possible without the help of others, however.

First of all, I would like to thank my supervisor Morten Hjorth-Jensen for his friendship, support, enthusiasm and advice during the last years. Through our countless discussions in his office or in picturesque Italian villages, I have learned a lot. He truly believes in me, and for that I am very grateful.

I would also like to thank my secondary supervisor Ragnar Winther, CEO at CMA, as well as senior adviser Helge Galdal at CMA, for continuous support, both financially and otherwise. At times when life has been less enjoyable, they have shown great kindness and understanding, cutting me some slack.

I have great colleagues and friends at CMA. I would especially like to thank former colleagues Halvor Møll Nilsen, Per Christian Moan and Jan Brede Thomassen for their collaboration, friendship, advice, and for the discussions we've had. Per Christian and Jan: Hopefully our Skyrme model project will be continued next year. Tore G. Halvorsen, partner in crime at CMA (the crime being physics), has been responsible for at least one laugh each day. I would also thank Dr. Giuseppe M. Coclite of University of Bari, Italy, who has been very helpful at the occasions he has visited CMA.

The constant encouragement of my many friends has been a comfort to me when I have been working at its hardest. To all of you, I'm really looking forward to going to the movies without thinking about electrons, having some brain capacity left for a board game, and having a beer at a friday quiz again.

When I was nine or ten years old, my father introduced me to BASIC. The shelves in the basement were also filled with strange and wonderful books on physics, chemistry and programming. To this day, I return to the basement for bedtime reading when I am visiting. So thank you, dad, for spurring my imagination!

Mom, dad and my sisters Camilla and Mathilde have been with my all of my life, and without their love and support, I would not be who or where I am today.

Last, but not at all least, Hilde, my better half, love of my life, I am profoundly grateful for your love and support. It must have been quite lonely at times, me being holed up in my cave and barely dropping by for some hours of sleep. Yes, I am going to fix those clothes hooks now, if you make some chili.

November 2008 Simen Kvaal
Oslo

Contents

Part I : Introduction

1 Background and theory

1.1 INTRODUCTION

On the surface, this thesis is about quantum dots. However, I admit that this is more or less an excuse to study many-body techniques, which I consider to be the *real* topic of the thesis. Even though some of the quantum dot applications of many-body methods are novel, the quantum dot-interested reader may be disappointed, while I think the many-body techniques-interested on the other hand will find more of interest. The research has been motivated not primarily by fascination of quantum dots, but rather the *ab initio* methods that are used to study them.

Ab initio many-body theory is, in many ways, a mature field, ranging from advanced perturbation theoretical approaches to Monte Carlo techniques, via coupled cluster methods and full configuration interaction. On the other hand, many-body theory is notoriously difficult, with many pitfalls and with, for the uninitiated, an obscure and esoteric way of speaking and formulating problems. In some cases, it is obvious that the theory still lacks a sound mathematical foundation, and that there are still many open yet very important questions to pose as well as answer. In addition, there is the curse of dimensionality, which makes good methods so hard to invent.

For this reason, I have focused on two main many-body techniques, and tried to do a thorough study of their properties when applied to quantum dots: Full configuration-interaction method (FCI, or "exact diagonalization") in a harmonic oscillator basis, and sub-cluster effective interactions as employed in recent years' no-core shell model calculations in nuclear physics. The reason for choosing quantum dots as subject of application is, (a) that it is interesting in itself, and (b), that harmonically confined quantum dots can be viewed as simplified nuclear systems, with lower spatial dimensionality and a well-defined, well-known interaction term. The knowledge gained should then have wide applicability in both quantum dot studies and nuclear physics, as well as some quantum chemistry problems. The reason for choosing the FCI method, was that other methods, such as coupled cluster (CC) and Hartree-Fock (HF) methods, are closely related to the FCI method. Insight can then be gained for these methods as well.

Another reason for studying the FCI method is the prospect of accurately computing the time-evolution of a system with a time-dependent Hamiltonian, such as a quantum dot manipulated with electromagnetic fields. The period of time for which such a calculation would be valid depends on the accuracy of the eigenvalues (or more precisely, their spacing). Except for the equation-of-motion coupled cluster method (see Section 2.5), FCI is the only *ab initio*

method that gives, in principle, all the eigenvalues and eigenfunctions of a many-body system.

The central part of this thesis deals with the analysis of the approximation properties of harmonic oscillator eigenfunctions, i.e., many-dimensional Hermite functions. As these are usually used as basis functions in the FCI and CC calculations, and in many HF-calculations as well, detailed knowledge of such properties is essential for understanding the numerical behaviour of virtually every application, in both nuclear physics and quantum dot studies. Surprisingly, except for important work on ordinary one-dimensional Hermite functions by Hille (1939), studies of hermite functions are hard to find in the literature. The analysis, carried out for the most part in Paper 2, results in unambiguous *a priori* error estimates for expansions of functions in a harmonic oscillator basis, as well as error estimates for FCI calculations.

Effective interactions are widely used in nuclear physics, and applying them to the simpler quantum dots could give great insight into the method, which is hard to obtain from the nuclear studies. Surprisingly, few studies of this kind have been done, even though it is fairly obvious that they are needed. As is shown in Papers 1 and 2, the quantum dot FCI calculations obtain a dramatic increase in convergence when using a two-body effective interaction.

Paper 3 reformulates and simplifies parts of the standard effective Hamiltonian theory, and points out a simpler and more transparent procedure than the one used today for computing the effective Hamiltonian used in no-core shell model calculations. I apply this procedure in all the other papers, and also give a thorough discussion of the two-body effective interaction in Paper 4.

This thesis is organized as follows. Part I continues with some preliminaries. In Section 1.2 we give a brief introduction to quantum dots. Following that, we discuss the formalism of second-quantization needed for discussing many-body theory in Section 1.3. Because of their importance, a gentle introduction to the properties of harmonic oscillator basis functions is given in Section 1.4; these are discussed in detail in Paper 2. Section 1.5 discusses some properties of the quantum dot Hamiltonian compared to the molecular Hamiltonian, and we discuss the variational principle in Section 1.6.

We are then ready to discuss many-body techniques in Chapter 2, starting with the FCI method in Section 2.1 before discussing effective Hamiltonians and interactions in Section 2.2. Section 2.3 discusses the scaling of the FCI method when a parallel implementation is considered, and Sections 2.4 and 2.5 briefly discuss the Hartree-Fock and coupled cluster methods, respectively.

Part II of the thesis contains the journal publications, referred to as Paper 1 through 4 in Part I.

1.2 QUANTUM DOTS

During the last twenty years, the research activity on so-called quantum dots has grown rapidly.[1] Put simply, quantum dots are nanometre-scale semiconductor devices confining a few electrons spatially. The quantum dots we consider here, so-called lateral quantum dots, are usually fabricated by etching techniques. Such methods are, despite their sophistication, essentially

[1] A search at ISI Web of Science reveals that the number of publications with topic "quantum dots" is approximately $n \approx 0.4(y-1985)^{3.1}$, where y is the year of publication.

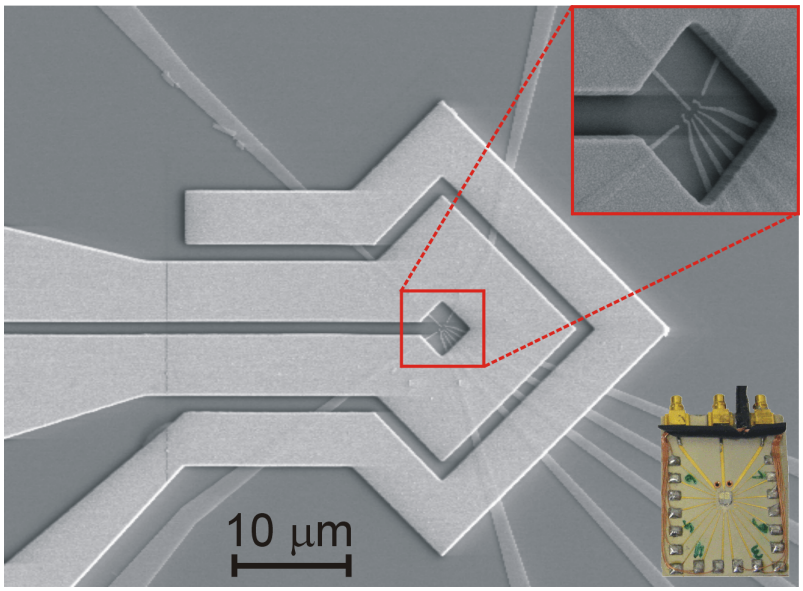

Figure 1.1: Scanning electron micrograph of a double quantum dot defined by electrostatic gates (expanded area) applied to a sandwich of GaAs/AlGaAs/GaAs, surrounded by a loop antenna that produces a magnetic field. Also shown is a sample holder optimized for radio frequency measurements on the double quantum dot. Image courtesy of the Nanophysics Group at the University of München, Germany.

macroscopic. Still, the resulting structures are small enough to allow behaviour in the quantum mechanical regime of the confined electrons, such as shell structure (Tarucha et al. 1996) and entanglement (Weiss et al. 2006). Moreover, the confinement parameters may be directly controlled via applied electromagnetic fields. For this reason, quantum dots are often called "designer atoms", and it is clear that these offer exciting possibilities to study elementary quantum mechanics and the transition to classical mechanics, direct manipulation and imaging of quantum states (Fitzgerald 2003), and so on.

For a general introduction to the topic, see the popularized article by Reed (1993) and the review by Reimann and Manninen (2002).

In Figure 1.1 a micrograph of a so-called double quantum dot (DQD) is shown. The starting point is a two-dimensional electron gas layer (2DEG), here a planar sheet of AlGaAs sandwiched between insulating GaAs layers. Metal gate electrodes are then applied to the top surface using lithographic etching techniques. Adjusting the voltage over some of these gates will define a double-well potential that will squeeze and confine a few electrons in the 2DEG, which otherwise were free to move in the plane. Other gates can again be used to load and remove *single electrons* from the DQD.

The DQD is actually a system of two lateral quantum dots coupled together. A model for this and similar quantum dots can be obtained in the effective mass approximation as a system of N interacting electrons of effective mass $m^* \approx 0.067 m_e$ in a double-well potential in $d = 2$ spatial dimensions. Such a double-well potential may be given by

$$V(\vec{r}) = \frac{1}{2} m^* \omega^2 \min\left\{ \|\vec{r} - \vec{a}\|^2, \|\vec{r} + \vec{a}\|^2 \right\},$$

where $\pm\vec{a}$ are the locations of the minima of the well, and ω is a parameter defining the char-

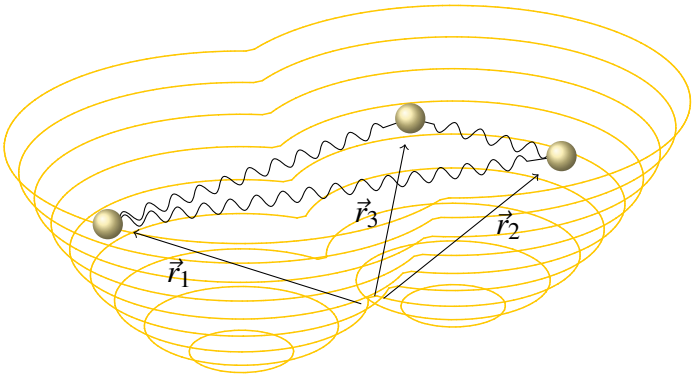

Figure 1.2: Illustration of quantum dot model. $N = 3$ electrons with coordinates $\vec{r}_i$ move in a potential trap $V(\vec{r})$ (gold wireframe) and interact via the Coulomb force; illustrated with squiggly lines. The classical motion of the electrons can be pictured by the rolling of small balls in a bowl, with additional repulsive forces

acteristic length unit a_0 of the well by $a_0 = \sqrt{\hbar/m\omega}$. Typical sizes are $a_0 \approx 20$ nm. Whenever $\|\vec{r}\| \gg \|\vec{a}\|$, the potential is essentially a harmonic oscillator. The Hamiltonian for this system reads

$$H = \left[\sum_{i=1}^{N} -\frac{\hbar^2}{2m^*}\nabla_i^2 + V(\vec{r}_i)\right] + \frac{e^2}{4\pi\epsilon_0\epsilon}\sum_{i<j}\frac{1}{r_{ij}}, \tag{1.1}$$

where $e^2/4\pi\epsilon_0 \approx 1.44$ eVnm, and where $\epsilon \approx 12$ is the dielectric of the surrounding semiconductor bulk. The electrons carry a spin degree of freedom $\sigma \in \{\pm 1\}$, and the total wavefunction for the system must be anti-symmetric with respect to interchanges of any two particles' coordinates $x_i = (\vec{r}_i, \sigma_1)$ and $x_j = (\vec{r}_j, \sigma_j)$.

Figure 1.2 illustrates the quantum dot model. The double-well potential is depicted along with some (classical) electrons. The motion of classical electrons would be that of sliding on the surface (viewed from above), taking into account the Coulomb repulsion between the electrons.

In this thesis, we shall almost exclusively discuss the so-called parabolic quantum dot, for which $\vec{a} = 0$. In this case, $V(\vec{r}) = m^*\omega^2\|\vec{r}\|^2/2$ which is a pure harmonic oscillator. Introducing the energy unit $\hbar\omega$ and length unit a_0, the Hamiltonian can be written on dimensionless form, viz,

$$H = \left[\sum_{i=1}^{N} -\frac{1}{2}\nabla_i^2 + \frac{1}{2}\|\vec{r}_i\|^2\right] + \lambda\sum_{i<j}\frac{1}{r_{ij}}, \tag{1.2}$$

where the interaction strength parameter λ is given by

$$\lambda = \frac{e^2}{4\pi\epsilon_0\epsilon}\frac{1}{\hbar\omega a_0} = \frac{e^2}{2\pi\epsilon_0\epsilon}\frac{m^* a}{\hbar^2} \approx 2.11.$$

This is a typical value in real quantum dots.

One of the possible uses for quantum dots is as basic constituents of future quantum computers. In one of the first proposed schemes, now a classic reference, Loss and DiVincenzo (1998) proposed to utilize the spins of coupled single-electron quantum dots (such as the DQD with $N = 2$ electrons) to encode qubits; the quantum-counterpart of a digital bit. However, one of the main obstacles turns out to be that of decoherence: Our model is overly simplistic, as small irregularities and interactions with the environment (for example, due to a nonzero temperature or the nuclei in the semiconductor bulk) breaks down the painstakingly engineered state of the system after very short time (Cerletti et al. 2005).

Our model Hamiltonian (1.1) or (1.2) should therefore not be interpreted as *the* Hamiltonian, but instead as a test case that must *at least* be tackled before we can predict the outcome of more realistic cases. Moreover, such an idealized model is very well suited for analysis of many-body methods.

1.3 SECOND QUANTIZATION

The quantum dot model described in the preceding section is very well suited for many-body techniques like full configuration interaction, Hartree-Fock, and the coupled cluster method. Before we can describe these methods, we will need to rewrite the Hamiltonian (1.2) using second quantization. This is a formalism which in an elegant way gets rid of difficulties such as wave-function symmetry and dependence on the number of particles N. The formulation of the many-body techniques then becomes much simpler.

The uninitiated may find this exposition rather brief, and I refer to any good text on many-body quantum mechanics, such as the books by Raimes (1972) and Lindgren and Morrison (1982), for details. The book by Ballentine (1998) also gives an introduction to the topic in a more mathematical way, discussing advanced concepts such as rigged Hilbert spaces.

Our goal is to find a few of the lowest eigenvalues of the Hamiltonian (1.2), i.e., we seek real numbers E_k and wavefunctions $\Psi_k = \Psi_k(x_1, x_2, \cdots, x_N)$ (where $x_i = (\vec{r}_i, \sigma_i)$, with $\sigma_i \in \{+, -\}$ being the electron spin degree of freedom) such that

$$H\Psi_k(x_1, x_2, \cdots, x_n) = E_k\Psi_k(x_1, x_2, \cdots, x_N).$$

The wavefunction Ψ_k is sought in the Hilbert space of anti-symmetric N-body functions, viz,

$$\Psi_k \in \mathscr{H}_N := \mathscr{H}_1 \wedge \mathscr{H}_1 \wedge \cdots \wedge \mathscr{H}_1,$$

where the single-particle space $\mathscr{H}_1$ is the space of square integrable functions over $\mathbb{R}^d \times \{\pm\}$, i.e.,

$$\mathscr{H}_1 := L^2(\mathbb{R}^d \times \{\pm\}) \approx L^2(\mathbb{R}^d) \otimes \mathbb{C}^2,$$

that is, $\mathbb{C}^2$-valued L^2-functions.

Given a complete orthonormal set $\{\phi_\alpha(x)\}_{\alpha=1}^{\infty}$ in $\mathscr{H}_1$, a corresponding set in $\mathscr{H}_N$ is conve-

niently given by Slater determinants. These are defined by

$$\Phi_{\alpha_1,\cdots,\alpha_N}(x_1,\cdots,x_N) := \frac{1}{\sqrt{N!}} \begin{vmatrix} \phi_{\alpha_1}(x_1) & \cdots & \phi_{\alpha_1}(x_N) \\ \vdots & & \vdots \\ \phi_{\alpha_N}(x_1) & \cdots & \phi_{\alpha_N}(x_N) \end{vmatrix},$$

where

$$\alpha_1 < \alpha_2 < \cdots < \alpha_N$$

is imposed to make the determinants unique. The indexing of $\phi_\alpha(x)$ by α may be arbitrary, as long as we have an ordering.

It is common to introduce a coordinate-free notation for wavefunctions using the so-called *ket*-notation, viz, $|\Psi\rangle$, $|\Phi_{\alpha_1,\cdots,\alpha_N}\rangle$, etc. One introduces a "basis" of kets $|x_1,x_2,\cdots,x_N\rangle$ so that any $|\Psi\rangle \in \mathscr{H}_N$, may be expanded as

$$|\Psi\rangle = \int \mathrm{d}x_1 \cdots \mathrm{d}x_N \, |x_1,\cdots,x_N\rangle\langle x_1,\cdots,x_N|\Psi\rangle,$$

where

$$\Psi(x_1,\cdots,x_N) = \langle x_1,\cdots,x_N|\Psi\rangle,$$

i.e., the wavefunction's value at $(x_1,\cdots,x_N)$ is the component of $|\Psi\rangle$ along the "basis vector" $|x_1,\cdots,x_N\rangle$. The integral $\int \mathrm{d}x_i$ is defined as

$$\int \mathrm{d}x_i := \sum_{\sigma_i} \int \mathrm{d}^d r.$$

We will furthermore sometimes use ket-notation $|\Psi\rangle$ for Hilbert space elements, and sometimes plain function-notation $\Psi(x_1,\cdots,x_N)$, depending on the context.

Let us introduce the so-called Fock space $\mathscr{H}_{\text{Fock}}$, which embodies the idea of a Hilbert space of functions containing *arbitrary* many particles. Simply by defining Slater determinants of N and $N'(\neq N)$ particles to be orthogonal to each other, we define

$$\mathscr{H}_{\text{Fock}} := \bigoplus_{N=0}^{\infty} \mathscr{H}_N.$$

The space $\mathscr{H}_0$ is defined as an arbitrary one-dimensional space, which is interpreted as containing zero particles. We pick a normalized $|-\rangle \in \mathscr{H}_0$ and call it *the vacuum*; the single "Slater determinant" of zero particles. So-called creation and annihilation operators $c_\alpha^\dagger$ and c_α (being Hermitian adjoints of each other) are defined for each orbital $\phi_\alpha(x)$. They are defined such that

$$|\Phi_{\alpha_1,\cdots,\alpha_N}\rangle = c_{\alpha_1}^\dagger c_{\alpha_2}^\dagger \cdots c_{\alpha_N}^\dagger |-\rangle. \tag{1.3}$$

Thus, $c_\alpha^\dagger : \mathscr{H}_N \to \mathscr{H}_{N+1}$ and $c_\alpha : \mathscr{H}_N \to \mathscr{H}_{N-1}$. The important anti-commutator relations

$$\{c_\alpha, c_\beta\} = \{c_\alpha^\dagger, c_\beta^\dagger\} = 0 \quad \text{and} \quad \{c_\alpha^\dagger, c_\beta\} = \delta_{\alpha,\beta}$$

follow from from Eqn. (1.3).

As a simple example of the usefulness of c_α and $c_\alpha^\dagger$, consider the *particle number operator* $\hat{N}$ defined by

$$\hat{N} := \sum_\alpha c_\alpha^\dagger c_\alpha,$$

where the caret notation distinguishes it from N. It is relatively easy to see that for any Slater determinant

$$\hat{N}|\Phi_{\alpha_1,\cdots,\alpha_N}\rangle = N|\Phi_{\alpha_1,\cdots,\alpha_N}\rangle,$$

that is, the Slater determinants are the eigenvectors of $\hat{N}$ with eigenvalue N. The eigenspace is simply $\mathscr{H}_N$.

The Hamiltonian (1.2) can also be written in terms of $c_\alpha^\dagger$ and c_α as

$$H = \sum_{\alpha\beta} h_\beta^\alpha c_\alpha^\dagger c_\beta + \frac{1}{2} \sum_{\alpha\beta\gamma\delta} u_{\gamma\delta}^{\alpha\beta} c_\alpha^\dagger c_\beta^\dagger c_\delta c_\gamma, \tag{1.4}$$

where the order of the indices in the last term should be noted. The matrix elements h_β^α and $u_{\gamma\delta}^{\alpha\beta}$ are defined by

$$h_\beta^\alpha := \int \mathrm{d}x\, \overline{\phi_\alpha(x)} \left(-\frac{1}{2}\nabla^2 + \frac{1}{2}\|\vec{r}\|^2 \right) \phi_\beta(x),$$

and

$$u_{\gamma\delta}^{\alpha\beta} := \lambda \int \mathrm{d}x_1 \mathrm{d}x_2\, \overline{\phi_\alpha(x_1)\phi_\beta(x_2)} \frac{1}{r_{12}} \phi_\gamma(x_1)\phi_\delta(x_2).$$

The new Hamiltonian (1.4) is seen to be independent of N, and is given naturally as an operator in the Fock space $\mathscr{H}_{\text{Fock}}$. As such, it is seen as a *particle number* conserving operator – the subspace $\mathscr{H}_N \subset \mathscr{H}_{\text{Fock}}$ is invariant under H, viz,

$$[H, \hat{N}] = 0.$$

This is seen by noting that the terms of H create and destroy the same number of particles. Notice, that the second-quantized Hamiltonian is really defined as an infinite matrix with respect to the Slater determinants.

We will take the single-particle orbitals $\phi_\alpha(x)$ to be eigenfunctions of the single-particle Harmonic oscillator. In $d = 2$ spatial dimensions, the indices α are then mapped one-to-one on the set (n, m, σ), where $n \geq 0$ and m are integers. The single-particle functions take the form $\phi_\alpha(x) = \varphi_{n,m}(\vec{r})\chi_\sigma$, where χ_σ are the spin-dependent basis functions; a basis for $\mathbb{C}^2$. The

functions $\varphi_{n,m}(\vec{r})$ are called Fock-Darwin orbitals, and are given in polar coordinates by

$$\varphi_{(n,m)}(r,\theta) := Ne^{im\theta}r^{|m|}L_n^{|m|}(r^2)e^{-r^2/2}, \tag{1.5}$$

where N is a normalization constant, and where $L_n^k(x)$ is the generalized Laguerre polynomial. The corresponding eigenvalues are $\epsilon_\alpha = 2n+|m|+1$. Notice, that we then obtain $h_\beta^\alpha = \epsilon_\alpha \delta_{\alpha,\beta}$.

The presentation of second-quantization given here is sketchy and omits some important details, such as whether it is *possible* at all to write Eqn. (1.2) as a matrix with respect to the chosen Slater determinant basis. For example, the bare interaction in the nuclear shell model is so strong that the matrix elements in the chosen basis are infinite, and one must do further analysis. Moreover, H is not even *defined* on the whole of $\mathscr{H}_N$. As it stands, H is a formal second-order differentiation operator, which is unnecessary restricting. In abstract partial differential equation analysis it is common to introduce a weak formulation which makes H a self-adjoint operator on a subspace $\mathscr{H}_N$, with a different norm. Typically, this would be the space of weakly differentiable functions. We touch upon this in the next section.

In this thesis, we mostly follow the physicist notation and formalism, in accordance with virtually all standard quantum mechanics texts. Ballentine (1998) gives a further account of the mathematical foundation of quantum mechanics. See Weidmann (1980) for a discussion of operators defined in terms of infinite matrices, and Babuska and Osborn (1996) for a discussion of the eigenvalue problem of self-adjoint operators and its variational formulation and subsequent approximation by the Ritz-Galerkin method. This *is* the FCI method, and using the Fock-Darwin single particle orbitals, it can be shown to fit perfectly into the framework so that convergence estimates hold for quite general interaction potentials. (See however Section 1.5.) With a little goodwill, this justifies the physicist's common view of an operator as a matrix, even in the infinite dimensional case.

1.4 PROPERTIES OF HARMONIC OSCILLATOR FUNCTIONS

As stated in the Introduction, an important part of the thesis is the analysis of the harmonic oscillator (HO) eigenfunctions in Paper 2 (with some surface-scratching in Paper 1), which generalize the standard Hermite functions. In this Section, I will give a general introduction to the ideas and concepts used to derive approximation properties. Hille (1939) gives a very detailed analysis of expansions in standard Hermite functions, but it is not easy to generalize his work to arbitrary dimensions, as the results are not proven or stated within the more modern framework of weak differentiation.

The standard Hermite functions are defined by

$$\phi_n(x) := [2^n n!\sqrt{\pi}]^{-1/2} H_n(x) e^{-x^2/2},$$

where $H_n(x)$, $n = 0, 1, \cdots$ are the usual Hermite polynomials. These obey the recurrence relation

$$H_{n+1}(x) = 2xH_n(x) - 2nH_{n-1}(x), \tag{1.6}$$

where we take $H_{-1} \equiv 0$ and where $H_0(x) = 1$.

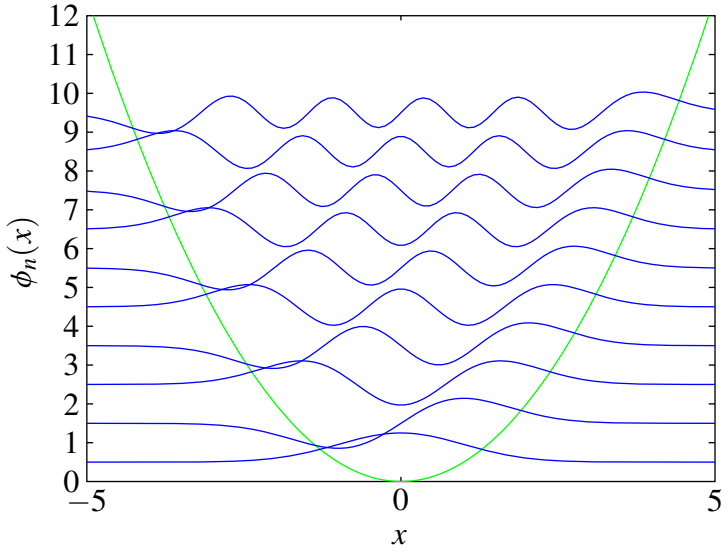

Figure 1.3: The ten first Hermite functions $\phi_n(x)$ (blue) plotted together with the harmonic potential $x^2/2$ (green). Each $\phi_n(x)$ is shifted vertically by $n+1/2$ for easy identification. This shift is equal to the eigenvalue of $\phi_n(x)$. Notice the penetration into the classically forbidden region by the Gaussian tail for each $\phi_n(x)$.

Now, the functions $\phi_n(x)$ constitute a complete orthonormal sequence in $L^2(\mathbb{R})$, and they are eigenfunctions of the one-dimensional HO Hamiltonian H_{HO} defined by

$$H_{\text{HO}} := -\frac{1}{2}\frac{\partial^2}{\partial x^2} + \frac{1}{2}x^2 = a_x^\dagger a_x + 1,$$

where

$$a_x := \frac{1}{\sqrt{2}}\left(x + \frac{\partial}{\partial x}\right), \quad \text{and} \quad a_x^\dagger := \frac{1}{\sqrt{2}}\left(x - \frac{\partial}{\partial x}\right)$$

are called ladder operators. The eigenvalue of ϕ_n is $n+1/2$, as is easily verified. The most important feature of $a_x^\dagger$ and a_x is that, for all n,

$$a_x^\dagger \phi_n(x) = \sqrt{n+1}\,\phi_{n+1}(x) \quad \text{and} \quad a_x \phi_n(x) = \sqrt{n}\,\phi_{n-1}(x).$$

This can be shown rather easily by using the recurrence formula (1.6). In Figure 1.3 a few of the Hermite functions are shown, translated vertically according to their HO energy.

If we consider an arbitrary $\psi \in L^2(\mathbb{R})$, it has a unique expansion in the Hermite functions, viz,

$$\psi(x) = \sum_{n=0}^{\infty} \langle \phi_n, \psi \rangle \phi_n(x) = \sum_{n=0}^{\infty} c_n \phi_n(x).$$

The coefficients satisfy

$$\|\psi\|^2 = \sum_{n=0}^{\infty} |c_n|^2 < +\infty, \tag{1.7}$$

which automatically implies that

$$|c_n| \longrightarrow 0 \quad \text{as} \quad n \longrightarrow \infty.$$

In fact, by the comparison test, $|c_n|$ must fall off faster than $n^{-1/2}$, viz,

$$|c_n| = o(n^{-1/2}).$$

If we assume, that for a given $\psi \in L^2(\mathbb{R})$, also $a_x^\dagger \psi \in L^2(\mathbb{R})$, we obtain

$$\|a_x^\dagger \psi\|^2 = \sum_{n=0}^{\infty} (n+1)|c_n|^2. \tag{1.8}$$

Comparing this with Eqn. (1.7), we see that the coefficients $|c_n|$ in this case must fall off faster, i.e.,

$$|c_n| = o(n^{-1}).$$

Moreover, we can easily see that $a_x^\dagger \psi \in L^2(\mathbb{R})$ if and only if $x\psi \in L^2(\mathbb{R})$ and $\partial_x \psi \in L^2(\mathbb{R})$. The first is equivalent to $\partial_x \hat{\psi} \in L^2(\mathbb{R})$, where the caret denotes the Fourier transform. Here, ∂_x is a shorthand for the partial derivative.

The notion of derivative we use here is the so-called *weak* derivative, which generalizes the classical one. The advantage of the weak derivative is that the space of k times weakly differentiable functions $H^k(\mathbb{R})$ becomes a Hilbert space. This space is defined by

$$H^1(\mathbb{R}) := \left\{ \psi \in L^2(\mathbb{R}) \,:\, \partial_x^j \psi \in L^2(\mathbb{R}) \; \forall j \leq k \right\} \tag{1.9}$$

with inner product

$$\langle \psi_1, \psi_2 \rangle_{H^k} := \sum_{j=0}^{k} \langle \partial_x^j \psi_1, \partial_x^j \psi_2 \rangle. \tag{1.10}$$

The spaces $H^k(\mathbb{R})$ can be generalized to arbitrary domains $\Omega \subset \mathbb{R}^n$ using weak partial derivatives of order $\leq k$. The definition of the weak derivative is not entirely trivial, and we refer to Evans (1998) for a general introduction. See also the discussion in Paper 2.

If $\psi(x)$ is known *a priori* to decay exponentially fast as $|x| \to \infty$, we obtain the following proposition:

Proposition 1 *Let $\psi \in L^2(\mathbb{R})$. Assume that, for all $m > 0$, $x^m \psi \in L^2(\mathbb{R})$ (implied by exponential decay). Then, $(a_x^\dagger)^k \psi \in L^2(\mathbb{R})$ if and only if $\partial_x^k \psi \in L^2(\mathbb{R})$, i.e., $\psi \in H^k(\mathbb{R})$. Equivalently,*

$$\sum_{n=0}^{\infty} n^m |c_n|^2 \; < \; +\infty. \tag{1.11}$$

The latter implies, in particular, that

$$|c_n| = o(n^{-(k+1)/2}). \tag{1.12}$$

In numerical applications, one usually does not observe an integral or half-integral exponent, as in Eqn. (1.12). Assume that $\psi \in H^k(\mathbb{R})$ but $\psi \notin H^{k+1}(\mathbb{R})$, i.e., ψ can be differentiated *at most* k times. The upper bound on the decay rate is now $|c_n| = o(n^{-(k+2)/2})$. This explains that the actual behaviour observed is often

$$|c_n| = o(n^{-(k+1+\epsilon)/2}), \quad 0 \leq \epsilon < 1.$$

Proposition 1 has an analogue for Fourier series, which is perhaps more well-known. Let $\psi \in L^2[0, 2\pi]$ be given by a Fourier series, viz,

$$\psi(x) = \sum_{n=-\infty}^{\infty} c_n \frac{e^{inx}}{\sqrt{2\pi}}.$$

Assume now that $\psi \in H^1[0, 2\pi]$. Differentiating the function $\exp(inx)/\sqrt{2\pi}$, we obtain

$$\partial_x \psi(x) = \sum_{n=-\infty}^{\infty} (in) c_n \frac{e^{inx}}{\sqrt{2\pi}}$$

with norm given by

$$\|\partial_x \psi(x)\|^2 = \sum_{n=-\infty}^{\infty} n^2 |c_n|^2,$$

which should be compared with Eqn. (1.8). An interesting point here is that differentiation in the Fourier case gives a weight n^2 in the sum, while the Hermite case only gives n^1. Notice that the Fourier basis functions only approximate over a bounded interval $[0, 2\pi]$, while the Hermite functions must deal with the whole line $\mathbb{R}$. Consequently, the width of the oscillations of $e^{inx}/\sqrt{2\pi}$ decreases faster than those of $\phi_n(x)$. Intuitively, $e^{inx}/\sqrt{2\pi}$ resolves details in the function $\psi(x)$ more efficiently.

In Paper 2 Proposition 1 is generalized to n-dimensional Hermite functions, being defined as tensor products of n one-dimensional Hermite functions. These constitute an orthonormal sequence for $L^2(\mathbb{R}^n)$, and are eigenfunctions for the n-dimensional HO Hamiltonian, i.e.,

$$\begin{aligned} H_{\text{HO}} = -\frac{1}{2}\nabla^2 + \frac{1}{2}\|\vec{r}\|^2 &= \sum_{i=1}^{n} \left(-\frac{1}{2}\frac{\partial^2}{\partial r_i^2} + \frac{1}{2} r_i^2 \right) \\ &= \sum_{i=1}^{n} \left(a_i^\dagger a_i + 1 \right). \end{aligned}$$

The n-dimensional results are completely analogous to the one-dimensional case, giving a rapid decay of the expansion coefficients if and only if ψ is many times (weakly) differentiable and decays sufficiently fast as $\|\vec{r}\| \to \infty$. Let me comment that the Slater determinants are eigenfunctions of H_{HO} with $n = Nd$, which automatically gives a starting point for the approximation properties of these as well.

The relevance of Proposition 1, is that when using HO eigenfunctions as basis in a many-body calculation, the convergence rate with respect to the basis size (as represented by, for example, the truncation parameter R in Section 2.1) depends precisely on how fast the coefficients

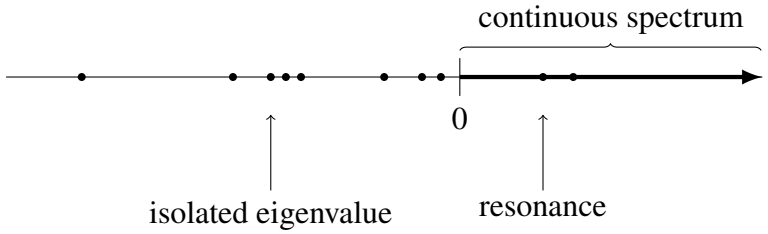

Figure 1.4: The spectrum of a molecular Hamiltonian in the Born-Oppenheimer approximation. There is a set of discrete, isolated eigenvalues $E_k < 0$, which may be infinitely many, and a continuous spectrum for $E > 0$. Moreover, there may be resonances, i.e., embedded discrete eigenvalues in the continuous spectrum

of the exact eigenfunction (or more precisely, the spin component functions) $\Psi(\vec{r}_1, \cdots, \vec{r}_N)$ fall off, which in turn is equivalent to the smoothness properties of the eigenfunction.

1.5 PROPERTIES OF THE SPECTRUM AND EIGENFUNCTIONS

We briefly mention some of the results from the spectral theory of Schrödinger operators and the analytic properties of electronic wavefunctions. In the light of the above discussion, the latter is especially interesting. The material is taken mostly from Hoffmann-Ostenhof et al. (1994) and Hislop and Sigal (1996).

The spectral theory of unbounded operators (such as H) is complex. There is a large amount of literature devoted to this, but most of the quantum mechanics-related literature is devoted to molecular problems, where the Hamiltonian describes a system of atomic nuclei and electrons in $d = 3$ dimensions. The central result states that the molecular Hamiltonian in the Born-Oppenheimer approximation (in which the positions of the nuclei are held fixed) has a point spectrum $\sigma_p \subset (-\infty, 0)$ (identical to the isolated eigenvalues and possibly empty) and a continuous spectrum $\sigma_c = [0, +\infty)$, consisting of approximate eigenvalues (whose "eigenvectors" are simply delta-function normalizable eigenfunctions, such as plane waves or the basis vectors $|x_1, \cdots, x_N\rangle$ of Section 1.3) and possibly embedded eigenvalues, i.e., resonances. This is illustrated in Figure 1.4. These concepts are perhaps most easily understood in the framework of rigged Hilbert space (Ballentine 1998).

When it comes to quantum dot Hamiltonians, the problem simplifies on one hand, but becomes more complicated on the other. First, the presence of the confining harmonic potential makes the continuous spectrum empty: The spectrum consists entirely of ordinary eigenvalues. Second, the two-dimensional Coulomb interaction actually violates the assumptions common in the literature (Hislop and Sigal 1996), namely that

$$\frac{1}{\|\vec{r}\|} \in L^2(\Omega), \quad \forall \Omega \in \mathbb{R}^3,$$

where Ω is assumed to be a bounded subset. To see this, note that the only non-trivial domains to check in both $d = 2$ and $d = 3$ are arbitrary domains containing $\vec{r} = 0$. Consider the unit

sphere $\Omega = \{\vec{r}\colon \|\vec{r}\| \leq 1\}$ for which we obtain the norm

$$\left\| \|\vec{r}\|^{-1} \right\|^2_{L^2(\Omega)} = \int_\Omega \left(\frac{1}{\|\vec{r}\|} \right)^2 \mathrm{d}^3 r = 4\pi \int_0^1 \frac{1}{r^2} r^2 \, \mathrm{d}r = 4\pi \ < +\infty.$$

In $d = 2$ dimensions, we obtain

$$\left\| \|\vec{r}\|^{-1} \right\|^2_{L^2(\Omega)} = \int_\Omega \frac{1}{\|\vec{r}\|^2} \, \mathrm{d}^2 r = 2\pi \int_0^1 \frac{1}{r^2} r \, \mathrm{d}r = \infty.$$

Thus, the Coulomb interaction is, in a sense, too strong in two dimensions, and we should really consider the problem further before going about and diagonalizing using the FCI method, since the variational formulation of the eigenvalue problem is, strictly speaking, not valid without further analysis (Babuska and Osborn 1996).

On the other hand, as argued in Paper 2, the known exact solutions in the two-particle case behave virtually identically in both $d = 2$ and $d = 3$. Moreover, Hoffmann-Ostenhof et al. (1994) have thoroughly analyzed the local analytic behaviour of many-electron wavefunctions in $d = 3$ dimensions. The central result is that near a so-called coalesce point $\xi_{\mathrm{CP}} = (\vec{r}_1, \cdots, \vec{r}_N)$, where at least one $r_{ij} = 0$, the wavefunction's 2^N spin components all can be written on the form

$$\Psi(\xi + \xi_{\mathrm{CP}}) = \|\xi\|^k P_k \left(\frac{\xi}{\|\xi\|} \right) (1 + a\|\xi\|) + O(\|\xi\|^{k+1}),$$

where P_k is a hyperspherical harmonic (a polynomial on the sphere S^{3N-1}) of degree k. Away from ξ_{CP}, $\Psi(\xi)$ is real analytic. The number k varies for coalesce points where a different number of the r_{ij} vanish. Thus, it is immediate, that $\Psi \in H^{\min(k)+1}(\mathbb{R}^{3N})$.

The actual behaviour of the FCI results fits very well with this for $d = 2$ dimensions as well, indicating that the technicality with respect to the interaction *should* resolve. The FCI calculations in Paper 2 clearly indicate that $\Psi \in K^{k+1}(\mathbb{R}^{2N})$ for some $k \geq 0$, where k varies for different eigenfunctions.

1.6 VARIATIONAL PRINCIPLE

We now discuss the *variational principle*, which is heavily relied upon by many many-body techniques in some way or another. The treatment by Babuska and Osborn (1996) is more detailed, but for our purposes the present discussion is sufficient.

Let $|\Psi\rangle \in \mathscr{H}_N$. The Rayleigh quotient $E[\Psi]$ is defined by

$$E[\Psi] := \frac{\langle \Psi | H | \Psi \rangle}{\langle \Psi | \Psi \rangle},$$

whenever this expression is finite. Physically, $E[\Psi]$ is the total energy of the quantum system in the state $|\Psi\rangle$.

Assume that the Hamiltonian is self-adjoint and bounded from below, and that its ground

state is $|\Psi_0\rangle$ with eigenvalue E_0. Any wavefunction $|\Psi\rangle$ will satisfy the variational principle

$$E[\Psi] \geq E[\Psi_0],$$

with equality if and only if $|\Psi\rangle = |\Psi_0\rangle$. Thus,

$$E_0 = \min_{|\Phi\rangle \in \mathscr{H}_N} E[\Phi].$$

Also the other eigenvalues and eigenfunctions can be characterized by similar principles (Babuska and Osborn 1996).

Estimates for the ground state can now be obtained by taking the minimum over subsets of $\mathscr{H}_N$. For example, the FCI ground state $|\Psi_0^{\mathrm{FCI}}\rangle$ can be characterized as

$$|\Psi_0^{\mathrm{FCI}}\rangle = \operatorname*{argmin}_{|\Phi\rangle \in \mathscr{P}} E[\Phi],$$

i.e., minimization of the energy when the wavefunction is allowed to be in the model space $\mathscr{P} \subset \mathscr{H}_H$ only. The Hartree-Fock method to be described in Section 2.4 minimizes $E[\Phi]$ over the nonlinear manifold of Slater determinants, when also the single-particle functions $\phi_\alpha(x)$ are allowed to vary.

2 Many-body techniques

2.1 CONFIGURATION INTERACTION METHOD

The configuration interaction method is perhaps the conceptually simplest of the common many-body techniques based on second quantization. It is also the most accurate, in the sense that it converges to the exact solution, and that the other methods are approximations to the FCI method. The main drawback of FCI is that the problem scales almost exponentially with the number of particles N, see Section 2.3. This is called the *curse of dimensionality* and is, in fact, the main obstacle and motivation for new many-body methods.

Let us select a finite number of Slater determinants $B := \{|\Phi_i\rangle\}\}_{i=1}^{m}$ with N particles. These span a finite-dimensional space $\mathscr{P} \subset \mathscr{H}_N$ called the model space. The FCI method is then simply a Ritz-Galerkin approximation with respect to $\mathscr{P}$ (Babuska and Osborn 1996). This is equivalent to the eigenvalue problem of the matrix H whose matrix elements are

$$\mathsf{H}_{i,j} = \langle \Phi_i | H | \Phi_j \rangle, \quad i,j \leq m.$$

Let us consider two widely used model spaces. Recall that the single-particle functions $\phi_\alpha(x) = \varphi_{n,m}(\vec{r})\chi_\sigma$ are eigenfunctions of the operator H_{HO} given by

$$H_{\text{HO}} = -\frac{1}{2}\nabla^2 + \frac{1}{2}\|\vec{r}\|^2,$$

which gives $h_\beta^\alpha = h_{(n',m',\tau)}^{(n,m,\sigma)} = \epsilon_\alpha \delta_{\alpha,\beta}$, with $\epsilon_{(n,m,\sigma)} = 2n + |m| + 1$ in two-dimensional systems. Let B be given by

$$B = B(R) := \left\{ |\Phi_{\alpha_1,\cdots,\alpha_N}\rangle \ : \ \sum_{i=1}^{N} \epsilon_{\alpha_i} - \frac{Nd}{2} \leq R \right\}.$$

Then B is a basis for what is commonly called *the energy cut model space*, as we include all the Slater determinants with single-particle energy less than $R + Nd/2$. Notice that the energy of a Slater determinant is on the form $R' + Nd/2$ where $R' \geq 0$ is an integer.

This is the basis in which I did most of the numerical simulations in the papers. Another basis B' is even more common to encounter, defined by

$$B' = B'(R) := \left\{ |\Phi_{\alpha_1,\cdots,\alpha_N}\rangle \ : \ \max_i\{\epsilon_{\alpha_i}\} - \frac{d}{2} \leq R \right\}.$$

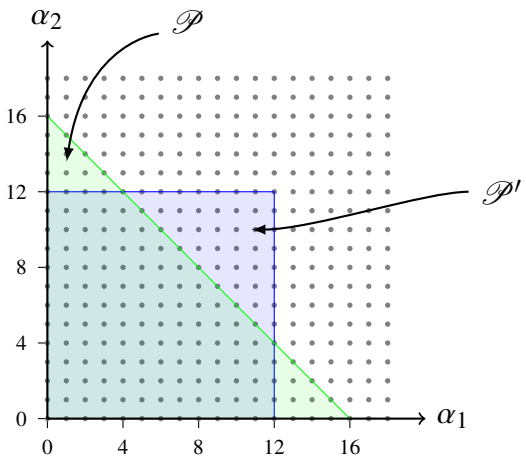

Figure 2.1: Illustration of $N = 2$ model spaces when $\epsilon_n = n + 1/2$. This is equivalent to a $d = 1$-dimensional harmonic oscillator. The Slater determinants included in each model space are on the form Φ_{α_1,α_2}. The shaded areas indicate with Slater determinants are included in $\mathscr{P}$, $R = 16$ (green) and $\mathscr{P}'$, $R = 12$ (blue), respectively.

The resulting model space $\mathscr{P}'$ is much bigger than $\mathscr{P}$, and is often called the *direct product model space*. Figure 2.1 illustrates $\mathscr{P}$ and $\mathscr{P}'$ in the case of $N = 2$ and $\epsilon_n = n + 1/2$, i.e., a one-dimensional system.

Which model space to choose is more or less a matter of taste. It is not obvious which is the better choice with respect to accuracy of the FCI method. Even though $\dim(\mathscr{P}')$ grows much faster with R than does $\dim(\mathscr{P})$, simple physical arguments indicate that $\mathscr{P}$ will include "more physically relevant" basis functions on average than $\mathscr{P}'$. As far as I know, no results in this direction have been published.

Papers 2 and 3 discuss the FCI method, properties of the Slater determinant basis functions, convergence of the eigenvalues with respect to R, etc, in detail.

Before we move on to the Hartree-Fock method, let us mention the results in Paper 2 on the error of the FCI method. For simplicity, we consider a one-dimensional one-particle problem, and we ignore spin. Let the exact (unknown) ground state eigenfunction $\psi(x) \in H^k(\mathbb{R})$ (where k is perhaps known from some analysis) be given by

$$\psi(x) = \sum_{n=0}^{\infty} c_n \phi_n(x), \quad |c_n| = o(n^{-(k+1+\epsilon)/2}),$$

where $\phi_n(x)$ are the standard Hermite functions considered in Section 1.4, and where the decay behaviour of $|c_n|$ is discussed in Section 1.4. The model spaces $\mathscr{P}$ and $\mathscr{P}'$ coincide in this case, and

$$B = B' = \{\phi_n(x)\}_{n=0}^{R}$$

is the FCI basis. The main result (Babuska and Osborn 1996) on the Ritz-Galerkin method states that the error ΔE in a non-degenerate eigenvalue (i.e., with unit multiplicity) is bounded

by

$$\Delta E \leq C \inf_{\phi\in\mathscr{P}} \|\psi-\phi\|_{\mathrm{HO}}^2$$
$$= C\|\psi - P\psi\|_{\mathrm{HO}}^2 = C\sum_{n=R+1}^{\infty}(n+\frac{1}{2})|c_n|^2, \tag{2.1}$$

where P projects orthogonally onto $\mathscr{P}$, and where where C is a constant. We have defined the HO-norm by

$$\|\psi\|_{\mathrm{HO}} := \langle\psi, H_{\mathrm{HO}}\psi\rangle^{1/2} = \left[\sum_{n=0}^{\infty}(n+\frac{1}{2})|\langle\phi_n,\psi\rangle|^2\right]^{1/2}$$

and used the fact that we expand the numerical wavefunction in eigenfunctions for $H_{\mathrm{HO}} = (-\partial_x^2 + x^2)/2$.

We can approximate the last sum in Eqn. (2.1) by an integral to obtain

$$\Delta E = O(R^{-(k+\epsilon-1)}), \tag{2.2}$$

which is valid for $k = 1$ if $\epsilon > 0$ and for $k > 1$. Otherwise, the integral approximation makes no sense. It turns out that Eqn. (2.2) is also valid in the general N-particle d-dimensional case, as described in Paper 2, assuming that the technicality of the Coulomb interaction in two dimensions resolves. The error estimate is discussed in more detail further down, in Section 2.3.

2.2 EFFECTIVE HAMILTONIANS

The many-body problem of the atomic nucleus is perhaps the most difficult many-body problem of modern physics: First, it has so many particles that a direct approach starting from the degrees of freedom from quantum chromodynamics is almost impossible, except when very few particles are present (Ishii, Aoki, and Hatsuda 2007). Second, there are too few particles to use statistical mechanics effectively. Furthermore, the fundamental interaction, i.e., the matrix elements $u_{\gamma\delta}^{\alpha\beta}$ are unknown, and one has to rely on phenomenological models. It is known that the interaction is very singular, with a so-called hard core potential growing rapidly towards infinity as $r_{ij} \to 0$; additionally, we have non-central tensor forces, violating conservation of orbital angular momentum. Finally, there is no natural centre to the system unlike the quantum dot model or the molecular system.

These considerations have led nuclear physicists on a 50-year long search (Bloch 1958; Bloch and Horowitz 1958) for ways to compute an *effective Hamiltonian*; a Hamiltonian that will reproduce exact eigenvalues of the full problem within a finite-dimensional model space.

A detailed account of the nuclear effective interaction theory is not possible to give here (for several reasons, of course); see Ellis and Osnes (1977), Hjorth-Jensen et al. (1995) and Dean et al. (2004). A lot of the theory also depends on perturbation theoretic approaches (Klein 1974; Shavitt and Redmon 1980; Lindgren and Morrison 1982; Schucan and Weidenmüller 1973). In-

stead, we will briefly discuss the most basic features of the standard theory. This is reformulated in Paper 3 in a geometric way, which relies heavily on the singular value decomposition (SVD), and leads to (in my opinion) a much simpler and transparent formalism.

An effective Hamiltonian H_{eff}, which is not unique, is usually defined as follows: Assume that $\mathscr{H}_N$ is finite-dimensional, $n = \dim(\mathscr{H}_N)$, and that P is the projector onto a model space $\mathscr{P} \subset \mathscr{H}_N$ with $m = \dim(\mathscr{P})$. Let G be such that

$$Qe^{-G}He^{G}P = Q\tilde{H}P = 0,$$

where Q is the orthogonal projector onto the complement of $\mathscr{P}$, i.e., $P+Q=1$. Then H_{eff} is defined by

$$H_{\text{eff}} := P\tilde{H}P.$$

This is to be interpreted as an operator defined *only* in $\mathscr{P}$.

Since similarity transforms preserve eigenvalues (i.e., $\tilde{H}$ has the same eigenvalues as H), the m eigenvalues of H_{eff} are identical to some of the n eigenvalues of H. If H has the spectral decomposition

$$H = \sum_{k=1}^{n} E_k |\Psi_k\rangle\langle\Psi_k|,$$

we assume that the eigenvalues E_k are arranged so that E_1 through E_m are reproduced by H_{eff}.

There are still many degrees of freedom in G to be determined. These fix the effective eigenvectors, i.e., the eigenvectors of H_{eff}. Two choices for G are common: An operator on the form $G = \omega = Q\omega P$ defined by

$$\omega(Q|\psi_k\rangle) = P|\psi_k\rangle, \quad \forall k \leq m$$

and the operator

$$G = \operatorname{artanh}(\omega - \omega^{\dagger}).$$

The first choice is called the Bloch-Brandow choice (Bloch 1958; Brandow 1967), and the second is the canonical Van Vleck choice (Van Vleck 1929). The first case leads to a non-Hermitian $H_{\text{eff}}^{\text{BB}}$, while the second a Hermitian $H_{\text{eff}}^{\text{c}}$ (where the superscript "c" stands for Canonical, see Paper 3.)

Finding the exact H_{eff} is usually out of question. Indeed, it is equivalent to the original diagonalization problem which we are trying to approximate. The usual way to tackle the problem is to expand H_{eff} in a perturbation series, with the interaction being the perturbation. To apply perturbation theory one must use the model space $\mathscr{P}$, where the unperturbed model space spectrum is separated from the excluded space spectrum. It has been known for some time, however, that this series is most likely to diverge in virtually all interesting cases in nuclear physics due to the presence of so-called intruder states, see Schucan and Weidenmüller (1973) and also Schaefer (1974) for a discussion.

The no-core shell model approach (basically FCI) was introduced in the 90's (Zheng et al.

1993), and today one can successfully handle, for example, the ^{12}C nucleus, i.e., an $N = 12$ problem (Navrátil, Vary, and Barrett 2000). The usual approach here is to compute the Hermitian effective Hamiltonian for the two-body problem, which can be computed more or less exactly, and to extract an effective interaction from this. Insertion into the full N-body problem then gives an approximation to the full Hermitian H_{eff}. This procedure is described in detail in Paper 4. Attempts at creating a three-body effective interaction have also been undertaken, using the same approach (Navrátil and Ormand 2003).

Let us give a general idea of the procedure. Formally, assume that $H = H^{(2)}$ for the two-body problem has been solved exactly, giving eigenvectors $|\Psi_k^{(2)}\rangle$ and eigenvalues $E_k^{(2)}$. By computing the two-body effective Hamiltonian in second quantization we obtain

$$H_{\text{eff}}^{(2)} = P^{(2)} \left[\sum_\alpha \epsilon_\alpha c_\alpha^\dagger c_\alpha + \frac{1}{2} \sum_{\alpha\beta\gamma\delta} \tilde{u}_{\gamma\delta}^{\alpha\beta} c_\alpha^\dagger c_\beta^\dagger c_\delta c_\gamma \right] P^{(2)},$$

where $P^{(2)}$ projects onto the two-body model space. The effective interaction matrix elements $\tilde{u}_{\gamma\delta}^{\alpha\beta}$ are then inserted into $H_{\text{eff}}^{(N)}$, which *in general is an N-body operator*, viz,

$$\begin{aligned} H_{\text{eff}}^{(N)} &= P^{(N)} \left[\sum_\alpha \epsilon_\alpha c_\alpha^\dagger c_\alpha + \frac{1}{N!} \sum_{\alpha_1\cdots\alpha_N} \sum_{\beta_1\cdots\beta_N} v_{\beta_1\cdots\beta_N}^{\alpha_1\cdots\alpha_N} c_{\alpha_1}^\dagger \cdots c_{\alpha_N}^\dagger c_{\beta_N} \cdots c_{\alpha_1} \right] P^{(N)} \\ &\approx P^{(N)} \left[\sum_\alpha \epsilon_\alpha c_\alpha^\dagger c_\alpha + \frac{1}{2} \sum_{\alpha\beta\gamma\delta} \tilde{u}_{\gamma\delta}^{\alpha\beta} c_\alpha^\dagger c_\beta^\dagger c_\delta c_\gamma \right] P^{(N)}. \end{aligned}$$

This is easily seen to be equivalent to simply replacing the matrix elements $u_{\gamma\delta}^{\alpha\beta}$ in the original Hamiltonian (1.4). It is crucial that the all the orbitals that appear in the space $\mathscr{P}^{(2)}$ also appear in $\mathscr{P}^{(N)}$ in order for this prescription to be well-defined.

In Papers 1, 2 and 4 the application of the two-body effective interaction to quantum dots is discussed. The motivation for this is two-fold: First, we may improve FCI calculations that already consume enormous amounts of CPU time worldwide. Second, the knowledge thereby gained may give a general insight into the behaviour of such effective interactions in an easier way than if we were to study the nuclear Hamiltonian directly.

2.3 SCALING AND ACCURACY

The curse of dimensionality is simply the fact that $\dim(\mathscr{P})$ grows almost exponentially with N. In this section, we study the effects of this on the accuracy and scaling with respect to parallelization of the FCI calculations. Consider the model space $\mathscr{P}'$, in which L single-particle orbitals can be occupied by the N particles without restriction. We assume the worst-case scenario with respect to the symmetries of H, i.e., that there are no observables Ω such that $[H,\Omega] = 0$, and we must include *all* Slater determinants in B' in our FCI calculation. Thus,

$$\dim(\mathscr{P}') = \binom{L}{N}.$$

Using a HO basis in d spatial dimensions and excluding spin, we obtain $L \approx R^d/d!$. To see this, consider the single-particle basis functions $\phi_\alpha(\vec{r})$ given by tensor products of d standard Hermite functions $\phi_{n_i}(r_i)$. (This gives no loss of generalization.) The energies are $\epsilon_\alpha - d/2 = n_1 + \cdots + n_d$, and the number L of $\phi_\alpha(\vec{r})$ with $\sum_{i=1}^d n_i \leq R$ approximately equals the volume of a d-dimensional hyperpyramid, being $1/d!$'th of the cube with sides R. Thus,

$$\dim(\mathscr{P}') \approx \frac{L^N}{N!} \approx \frac{1}{d!^N N!} R^{Nd}. \tag{2.3}$$

For the model space $\mathscr{P}$ the growth is similar. The spinless model space is characterized by those Slater determinants for which

$$\sum_{i=1}^N \epsilon_{\alpha_i} - \frac{Nd}{2} = \sum_{i=1}^N \sum_{k=1}^d n_{i,k} \leq R.$$

This time, the hyperpyramid is in Nd dimensions, so that the number of possibilites is approximately $R^{Nd}/(Nd)!$. We obtain an additional factor $1/N!$ due to the permutation symmetry of the Slater determinants. Hence,

$$\dim(\mathscr{P}) \approx \frac{1}{(Nd)!N!} R^{Nd}. \tag{2.4}$$

Let us consider, for simplicity, the problem of storing a single vector on a supercomputer cluster with n_{cpu} nodes, each having the capability of storing M_{cpu} floating point numbers. In a real setting, we need to store several vectors and maybe the Hamiltonian matrix, which has *at least* $\sim \dim(\mathscr{P})$ nonzero entries. Therefore, we set

$$n_{\text{cpu}} M_{\text{cpu}} = \dim(\mathscr{P}),$$

which is a conservative estimate on the requirements of the supercomputer. Using Eqns. (2.3) and (2.4), the largest model space parameter R that the supercomputer can handle becomes

$$R \approx (M_{\text{cpu}} n_{\text{cpu}} A)^{1/Nd},$$

where $A = d!^N N!$ for the model space $\mathscr{P}'$, and $A = (Nd)!N!$ for $\mathscr{P}$, respectively. Considering the estimate (2.2) for the error ΔE in a non-degenerate eigenvalue, we assume

$$\Delta E \approx C R^{-\alpha}, \quad \alpha > 0.$$

The error in the FCI calculation on the supercomputer becomes, roughly,

$$\Delta E \approx C (M_{\text{cpu}} n_{\text{cpu}} A)^{-\alpha/Nd}$$

If we compare the performance with $n_{\text{cpu}} = 1$, i.e., a single desktop computer, the error is improved by a factor

$$n_{\text{cpu}}^{-\alpha/Nd},$$

a very small number for interesting computations. For example, halving the error requires $n_{\text{cpu}}^{1/2} = 2^{Nd/\alpha}$ nodes. In Paper 2 we see that $\alpha \approx 1.4$ for the ground state of $N = 5$ particles in $d = 2$ dimensions, which requires about

$$n_{\text{cpu}}^{\frac{1}{2}} = 2^{10/1.5} \approx 100 \text{ nodes}$$

to halve the error. Halving the error again would need $\sim 10,000$ nodes. For $N = 4$ particles, $\alpha \approx 1.4$, giving

$$n_{\text{cpu}}^{\frac{1}{2}} = 2^{8/1.4} \approx 50 \text{ nodes},$$

which is still very large for halving the error, requiring about $2,500$ nodes to halve the error again.

These considerations lend support to the idea that running FCI codes in parallel is not that useful. The combination of slow convergence with respect to R and the curse of dimensionality, leads to a very small benefit from parallelization. On the other hand, if one utilizes the effective interaction, the convergence rate is improved to $\alpha \approx 3.8$ for $N = 5$. Then, we would require only $n_{\text{cpu}} \approx 6$ nodes to halve the error.

For $N = 4$, $\alpha \approx 4.6$, requiring $n_{\text{cpu}} \approx 3$ nodes. It also seems, that the constant C becomes smaller when using the effective interaction, improving the error even more.

In conclusion, using a two-body effective interaction – which will *not* make the scheme more complicated – will improve the accuracy of parallel quantum dot calculations drastically. Even a single desktop computer with effective interactions will rival parallel implementations that use the bare Coulomb interaction.

2.4 HARTREE-FOCK METHOD

The exact eigenfunction $\Psi_k(x_1, x_2, \cdots, x_N) \in \mathscr{H}_N$ of H is, on average, extremely complicated, as a function of N electron coordinates. Even if the basis functions used for $\mathscr{H}_N$ are Slater determinants, which are fairly simple to visualize, linear combinations of such are not. The function $|\Psi_k\rangle$ would be a Slater determinant only if the interactions were absent. Since in this case the electrons are independent, we say that their motion is uncorrelated, even though a degree of statistical correlation is present due to anti-symmetry. The Coulomb interaction introduces strong correlations, so that the probability of locating a particle at, say $\vec{r}$, depends strongly on the whereabouts of the others.

With these considerations at hand, it is natural to try and find a Hamiltonian describing electrons that move independently without interacting. We therefore consider the interaction as a perturbation and seek a modified single-particle potential $\tilde{V}(\vec{r})$ such that the corresponding ground state Slater determinant $|\Phi^{\text{HF}}\rangle$ has a minimum variational energy $E[\Phi^{\text{HF}}]$, i.e.,

$$|\Phi^{\text{HF}}\rangle := \underset{|\Phi\rangle \in \mathscr{S}}{\operatorname{argmin}} \frac{\langle \Phi | H | \Phi \rangle}{\langle \Phi | \Phi \rangle}, \tag{2.5}$$

as discussed in Section 1.6. Here $\mathscr{S}$ consists of all N-electron functions that can be written as

Slater determinants, with arbitrary orthonormal single-particle functions. The solution $|\Phi_{\rm HF}\rangle$ to this problem is then the optimal independent particle (i.e., uncorrelated) picture of the interacting system. This is the Hartree-Fock method, and it is called a *mean-field* method, since the interaction is replaced by an "average" particle-independent potential, in a very specific sense.

Let $u(i,j) = u(x_i, x_j) = \lambda / r_{ij}$ be the interaction between particles i and j. The Hamiltonian (1.2), where we now replace the harmonic potential with a more general $V(\vec{r})$, can then be written

$$\begin{aligned} H &= \sum_{i=1}^{N} h(i) + \sum_{i<j} u(i,j) \\ &= \left[\sum_{i=1}^{N} h(i) + f(i) \right] + \left[\sum_{i<j}^{N} u(i,j) - \sum_{i=1}^{N} f(i), \right] \end{aligned}$$

where

$$f(i) := \tilde{V}(\vec{r}_i) - V(\vec{r}_i)$$

is called the *fluctuation potential*, and is the modification of $V(\vec{r}_i)$ needed to obtain the Hartree-Fock single-particle potential $\tilde{V}$. Equation (2.5) leads to a coupled non-linear set of equations called the Hartree-Fock equations. It has the form of a non-linear eigenvalue problem for the eigenfunctions $\psi_\alpha(x)$ of $h+f$ with corresponding eigenvalues ϵ_α, and reads

$$\left[h + \int \rho(y,y) u(x,y)\, \mathrm{d}y \right] \psi_\alpha(x) - \int \rho(x,y) u(x,y) \psi_\alpha(y)\, \mathrm{d}y = \epsilon_\alpha \psi_\alpha(x), \tag{2.6}$$

where

$$\rho(x,y) := \sum_{\alpha=1}^{N} \overline{\psi_\alpha(x)} \psi_\alpha(y).$$

The action of $f = f(\psi_1, \cdots, \psi_N)$ on an arbitrary $\phi \in \mathscr{H}_1$ depends on the unknown single-particle functions ψ_α, viz,

$$f\phi(x) = \left[\int \rho(y,y) u(x,y)\, \mathrm{d}y \right] \phi(x) - \int \rho(x,y) u(x,y) \phi(y)\, \mathrm{d}y,$$

where the last term, called the exchange term, is seen to be *non-local*, in contrast to ordinary potential function operators.

The Hartree-Fock solution is the Slater determinant constructed from the N first $\psi_\alpha(x)$, viz,

$$|\Phi^{\rm HF}\rangle = b_1^\dagger b_2^\dagger \cdots b_N^\dagger |-\rangle,$$

where $b_\alpha^\dagger$ creates a particle in the single-particle orbital $\psi_\alpha(x)$. The Hartree-Fock energy $E^{\rm HF} = E[\Phi^{\rm HF}]$ can be shown to be (Gross et al. 1991)

$$E^{\rm HF} = [\Phi_{\rm HF}] = \frac{1}{2} \sum_{i=1}^{N} \epsilon_i + \langle \psi_i | h | \psi_i \rangle.$$

To solve the Hartree-Fock equations (2.6), one usually uses fix-point iterations, starting with the original single-particle functions $\phi_\alpha(x)$. Thus, one iterates

$$\left[h + f(\psi_1^{(k)}, \cdots \psi_N^{(k)})\right] \psi_\alpha^{(k+1)}(x) = \epsilon_\alpha^{(k+1)} \psi_\alpha(x)^{(k+1)},$$

with the initial condition $\psi_\alpha^{(0)} = \phi_\alpha$. On each step, an infinite set of eigenfunctions are found (in principle), and the lowest-lying are chosen for the next iteration.

The Hartree-Fock orbitals $\psi_\alpha(x)$ are called *canonical*, because they constitute the best possible non-correlated single-particle basis functions, in contrast to the original $\phi_\alpha(x)$, which were arbitrary. It is common practice in for example quantum chemistry, to do FCI calculations in the Slater determinant basis generated by the Hartree-Fock orbitals $\psi_\alpha(x)$.

For a detailed account of the properties of the Hartree-Fock method, such as convergence issues, see Schneider (2006) and Lions (1987). For an application to parabolic quantum dots, see Waltersson and Lindroth (2007).

2.5 COUPLED CLUSTER METHOD

The coupled-cluster method (CC) is today probably the most powerful *ab initio* method to obtain ground state eigenvalues of many-body problems. It was introduced in the context of nuclear physics by Coester and Kümmel around 1960. While it gained little attention in nuclear physics communities, with only sporadic applications before the 1990's, quantum chemists took on to the idea and developed the method further (Kümmel 1991).

Coupled cluster calculations have been very successful for molecular problems (Bartlett and Musiał 2007), and in recent years, nuclear physicists have been further developing and applying the CC method to nuclei hitherto out of reach of FCI (Dean and Hjorth-Jensen 2004). To name an example, Hagen et al. (2008) have computed the ground state energy of ^{48}Ca (an $N = 48$ problem in $d = 3$ dimensions) to about ten percent accuracy. Keeping in mind that if the corresponding calculation should be done with FCI we would have $\dim(\mathscr{P}) \approx 10^{71}$, it is clear that such CC calculations are a huge step forward, and that FCI is hard pressed to compete with the results, see for example the heated correspondence between Dean et al. (2008) and Roth and Navrátil (2007, 2008). For a detailed analysis of the CC method, see the technical report by Schneider (2006).

Recently, the singles and doubles CC method has been used on quantum dots, see for examlpe Heidari et al. (2007). We mention here also the so-called equation of motion CC method (Stanton and Bartlett 1993), which is able to extract other eigenfunctions and eigenvalues than the ground state. Henderson et al. (2003) have used it on parabolic quantum dots.

In this section we consider a simplified description of the CC method, outlining the features more than giving calculational recipes.

Consider an N-body problem, and let the model space $\mathscr{P}'$ be given, with truncation parameter R. In this section, we shall for simplicity assume that the Hamiltonian is *defined* by it's projection onto $\mathscr{P}'$, i.e., that FCI is *defined* to be exact. In other words, we work in a finite-dimensional Hilbert space.

Let $|\Phi_0\rangle \in B'$ be an arbitrary Slater determinant in the basis for $\mathscr{P}'$, say, the (unperturbed)

ground state, viz,

$$|\Phi_0\rangle = c_1^\dagger c_1^\dagger \cdots c_N^\dagger |-\rangle.$$

By reordering the orbitals $\phi_\alpha(x)$, this form is always possible. Let us define an *excitation operator* T_k by

$$T_k := \frac{1}{k!^2} \sum_{a_1,\cdots,a_k=1}^{N} \sum_{\beta_1,\cdots,\beta_k=N+1}^{L} t_{a_1,\cdots,a_k}^{\beta_1,\cdots,\beta_k} c_{\beta_1}^\dagger \cdots c_{\beta_k}^\dagger c_{a_k} \cdots c_{a_1}, \tag{2.7}$$

parametrized by excitation coefficients (usually called amplitudes) $t_{a_1,\cdots,a_k}^{\beta_1,\cdots,\beta_k}$, where the Latin indices take values $a_i \leq N$ only, and the Greek indices take values $\beta_i > N$ only. Each term, when applied to $|\Phi_0\rangle$, moves k particles "up" from the N first orbitals into the remaining $L-N$. Notice, that *all* $|\Phi\rangle \in B'$ can be written on the form $T_k|\Phi_0\rangle$, for suitable excitation amplitudes, see Eqn. (2.9) below.

It can now be shown, that any $|\Psi\rangle \in \mathscr{P}'$ with $\langle\Phi_0|\Psi\rangle = 1$ can be written

$$|\Psi\rangle = e^T|\Phi_0\rangle, \quad \text{where} \quad T = \sum_{k=1}^{N} T_k.$$

In particular, assuming that we can normalize the exact ground state $|\Psi_0\rangle$ (identical to the FCI ground state in the model space $\mathscr{P}'$) so that $\langle\Phi_0|\Psi_0\rangle = 1$, we have

$$E_0 = \langle\Phi_0|e^{-T}He^T|\Phi_0\rangle = \langle\Phi_0|\tilde{H}|\Phi_0\rangle.$$

Using the Baker-Campbell-Hausdorff formula, we obtain the well-known expansion

$$\tilde{H} = H + [H,T] + \frac{1}{2!}[[H,T],T] + \frac{1}{3!}[[[H,T],T],T] + \frac{1}{4!}[[[[H,T],T],T],T] + \cdots$$

Using the fact that the Hamiltonian (1.4) contains only up to two-body terms, it is straightforward to show that all the terms not listed in this expansion *vanish identically*. We obtain the following equations:

$$\begin{aligned} E_0 &= \langle\Phi_0|\tilde{H}|\Phi_0\rangle = \langle\Phi_0|H(1+T_2+\frac{1}{2}T_1^2)|\Phi_0\rangle \\ 0 &= \langle\Phi|e^{-T}He^T|\Phi_0\rangle, \quad \forall\Phi \in B', \Phi \neq \Phi_0. \end{aligned} \tag{2.8}$$

It is interesting to note, that E_0 only depends on T_1 and T_2, while $|\Psi_0\rangle$ depends on all the T_k. In Eqn (2.8), $|\Phi\rangle$ can be written on the form

$$|\Phi\rangle = c_{\beta_1}^\dagger c_{\beta_2}^\dagger \cdots c_{\beta_k}^\dagger c_{a_k} \cdots c_{a_2} c_{a_1} |\Phi_0\rangle. \tag{2.9}$$

Inserting this into Eqn. (2.8), one obtains a set of nonlinear equations for the excitation amplitudes t_a^β, $t_{a_1,a_2}^{\beta_1,\beta_2}$, etc, which can be solved by iterative techniques. We will not list the equations here, as they are quite complicated.

We have not yet introduced any approximation, and the number of unknowns is presently

$\dim(\mathscr{P}')$, so that the problem is, in fact, no simpler than the FCI problem. We therefore truncate the expansion T at, say, two-particle excitations, i.e.,

$$T \approx T_1 + T_2,$$

and solve the resulting nonlinear equations. This is referred to as the "singles and doubles coupled cluster method" (CCSD). By truncating at T_3, we obtain the "singles, doubles and triplets" method (CCSDT), and so on, producing successively more complicated non-linear equations.

An important feature of the CC method is that it is not variational. The ground state energy computed is not *a priori* an upper bound on the ground state energy. On the other hand, it scales much better with increasing model space size than does the FCI method.

3 Introduction to the papers

3.1 A READER'S GUIDE

There are four papers in this thesis. At the time of writing, Papers 1 and 3 have been published, while Papers 2 and 4 is awaiting editorial decisions. They are presented in chronological order with respect to submission to the journals.

Paper 1

Paper 1, written in collaboration with Morten Hjorth-Jensen and Halvor Møll Nilsen, is a study of one-dimensional quantum dots, focusing on the two-particle case. It may be considered as a preliminary study of the general case, which is the topic for Paper 2. The one-dimensional two-particle parabolic quantum dot is reduced to a one-dimensional problem by applying centre of mass-coordinates, in which only the relative coordinate problem is non-trivial, having Hamiltonian

$$H_{\text{rel}} = -\frac{1}{2}\frac{\partial^2}{\partial x^2} + \frac{1}{2}x^2 + U(\sqrt{2}|x|),$$

where U is the interaction potential. The effects of the trap alone was studied by replacing U with some other potential $v(x)$, producing the one-body Hamiltonian. Arguments along the line of Section 1.4 are then used to analyze and discuss the numerical properties of the full configuration interaction (FCI) method in this particular case.

Paper 2

After finishing Paper 1 (which admittedly bears marks of being my first publication), I tried to handle the general case: N electrons in d dimensions. In the end it sorted out, but not exactly as I thought, however. The keen reader may have noticed an error in Paper 1 concerning the decay of the coefficients $|c_n|$ in Sec. III C: $x^k\psi(x) \in L^2(\mathbb{R})$ and $\partial_x^k\psi(x) \in L^2(\mathbb{R})$ are *not* sufficient conditions for $\psi(x) \in H^k(\mathbb{R})$ – the correct condition is $x^j\partial_x^{k-j}\psi(x) \in L^2(\mathbb{R})$ for all $0 \leq j \leq k$. However, as shown in Paper 2 and indicated in Section 1.4, this has no bearing on the result when we consider exponentially decaying functions $\psi(x)$.

Paper 2 develops a series of results concerning approximation properties of n-dimensional Hermite functions, defined as tensor products of standard one-dimensional Hermite functions. These show that for an FCI calculation where the exact wavefunction is known to be non-

smooth, the convergence will be at most algebraic, cf. Eqn. (2.2). This is demonstrated with numerical simulations. It is also demonstrated numerically that the different eigenfunctions $|\Psi_k\rangle$ have differing smoothness properties, in accordance with the results mentioned in Section 1.5. By applying a two-electron effective interaction, the convergence with respect to basis size is seen to accelerate drastically. This motivates further analysis of the effective interactions themselves.

Paper 3

Paper 3 deals with effective Hamiltonians at the stage before we extract an effective interaction. It gives a description of the common effective Hamiltonians which I have termed "geometric" due to its extensive use of the characterization of pairs of linear subspaces by so-called canonical angles and vectors. The canonical angles generalizes angles between vectors to angles between general subspaces. The singular value decomposition is essential here. I also discuss the consequences of symmetries in the system (i.e., observables S such that $[H,S]=0$), and demonstrate that it is important to reflect such symmetries in the model space. That is, if angular momentum is conserved, viz, $[H,L_z]=0$, then the model space should be rotationally symmetric, viz, $[P,L_z]=0$.

I continue to propose a new way to compute the effective interaction in the sub-cluster case, such as employed in all the other papers. The standard method is somewhat more complicated (Navrátil, Kamuntavicius, and Barrett 2000).

Paper 4

Paper 4 implements the effective two-body interaction and describes it in detail for the Coulomb case. The algorithm is also used in Papers 1 and 2, but I felt there was no room and that it was inappropriate to spend much space on it there and then. Also, my own knowledge of the method had increased since Paper 1 was written, so that a relatively succinct and clear description could be given.

The main contribution of Paper 4 is however an open source implementation of the FCI method with effective two-body interactions called OpenFCI. The idea is that an openly available code released under the Gnu GPL and documented in a scientific journal will spur more activity among students and researchers new to the field. OpenFCI is also well-suited as starting point for implementations of Hartree-Fock, coupled cluster methods and so on.

3.2 DISCUSSION AND OUTLOOK

Much of this work has been devoted to and motivated by the convergence properties of the FCI method with respect to the basis size parameter R. Let us summarize and discuss some of the findings.

Properties of the harmonic oscillator basis

The harmonic oscillator (HO) basis is on one side very well suited for many-body calculations, since it easily allows for manipulation of operators using centre-of-mass and relative coordinates. Furthermore, HO basis functions easily accommodate various common symmetries, such as total angular momentum and reflection symmetries. On the other hand, it has problems resolving the non-smooth wavefunctions that invariably appear as eigenfunctions of the quantum dot Hamiltonian. This has the important consequence that one will *never* achieve better convergence than algebraic convergence, i.e., of $R^{-\alpha}$-type, when using FCI.

The FCI convergence estimates have obvious consequences for the coupled cluster (CC) class of methods, and the approximation estimates for the HO basis functions can prove to be useful for analyzing this class of methods from first principles as well.

Other methods in other areas of research may benefit from the theory as well, such as approximating general partial differential equations using pseudospectral methods (Boyd 2001).

Properties of the effective two-body interaction

In Papers 1 and 2, it was demonstrated that the effective two-body interaction improves the convergence of the FCI calculations by up to several orders of magnitude, for example for systems containing $N = 5$ electrons. For $N > 6$, it is difficult to get good results using FCI anyway, because of the extreme increase in basis size. However, what if the effective interaction could be utilized in, say, a coupled cluster calculation? We can assume that the error in a coupled cluster with singles and doubles calculation (cf. Section 2.5) is comparable to that of the FCI calculation. Can the error be reduced by the same order of magnitude in the CC case as in the FCI case? To me, it seems very likely. Studies in this direction are obvious candidates for future research.

On the other hand, I suspect that the improvement the two-body effective interaction offers would decrease with increasing N. Studies in this direction would be feasible if the effective interaction-approach to coupled cluster calculations works. This would be highly interesting – both with respect to reaching higher N and understanding the effective interactions.

We have not studied the properties of the *wavefunctions* when using effective two-body interactions. It is well-known that even if an effective Hamiltonian may reproduce nuclear spectra, the transition probabilities may be completely wrong. Thus, a study of the error in the wavefunctions using different norms should be undertaken.

Consequences for other physical systems

Can we extrapolate the results obtained for quantum dots to other systems, such as the no-core nuclear shell model? How closely related are the different models? The no-core shell model is formally equivalent to the parabolic quantum dot model, except for the complications mentioned in Section 2.2 concerning a lack of natural centre of the system and the unknown interaction properties. The spectrum of the nucleus is *not* purely discrete, so some work must be done in order to apply what we have learned. It should be evident, however, that an interesting approach to nuclear properties may come from applying the approximation properties of Hermite functions in the other direction, so to speak. By studying the numerical eigenfunctions, one may

extract information about the system. For example, if a certain $R^{-\alpha}$-behaviour is found in the FCI coefficients, conclusions about the cusps and similar in the wavefunctions may be drawn.

Properties of many-body effective interactions

In the nuclear physics community, the need for more accurate effective interactions, i.e., three-body interactions, is realized. Moreover, there are *fundamental* three-body forces that need to be accounted for. A study of such three-body effective interactions in the quantum dot model may give significant insight into the properties of such.

The reason why the effective two-body interaction can be computed unambiguously *in the Coulomb case*, is that the two-body central force problem is classically integrable. (The nuclear forces have non-central terms, so conclusions for nuclei cannot be drawn in this way.) By transforming to the centre-of-mass frame and separating out angular momentum, we obtain a one-dimensional radial equation, which has no degeneracies, as discussed in Paper 4. In particular, *all* eigenvalues of the two-body quantum dot are complex analytic functions of the interaction strength λ. This rules out the existence of intruder states in this case.

If we move to the three-body problem, however, it is *almost certainly* classically chaotic, a fact that can be assessed by numerical simulations (Ott 1993). Is is well-known that the helium atom, for example, exhibits classically chaotic motion. The attempt at creating a three-body effective interaction will then necessarily have to deal with this fact, since in classically non-integrable systems *there will be intruder states*. Perturbation theory is therefore likely to fail, and selecting the "proper" eigenpairs for an effective Hamiltonian is not trivial.

Research along this direction will almost certainly prove very interesting.

Do we need the extra convergence?

This thesis has been about striving for greater accuracy in eigenvalues. But is it really necessary? Can we not be happy, so to speak, with what we've got? After all, the quantum dot model is only a model, and a rough one as well.

On the other hand, in future technologies, being able to successfully predict the outcome of an experiment from first principles is crucial. Even if our models are inaccurate, future models based on the same ideas may be much better. To be able to simulate a system under the influence of a time-dependent perturbation, such as a laser, also requires highly accurate eigenvalues in order to work, as the the time limit of accurate simulations is directly proportional to the largest energy difference error.

Additionally, there is the desire to find out all there is to know about a given model. Good and well-understood numerical methods are then essential. The impact on the amassed knowledge on fundamental quantum systems when good numerical tools are available should not be underestimated. Thus, we should strive for faster, more accurate, and economical methods.

References

Babuska, I. and J. Osborn (1996). *Handbook of Numerical Analysis: Finite Element Methods*, Volume 2. North-Holland.

Ballentine, L. (1998). *Quantum Mechanics: A Modern Development*. World Scientific.

Bartlett, R. J. and M. Musiał (2007). Coupled-cluster theory in quantum chemistry. *Reviews of Modern Physics 79*, 291.

Bloch, C. (1958). Sur la théorie des perturbations des états liés. *Nuclear Physics 6*, 329.

Bloch, C. and J. Horowitz (1958). Sur la détermination des premiers états d'un système de fermions dans le cas dégénéré. *Nuclear Physics 8*, 91.

Boyd, J. (2001). *Chebyshev and Fourier Spectral Methods*. Springer.

Brandow, B. (1967). Linked-cluster expansions for the nuclear many-body problem. *Reviews of Modern Physics 39*, 771.

Cerletti, V., W. A. Coish, O. Gywat, and D. Loss (2005). Recipes for spin-based quantum computing. *Nanotechnology 16*, R27.

Dean, D., T. Engeland, M. Hjorth-Jensen, M. Kartamyshev, and E. Osnes (2004). Effective interactions and the nuclear shell-model. *Progress in Particle and Nuclear Physics 53*, 419.

Dean, D. J., G. Hagen, M. Hjorth-Jensen, T. Papenbrock, and A. Schwenk (2008). Comment on "ab initio study of ^{40}Ca with an importance-truncated no-core shell model". *Physical Review Letters 101*, 119201.

Dean, D. J. and M. Hjorth-Jensen (2004, May). Coupled-cluster approach to nuclear physics. *Physical Review C 69*, 054320.

Ellis, P. and E. Osnes (1977). An introductory guide to effective operators in nuclei. *Reviews of Modern Physics 49*, 777.

Evans, L. (1998). *Partial Differential Equations*, Volume 19 of *Graduate Studies in Mathematics*. AMS.

Fitzgerald, R. (2003). An optical probe can map quantum dot wavefunctions. *Physics Today 56*, 14.

Gross, E., E. Runge, and O. Heinonen (1991). *Many-particle theory*. Adam Hilger.

Hagen, G., T. Papenbrock, D. J. Dean, and M. Hjorth-Jensen (2008). Medium-mass nuclei from chiral nucleon-nucleon interactions. *Physical Review Letters 101*, 092502.

Heidari, I., S. Pal, B. S. Pujari, and D. G. Kanhere (2007). Electronic structure of spherical quantum dots using coupled cluster method. *Journal of Chemical Physics 127*, 114708.

Henderson, T., K. Runge, and R. Bartlett (2003, JAN 15). Excited states in artificial atoms via equation-of-motion coupled cluster theory. *Physical Review B 67*, 045320.

Hille, E. (1939). Contributions to the theory of Hermitian series. *Duke Mathematical Journal 5*, 875.

Hislop, P. and I. Sigal (1996). *Introduction to Spectral Theory With Applications to Schrödinger Operators*, Volume 113 of *Applied Mathematical Sciences*. Springer.

Hjorth-Jensen, M., T. Kuo, and E. Osnes (1995). Realistic effective interactions for nuclear systems. *Physics Reports 261*, 125.

Hoffmann-Ostenhof, M., T. Hoffmann-Ostenhof, and H. Stremnitzer (1994). Local properties of coulombic wave functions. *Communications in Mathematical Physics 163*, 185.

Ishii, N., S. Aoki, and T. Hatsuda (2007). Nuclear force from lattice qcd. *Physical Review Letters 99*, 022001.

Klein, D. (1974). Degenerate perturbation theory. *Journal of Chemical Physics 61*, 786.

Kümmel, H. (1991, March). Origins of the coupled cluster method. *Theoretical Chemistry Accounts: Theory, Computation, and Modeling 80*, 81.

Lindgren, I. and J. Morrison (1982). *Atomic Many-Body Theory*. Springer.

Lions, P.-L. (1987). Solutions of Hartree-Fock Equations for Coulomb Systems. *Communications in Mathematical Physics 109*, 33.

Loss, D. and D. P. DiVincenzo (1998, Jan). Quantum computation with quantum dots. *Physical Review A 57*, 120.

Navrátil, P., G. P. Kamuntavicius, and B. R. Barrett (2000). Few-nucleon systems in a translationally invariant harmonic oscillator basis. *Physical Review C 61*, 044001.

Navrátil, P. and W. E. Ormand (2003, Sep). Ab initio shell model with a genuine three-nucleon force for the p-shell nuclei. *Physical Review C 68*, 034305.

Navrátil, P., J. Vary, and B. Barrett (2000). Large-basis ab initio no-core shell model and its application to 12C. *Physical Review C 62*, 054311.

Ott, E. (1993). *Chaos in dynamical systems*. Cambridge.

Raimes, S. (1972). *Many-Electron Theory*. North-Holland.

Reed, M. (1993). Quantum Dots. *Scientific American 268*, 118.

Reimann, S. M. and M. Manninen (2002). Electronic structure of quantum dots. *Reviews of Modern Physics 74*, 1283.

Roth, R. and P. Navrátil (2007). Ab initio study of ^{40}Ca with an importance-truncated no-core shell model. *Physical Review Letters 99*, 092501.

Roth, R. and P. Navrátil (2008). *Physical Review Letters 101*, 119202.

Schaefer, P. (1974). Analytic Properties of the Effective Interaction in Nuclei Investigated on Simple Models. *Annals of Physics 87*, 375.

Schneider, R. (2006). Analysis of the Projected Coupled Cluster Method in Electronic Structure Calculations. Technical report, Technische Universität Berlin. Part of DFG (Deutsche Forschunggemeinschaft) Priority Program 1145.

Schucan, T. and H. Weidenmüller (1973). Perturbation Theory for the Effective Interaction in Nuclei. *Annals of Physics 76*, 483.

Shavitt, I. and L. T. Redmon (1980). Quasidegenerate perturbation theories. a canonical van vleck formalism and its relationship to other approaches. *Journal of Chemical Physics 73*, 5711.

Stanton, J. F. and R. J. Bartlett (1993). The equation of motion coupled-cluster method. A systematic biorthogonal approach to molecular excitation energies, transition probabilities, and excited state properties. *Journal of Chemical Physics 98*, 7029.

Tarucha, S., D. Austing, T. Honda, R. van der Hage, and L. Kouwenhoven (1996). Shell filling and spin effects in a few electron quantum dot. *Physical Review Letters 77*, 3613.

Van Vleck, J. (1929). On sigma-type doubling and electron spin in the spectra of diatomic molecules. *Physical Review 33*, 467.

Waltersson, E. and E. Lindroth (2007). Many-body perturbation theory calculations on circular quantum dots. *Physical Review B 76*, 045314.

Weidmann, J. (1980). *Linear Operators in Hilbert Spaces*. New York, Heidelberg, Berlin: Springer-Verlag.

Weiss, S., M. Thorwart, and R. Egger (2006). Charge qubit entanglement in double quantum dots. *Europhysics Letters 76*, 905.

Zheng, D. C., B. R. Barrett, L. Jaqua, J. P. Vary, and R. J. McCarthy (1993, Sep). Microscopic calculations of the spectra of light nuclei. *Physical Review C 48*, 1083.

Part II : Papers

1 Effective interactions, large-scale diagonalization, and one-dimensional quantum dots

This paper appeared in volume 76 of Physical Review B, 2007.

Effective interactions, large-scale diagonalization, and one-dimensional quantum dots

Simen Kvaal,[1,*] Morten Hjorth-Jensen,[2,1] and Halvor Møll Nilsen[1]
[1]*Centre of Mathematics for Applications, University of Oslo, N-0316 Oslo, Norway*
[2]*Department of Physics, University of Oslo, N-0316 Oslo, Norway*
(Received 18 April 2007; published 17 August 2007)

The widely used large-scale diagonalization method using harmonic oscillator basis functions (an instance of the Rayleigh-Ritz method [S. Gould, Variational Methods for Eigenvalue Problems: An Introduction to the Methods of Rayleigh, Ritz, Weinstein, and Aronszajn (Dover, New York, 1995)], also called a spectral method, configuration-interaction method, or "exact diagonalization" method) is systematically analyzed using results for the convergence of Hermite function series. We apply this theory to a Hamiltonian for a one-dimensional model of a quantum dot. The method is shown to converge slowly, and the nonsmooth character of the interaction potential is identified as the main problem with the chosen basis, while, on the other hand, its important advantages are pointed out. An effective interaction obtained by a similarity transformation is proposed for improving the convergence of the diagonalization scheme, and numerical experiments are performed to demonstrate the improvement. Generalizations to more particles and dimensions are discussed.

DOI: 10.1103/PhysRevB.76.085421 PACS number(s): 73.21.La, 71.15.−m, 31.15.Pf

I. INTRODUCTION

Large-scale diagonalization is widely used in many areas of physics, from quantum chemistry[1] to nuclear physics.[2] It is also routinely used to obtain spectra of model quantum dots, see, for example, Refs. 3–19. The method is based on a projection of the model Hamiltonian onto a finite-dimensional subspace of the many-body Hilbert space in question, hence the method is an instance of the Rayleigh-Ritz method.[20] Usually, one takes the stance that the many-body Hamiltonian is composed of two parts $\hat{H}_0$ and $\hat{H}_1$, treating the latter as a perturbation of the former, whose eigenfunctions are assumed to be a basis for the Hilbert space. This leads to a matrix diagonalization problem, hence the name of the method. As $\hat{H}_1$ often contains the interaction terms of the model, "perturbing" the electronic configuration states of $\hat{H}_0$, the method is also called the configuration-interaction method. In the limit of an infinite basis, the method is *in principle* exact, and for this reason, it is also called "exact diagonalization." Usually, however, this method is far from exact, as $\hat{H}_1$ is rarely a small perturbation (in a sense to be specified in Sec. III E), while limited computing resources yield a tight bound on the number of degrees of freedom available per particle.

In this work, we provide mathematical convergence criteria for configuration-interaction calculations. More specifically, we address this problem in the case where $\hat{H}_0$ is a harmonic oscillator (or HO for short), concentrating on a simple one-dimensional problem. A common model for a quantum dot is, indeed, a perturbed harmonic oscillator, and using HO basis functions is also a common approach in other fields of many-body physics and partial differential equations settings in general, as it is also known as the Hermite spectral method.[21] When we, in the following, refer to the configuration-interaction method, or CI for short, it is assumed that a HO basis is used.

Studying a one-dimensional problem may seem unduly restrictive, but will, in fact, enable us to treat realistic multi-dimensional problems as well due to the symmetries of the harmonic oscillator. Moreover, we choose a worst-case scenario, in which the interaction potential decays very slowly. We argue that the nature of the perturbation $\hat{H}_1$, i.e., the nonsmooth character of the Coulomb potential or the trap potential, hampers the convergence properties of the method. To circumvent this problem and improve the convergence rate, we construct an effective two-body interaction via a similarity transformation. This approach, also using a HO basis, is routinely used in nuclear physics,[22–24] where the interactions are of a completely different nature.

The effective interaction is defined for a smaller space than the original Hilbert space, but it reproduces exactly the lowest-lying eigenvalues of the full Hamiltonian. This can be accomplished by a technique introduced by Suzuki and Okamoto.[25–28] Approaches based on this philosophy for deriving effective interactions have been used with great success in the nuclear many-body problem.[22–24] For light nuclei, it provides benchmark calculations of the same quality as Green's function Monte Carlo methods or other *ab initio* methods. See, for example, Ref. 29 for an extensive comparison of different methods for computing properties of the nucleus ^{4}He. It was also used in a limited comparative study of large-scale diagonalization techniques and stochastic variational methods applied to quantum dots.[30]

We demonstrate that this approach to the CI method for quantum dots yields a considerable improvement to the convergence rate. This has important consequences for studies of the time development of quantum dots with two or more electrons, as reliable calculations of the eigenstates are crucial ingredients in studies of coherence. This is of particular importance in connection with the construction of quantum gates based on quantum dots.[31] Furthermore, the introduction of an effective interaction allows for studies of many-electron quantum dots via other many-body methods like resummation schemes such as various coupled cluster theories as well. As the effective interaction is defined only within the model space, systematic and controlled convergence studies of these methods in terms of the size of this space are possible.

The article is organized as follows: In Sec. II, the model quantum dot Hamiltonian is discussed. In Sec. III, we discuss the CI method and its numerical properties. Central to this section are results concerning the convergence of Hermite function series.[32,33] We also demonstrate the results with some numerical experiments.

In Sec. IV, we discuss the similarity transformation technique of Suzuki and Okamoto [25–28] and replace the Coulomb term in our CI calculations with this effective interaction. We then perform numerical experiments with the modified method and discuss the results.

We conclude the article with generalizations to more particles in higher dimensions and possible important applications of the modified method in Sec. V.

II. ONE-DIMENSIONAL QUANTUM DOTS

A widely used model for a quantum dot containing N charged fermions is a perturbed harmonic oscillator with Hamiltonian

$$\hat{H} = \sum_{j=1}^{N} \left[-\frac{1}{2}\nabla_j^2 + \frac{1}{2}\|\vec{r}_j\|^2 + v(\vec{r}_j) \right] + \sum_{j=1}^{N} \sum_{k=j+1}^{N} U(\|r_j - r_k\|), \tag{1}$$

where $\vec{r}_j \in \mathbb{R}^2$, $j=1,\ldots,N$ are each particle's spatial coordinate, $v(\vec{r})$ is a small modification of the HO potential $\|\vec{r}\|^2/2$, and $U(r)$ is the Coulomb interaction, viz., $U(r)=\lambda/r$, where λ is a constant. Modeling the quantum dot geometry by a perturbed harmonic oscillator is justified by self-consistent calculations,[34–36] and is the stance taken by many other authors using the large-scale diagonalization technique as well.[3–5,8–10,12,14–18] The potential modification $v(\vec{r})$ is chosen to emulate different trap geometries, such as a double well or a flat-bottomed well. For instance, in Ref. 16, a nonsmooth perturbation in two dimensions of the form $v(x,y)=-A|x| - B|y|$ is used, creating four coupled wells. In this article, we use a Gaussian perturbation in one dimension [cf. Eq. (11)].

Electronic structure calculations amount to finding eigenpairs (E,Ψ), e.g., the ground state energy and wave function, such that

$$\hat{H}\Psi = E\Psi, \quad \Psi \in \mathcal{H} \quad \text{and } E \in \mathbb{R}.$$

Here, even though the Hamiltonian only contains spatial coordinates, the eigenfunction Ψ is a function of both the spatial coordinates $\vec{r}_k \in \mathbb{R}^2$ and the spin degrees of freedom $\sigma_k \in \{-1/2, +1/2\}$, i.e.,

$$\mathcal{H} = L_2(\mathbb{R}^{2N}) \otimes \mathbb{C}^2.$$

The actual Hilbert space is the space of the *antisymmetric* functions, i.e., functions Ψ for which

$$\Psi(x_{P(1)}, x_{P(2)}, \ldots, x_{P(N)}) = \mathrm{sgn}(P)\Psi(x_1, x_2, \ldots, x_N),$$

for all permutations P of N symbols. Here, $x_k=(\vec{r}_k,\sigma_k)$.

For simplicity, we concentrate on one-dimensional quantum dots. Even though this is not an accurate model for real quantum dots, it offers several conceptual and numerical advantages. Firstly, the symmetries of the harmonic oscillator makes the numerical properties of the configuration-interaction method of this system very similar to a two or even three-dimensional model, as the analysis extends almost directly through tensor products. Secondly, we may investigate many-body effects for moderate particle numbers N while still allowing a sufficient number of HO basis functions for unambiguously addressing accuracy and convergence issues in numerical experiments.

In this article, we further focus on two-particle quantum dots. Incidentally, for the two-particle case, one can show that the Hilbert space of antisymmetric functions is spanned by functions of the form

$$\Psi(\vec{r}_1,\sigma_1,\vec{r}_2,\sigma_2) = \psi(\vec{r}_1,\vec{r}_2)\chi(\sigma_1,\sigma_2),$$

where the spin wave function χ can be taken as symmetric or antisymmetric with respect to particle exchange, leading to an antisymmetric or symmetric spatial wave function ψ, respectively. Inclusion of a magnetic field $\vec{B}$ poses no additional complications,[37] but for simplicity, we presently omit it. Thus, it is sufficient to consider the spatial problem and produce properly symmetrized wave functions.

Due to the peculiarities of the bare Coulomb potential in one dimension,[38,39] we choose a screened approximation $U(x_1-x_2;\lambda,\delta)$ given by

$$U(x;\lambda,\delta) = \frac{\lambda}{|x| + \delta},$$

where λ is the strength of the interaction and $\delta>0$ is a screening parameter which can be interpreted as the width of the wave function orthogonal to the axis of motion. This choice is made since it is nonsmooth, like the bare Coulomb potential in two and three dimensions. The total Hamiltonian then reads

$$\hat{H} = -\frac{1}{2}\left(\frac{\partial^2}{\partial x_1^2} + \frac{\partial^2}{\partial x_2^2}\right) + \frac{1}{2}(x_1^2 + x_2^2) + v(x_1) + v(x_2) + U(x_1 - x_2;\lambda,\delta). \tag{2}$$

Observe that for $U=0$, i.e., $\lambda=0$, the Hamiltonian is separable. The eigenfunctions of $\hat{H}$ (disregarding proper symmetrization due to the Pauli principle) become $\psi_{n_1}(x_1)\psi_{n_2}(x_2)$, where $\psi_n(x)$ are the eigenfunctions of the trap Hamiltonian $\hat{H}_t$ given by

$$\hat{H}_t = -\frac{1}{2}\frac{\partial^2}{\partial x^2} + \frac{1}{2}x^2 + v(x). \tag{3}$$

Similarly, for a vanishing trap modification $v(x)=0$, the Hamiltonian is separable in (normalized) center-of-mass coordinates given by

$$X = \frac{x_1 + x_2}{\sqrt{2}} \quad \text{and} \quad x = \frac{x_1 - x_2}{\sqrt{2}}.$$

Indeed, any orthogonal coordinate change leaves the HO Hamiltonian invariant (see Sec. III), and hence

$$\hat{H} = -\frac{1}{2}\left(\frac{\partial^2}{\partial X^2} + \frac{\partial^2}{\partial x^2}\right) + \frac{1}{2}(X^2 + x^2) + v[(X+x)/\sqrt{2}] + v[(X-x)/\sqrt{2}] + U(\sqrt{2}x;\lambda,\delta).$$

The eigenfunctions become $\phi_n(X)\psi_m(x)$, where $\phi_n(X)$ are the Hermite functions, i.e., the eigenfunctions of the HO Hamiltonian (see Sec. III), and where $\psi_m(x)$ are the eigenfunctions of the interaction Hamiltonian, viz.,

$$\hat{H}_i = -\frac{1}{2}\frac{\partial^2}{\partial x^2} + \frac{1}{2}x^2 + U(\sqrt{2}x;\lambda,\delta). \tag{4}$$

Odd (even) functions $\psi_m(x)$ yield antisymmetric (symmetric) wave functions with respect to particle interchange.

III. CONFIGURATION-INTERACTION METHOD

A. Harmonic oscillator and model spaces

The configuration-interaction method is an instance of the Rayleigh-Ritz method,[20] employing eigenfunctions of the unperturbed HO Hamiltonian as basis for a finite-dimensional Hilbert space $\mathcal{P}$, called the model space, onto which the Hamiltonian (1), or in our simplified case, the Hamiltonian (2), is projected and then diagonalized. As mentioned in Sec. I, this method is, in principle, exact, if the basis is large enough.

We write the N-body Hamiltonian (1) as

$$\hat{H} = \hat{H}_0 + \hat{H}_1,$$

with $\hat{H}_0$ being the HO Hamiltonian, viz.,

$$\hat{H}_0 = -\frac{1}{2}\sum_{j=1}^{N}\nabla_j^2 + \frac{1}{2}\sum_{j=1}^{N}\|\vec{r}_j\|^2,$$

and $\hat{H}_1$ being a perturbation of $\hat{H}_0$, viz.,

$$\hat{H}_1 = \sum_{j=1}^{N} v(\vec{r}_j) + \sum_{j=1}^{N}\sum_{k=j+1}^{N} U(\|r_j - r_k\|).$$

For a simple one-dimensional model of two particles, we obtain

$$\hat{H}_0 = \hat{h}(x_1) + \hat{h}(x_2),$$

where $\hat{h}(x)$ is the well-known one-dimensional harmonic oscillator Hamiltonian, viz.,

$$\hat{h}(x) = -\frac{1}{2}\frac{\partial^2}{\partial x^2} + \frac{1}{2}x^2.$$

Clearly, $\hat{H}_0$ is just a two-dimensional HO Hamiltonian, if we disregard symmetrization due to the Pauli principle. For the perturbation, we have

$$\hat{H}_1 = v(x_1) + v(x_2) + \frac{\lambda}{|x_1 - x_2| + \delta}.$$

In order to do a more general treatment, let us recall some basic facts about the harmonic oscillator.

If we consider a single particle in D-dimensional space, it is clear that the D-dimensional harmonic oscillator Hamiltonian is the sum of one-dimensional HO Hamiltonians for each Euclidean coordinate, viz.,

$$\hat{h}^{(D)} = -\frac{1}{2}\nabla^2 + \frac{1}{2}\|\vec{x}\|^2 = \sum_{k=1}^{D}\hat{h}(x_k). \tag{5}$$

We indicate the variables on which the operators depend by parentheses if there is danger of confusion. Moreover, the HO Hamiltonian for N (distinguishable) particles in d dimensions is simply $\hat{h}^{(Nd)}$. The D-dimensional HO Hamiltonian is manifestly separable, and the eigenfunctions are

$$\Phi_{\vec{n}}(\vec{x}) = \prod_{k=1}^{D}\phi_{n_k}(x_k),$$

with energies

$$\epsilon_{\vec{n}} = \frac{D}{2} + \sum_{k=1}^{D} n_k,$$

where $\vec{n}$ denotes the multi-index of quantum numbers n_k. The one-dimensional HO eigenfunctions are given by

$$\phi_n(x) = (2^n n!\,\pi^{1/2})^{-1/2} H_n(x) e^{-x^2/2},$$

where $H_n(x)$ are the usual Hermite polynomials. These functions are the Hermite functions and are treated in further detail in Sec. III C.

As for the discretization of the Hilbert space, we employ a so-called energy-cut model space $\mathcal{P}$, defined by the span of all HO eigenfunctions with energies up to a given $\epsilon = N_{\max} + D/2$, viz.,

$$\mathcal{P} := \mathrm{sp}\left\{\Phi_{\vec{n}}(\vec{x}) \middle| 0 \leqslant \sum_k n_k \leqslant N_{\max}\right\},$$

where we bear in mind that the $D = Nd$ dimensions are distributed among the N particles.

For the one-dimensional model with only one particle, the model space reduces to

$$\mathcal{P}_1 = \mathrm{sp}\{\phi_n(x) | 0 \leqslant n \leqslant N_{\max}\}. \tag{6}$$

Thus, one particle is associated with one integer quantum number n, denoting the "shell number where the particle resides," in typical terms. For two particles, we get

$$\mathcal{P}_2 = \mathrm{sp}\{\phi_{n_1}(x_1)\phi_{n_2}(x_2) | 0 \leqslant n_1 + n_2 \leqslant N_{\max}\}.$$

We illustrate this space in Fig. 1.

Proper symmetrization must also be applied. However, the Hamiltonian (1) commutes with particle permutations, meaning that the eigenfunctions *will* be symmetric or antisymmetric, assuming that the eigenvalues are distinct. In the case of degeneracy, we may simply produce (anti)symmetric eigenfunctions by taking linear combinations.

We mention that other model spaces can also be used; most common is perhaps the *direct product model space*, defined by N direct products of $\mathcal{P}_1$ rather than a cut in energy as above.

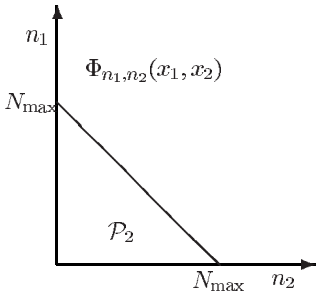

FIG. 1. Two-body model space defined by a cut in energy. The two-body state has quantum numbers n_1 and n_2, the sum of which does not exceed $N_{\max}$.

B. Coordinate changes and the harmonic ascillator

It is obvious that any orthogonal coordinate change $\vec{y}=S\vec{x}$, where $S^TS=1$, commutes with $\hat{h}^{(D)}$. In particular, energy is conserved under the coordinate change. Therefore, the eigenfunctions of the transformed Hamiltonian will be a linear combination of the original eigenfunctions of the same energy, viz.,

$$\Phi_{\vec{n}}(S\vec{x}) = \sum_{\vec{n}'} \langle \Phi_{\vec{n}'}, \hat{T}\Phi_{\vec{n}} \rangle \Phi_{\vec{n}'}(\vec{x}),$$

where the sum is over all $\vec{n}'$ such that $\epsilon_{\vec{n}'}=\epsilon_{\vec{n}}$. Here, $\hat{T}$ performs the coordinate change, viz.,

$$\hat{T}\Phi_{\vec{n}}(\vec{x}) = \Phi_{\vec{n}}(S\vec{x}), \tag{7}$$

where $\hat{T}$ is unitary. Also note that energy conservation implies that $\mathcal{P}$ is invariant with respect to the coordinate change, implying that the CI method is equivalent in the two coordinate systems.

An important example is the center-of-mass transformation introduced in Sec. II. This transformation is essential when we want to compute the Hamiltonian matrix since the interaction is given in terms of these coordinates.

Observe that in the case when the Hamiltonian is, in fact, separated by such a coordinate change, the formulation of the *exact* problem using HO basis is equivalent to two one-particle problems using HO basis in the new coordinates.

C. Approximation properties of the Hermite functions

In order to understand the accuracy of the CI method, we need to study the approximation properties of the Hermite functions. Note that all the Hermite functions $\phi_n(x)$ spanning $L_2(\mathbb{R})$ are *smooth*. Indeed, they are holomorphic in the entire complex plane. Any finite linear combination of these will yield another holomorphic function, so any nonsmooth function will be badly approximated. This simple fact is sadly neglected in the configuration-interaction literature, and we choose to stress it here: Even though the Hermite functions are simple to compute and deal with, arising in a natural way from the consideration of a perturbation of the HO and obeying a wealth of beautiful relations, they are not very well suited for the computation of functions whose smoothness is less than infinitely differentiable or whose decay behavior for large $|x|$ is algebraic, i.e., $f(x)=o(|x|^\beta)$ for some $\beta<0$. Due to the direct product nature of the N-body basis functions, it is clear that these considerations are general and not restricted to the one-dimensional one-particle situation.

Consider an expansion $\psi(x)=\Sigma_{n=0}^{\infty}c_n\phi_n(x)$ in Hermite functions of an arbitrary $\psi\in L_2(\mathbb{R})$. The coefficients are given by

$$c_n = \langle \phi_n, \psi \rangle = \int_{-\infty}^{\infty} \psi(x)\bar{H}_n(x)e^{-x^2/2}dx.$$

Here, $\bar{H}_n(x)=(2^n n!\sqrt{\pi})^{-1/2}H_n(x)$ are the normalized Hermite polynomials. If $\psi(x)$ is well approximated by the basis, the coefficients c_n will decay quickly with increasing n. The *least* rate of convergence is a direct consequence of

$$\|\psi\|^2 = \sum_{n=0}^{\infty} |c_n|^2 < \infty,$$

hence we must have $|c_n|=o(n^{-1/2})$. (This is *not* a sufficient condition, however.) With further restrictions on the behavior of $\psi(x)$, the decay will be faster. This is analogous to the faster decay of Fourier coefficients for smoother functions,[40] although for Hermite functions smoothness is not the only parameter as we consider an infinite domain. In this case, another equally important feature is the decay of $\psi(x)$ as $|x|$ grows, which is intuitively clear given that all the Hermite functions decay as $\exp(-x^2/2)$.

Let us prove this assertion. We give here a simple argument due to Boyd,[32] but we strengthen the result somewhat.

To this end, assume that $\psi(x)$ has k square integrable derivatives (in the weak sense) and that $x^m\psi(x)$ is square integrable for $m=0,1,\ldots,k$. Note that this is a sufficient condition for

$$a^\dagger\psi(x) = \frac{1}{\sqrt{2}}[x\psi(x) - \psi'(x)],$$

and $(a^\dagger)^2\psi(x)$ up to $(a^\dagger)^k\psi(x)$ to be square integrable as well. Here, $a^\dagger$ and its Hermitian conjugate a are the well-known ladder operators for the harmonic oscillator.[41]

Using integration by parts, the formula for c_n becomes

$$c_n = \int_{-\infty}^{\infty} \psi(x)\bar{H}_n(x)e^{-x^2/2}dx$$

$$= (n+1)^{-1/2}\int_{-\infty}^{\infty} [a^\dagger\psi(x)]\bar{H}_{n+1}(x)e^{-x^2/2}dx,$$

or

$$c_n = (n+1)^{-1/2}d_{n+1},$$

where d_n are the Hermite expansion coefficients of $a^\dagger\psi(x)\in L_2$. Since $\Sigma|d_n|^2<\infty$ by assumption, we obtain

$$\sum_{n=0}^{\infty} n|c_n|^2 < \infty,$$

implying

$$c_n = o(n^{-1}).$$

Repeating this argument k times, we obtain the estimate

$$c_n = o[n^{-(k+1)/2}].$$

It is clear that if $\psi(x)$ is infinitely differentiable and if, in addition, $\psi(x)$ decays faster than any power of x, such as, for example, exponentially decaying functions or functions behaving like $\exp(-\alpha x^2)$, c_n will decay faster than *any* power of $1/n$, so-called infinite-order convercence or spectral convergence. Indeed, Hille[33] gives results for the decay of the Hermite coefficients for a wide class of functions. The most important for our application being the following: If $\psi(x)$ decays as $\exp(-\alpha x^2)$, with $\alpha > 0$, and if $\tau > 0$ is the distance from the real axis to the nearest pole of $\psi(x)$ (when considered as a complex function), then

$$|c_n| = O(n^{-1/4} e^{-\tau\sqrt{2n+1}}), \tag{8}$$

a very rapid decay for even moderate τ.

An extremely useful property[32] of the Hermite functions is the fact that they are uniformly bounded, viz.,

$$|\phi_n(x)| \leqslant 0.816, \quad \forall\, x,n.$$

As a consequence, the *pointwise* error in a truncated series is almost everywhere bounded by

$$\left| \psi(x) - \sum_{n=0}^{N_{\max}} c_n \phi_n(x) \right| \leqslant 0.816 \sum_{n=N_{\max}+1}^{\infty} |c_n|.$$

Thus, estimating the error in the expansion amounts to estimating the sum of the neglected coefficients. If $|c_n| = o(n^{\alpha})$,

$$\left| \psi(x) - \sum_{n=0}^{N_{\max}} c_n \phi_n(x) \right| = o(N_{\max}^{\alpha+1}) \quad \text{a.e.}$$

For the error in the mean,

$$\left\| \psi(x) - \sum_{n=0}^{N} c_n \phi_n(x) \right\| = O(N_{\max}^{\alpha+1/2}), \tag{9}$$

as is seen by approximating $\Sigma_{n=N_{\max}+1}^{\infty} |c_n|^2$ by an integral.

In the above, "almost everywhere," or "a.e." for short, refers to the fact that we do not distinguish between square integrable functions that differ on a point set of Lebesgue measure zero. Moreover, there is a subtle distinction between the notations $O(g(n))$ and $o(g(n))$. For a given function f, $f(n) = o(g(n))$ if $\lim_{n\to\infty} |f(n)/g(n)| = 0$, while $f(n) = O(g(n))$ if we have $\lim_{n\to\infty} |f(n)/g(n)| < \infty$, a slightly weaker statement.

D. Application to the interaction potential

Let us apply the above results to the eigenproblem for a perturbed one-dimensional harmonic oscillator, i.e.,

$$\psi''(x) = [x^2 + 2f(x) - 2E]\psi(x), \tag{10}$$

which is also applicable when the two-particle Hamiltonian (2) is separable, i.e., when $U=0$ or $v=0$.

It is now clear that under the assumption that $f(x)$ is k times differentiable (in the weak sense), and that $f(x) = o(|x|^2)$ as $|x| \to \infty$, the eigenfunctions will be $k+2$ times (weakly) differentiable and decay as $\exp(-x^2/2)$ for large $|x|$. Hence, the Hermite expansion coefficients of $\psi(x)$ will decay as $o(n^{\alpha})$, $\alpha = -(k+3)/2$.

If we further assume that $f(x)$ is analytic in a strip of width $\tau > 0$ around the real axis, the same will be true for $\psi(x)$ such that we can use Eq. (8) to estimate the coefficients.

A word of caution is, however, at its place. Although we have argued that if a given function can be differentiated k times (in the weak sense), then the coefficients decay as $o(n^{\alpha})$, $\alpha = -(k+1)/2$, it may happen that this decay "kicks in" too late to be observable in practical circumstances.

Consider, for example, the following function:

$$g(x) = \frac{e^{-x^2/2}}{|x| + \delta},$$

which has exactly one (almost everywhere continuous) derivative and decays as $\exp(-x^2/2)$. However, the derivative is seen to have a jump discontinuity of magnitude $2/\delta^2$ at $x=0$. From the theory, we expect $o(n^{-1})$ decay of the coefficients, but for small δ the first derivative is badly approximated, so we expect to observe only $o(n^{-1/2})$ decay for moderate n, due to the fact that the rate of decay of the coefficients of $g(x)$ are *explicitly* given in terms of the coefficients of $a^{\dagger} g(x)$.

In Fig. 2, the decay rates at different n and for various δ are displayed. The decay rate α is computed by estimating the slope of the graph of $\ln |c_n|$ versus $\ln n$, a technique used throughout this article. Indeed, for small δ, we observe only $\alpha \approx -1/2$ convergence in practical settings, where n is moderate, while larger δ gives $\alpha \approx -1$ even for small n.

The above function was chosen due to its relation to the interaction Hamiltonian (4). Indeed, its coefficients are given by

$$c_n = \langle \phi_n, g \rangle = \langle \phi_n, U(x;1,\delta)\phi_0 \rangle,$$

i.e., proportional to the first row of the interaction matrix. Moreover, due to Eq. (10), the ground state ψ of the interaction Hamiltonian has a second derivative with similar behavior near $x=0$ as $g(x)$. Thus, we expect to observe $\alpha \approx -3/2$, rather than $\alpha \approx -2$, for the available range of n in the large-scale diagonalization experiments.

We remark here that it is quite common to model quantum dot systems using nonsmooth potentials[42] $v(\vec{r})$ and even to use the CI method with HO basis functions on these models.[16,43,44] The present analysis clearly shows that the CI method will behave badly with such potentials.

E. Numerical experiments

We wish to apply the above analysis by considering the model Hamiltonian.[2] We first consider the case where $v(x) = 0$ or $U(x) = 0$, respectively, which reduces the two-particle problem to one-dimensional problems through separation of variables, i.e., the diagonalization of the trap Hamiltonian $\hat{H}_t$ and the interaction Hamiltonian $\hat{H}_i$ in Eqs. (3) and (4). Then we turn to the complete nonseparable problem.

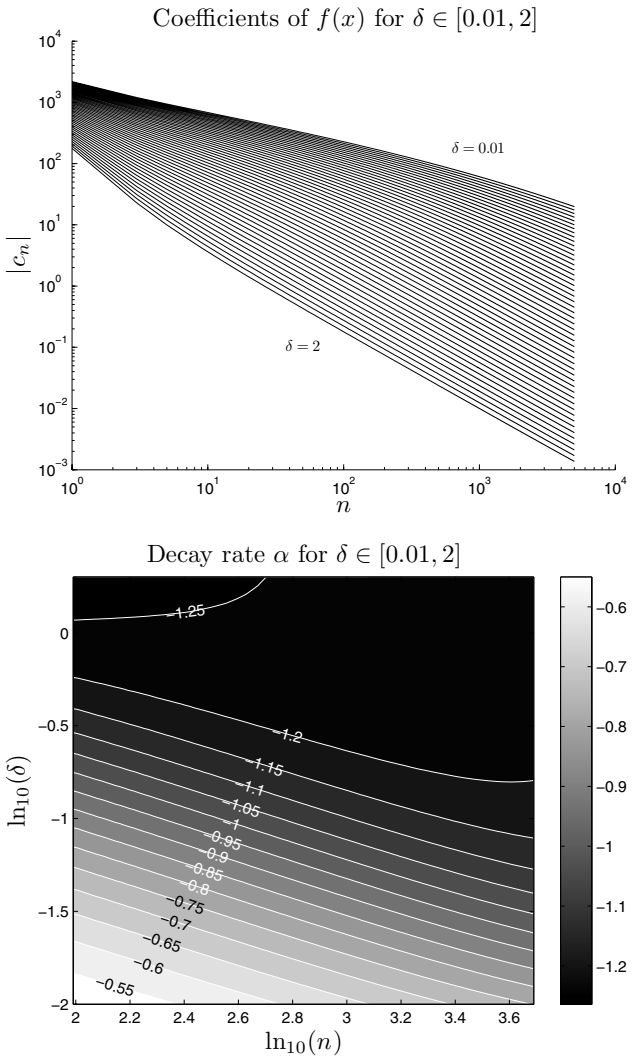

FIG. 2. (Top) Coefficients $|c_n|$ of the function $\exp(-x^2/2)/(|x|+\delta)$ for $\delta \in [0.01, 2]$, $n=0, 2, \ldots, 5000$. (Bottom) Estimated decay rate α of $|c_n|$, i.e., slope of the graphs in the left panel.

For simplicity, we consider the trap $x^2/2+v(x)$ with

$$v(x) = Ae^{-C(x-\mu)^2}, \quad A, C > 0, \quad \mu \in \mathbb{R}, \tag{11}$$

which gives rise to a double-well potential or a single-well potential, depending on the parameters, as depicted in Fig. 3. The perturbation is everywhere analytic and rapidly decaying. This indicates that the corresponding configuration-interaction energies and wave functions also should converge rapidly. In the numerical experiments below, we use $A=4$, $C=2$, and $\mu=0.75$, creating the asymmetric double well in Fig. 3.

For the interaction Hamiltonian $\hat{H}_i$ and its potential $x^2/2+U(\sqrt{2}x;\lambda,\delta)$, we arbitrarily choose $\lambda=1$ and $\delta=0.01$, giving a moderate jump discontinuity in the derivative.

As these problems are both one-dimensional, the model space reduces to $\mathcal{P}_1$ as given in Eq. (6). Each problem then amounts to diagonalizing a matrix $\mathbf{H}$ with elements

$$\mathbf{H}_{n,m} = \langle \phi_n, \hat{H}_{t,i} \phi_m \rangle = \left(n + \tfrac{1}{2}\right) \delta_{n,m} + \int_{-\infty}^{\infty} \phi_n(x) f(x) \phi_m(x) dx,$$

$$0 \leq n,\ m \leq N_{\max},$$

with $f(x)=v(x)$ or $f(x)=U(\sqrt{2}x;1,0.01)$. We compute the matrix to the desired precision using Gauss-Legendre quadrature. In order to obtain reference eigenfunctions and eigenvalues, we use a constant reference potential method[45] implemented in the MATSLISE package[46] for MATLAB. This yields results accurate to about 14 significant digits.

In Fig. 4 (left), the magnitude of the coefficients of the exact ground states alongside the ground state energy error and wave function error (right) is graphed for each Hamiltonian, using successively larger $N_{\max}$. The coefficients of the exact ground states decay according to expectations, as we clearly have spectral convergence for the $\hat{H}_t$ ground state and $o(n^{-1.57})$ convergence for the $\hat{H}_i$ ground state.

These aspects are clearly reflected in the CI calculations. Both the $\hat{H}_t$ ground state energy and wave function converge spectrally with increasing $N_{\max}$, while for $\hat{H}_i$ we clearly have algebraic convergence. Note that for $\hat{H}_t$, $N_{\max} \sim 40$ yields a ground state energy accurate to $\sim 10^{-10}$, and that such precision would require $N_{\max} \sim 10^{12}$ for $\hat{H}_i$, which converges only algebraically.

Intuitively, these results are easy to understand: For the trap Hamiltonian, a modest value of $N_{\max}$ produces almost exact results, since the exact ground state has extremely small components outside the model space. This is not possible for the interaction Hamiltonian, whose exact ground state is poorly approximated in the model space alone.

If we consider the complete Hamiltonian (2), we now expect the error to be dominated by the low-order convergence of the interaction Hamiltonian eigenproblem. Figure 4 also shows the error in the ground state energy for the corresponding two-particle calculation, and the error is, indeed, seen to behave identically to the $\hat{H}_i$ ground state energy error. (That the energy error curve is almost on top of the error in the *wave function* for $\hat{H}_i$ is merely a coincidence.)

It is clear that the nonsmooth character of the potential U destroys the convergence of the method. The eigenfunctions will be nonsmooth, while the basis functions are all very smooth. Of course, a nonsmooth potential $v(x)$ would destroy the convergence as well.

In this sense, we speak of a "small perturbation $\hat{H}_1$" if the eigenvalues and eigenfunctions of the total Hamiltonian converge spectrally. Otherwise, the perturbation is so strong that the very smooth property of the eigenfunctions vanish. In our case, even for arbitrarily small interaction strengths λ, the eigenfunctions are nonsmooth, so that the interaction is never small in the sense defined here. On the other hand, the trap modification $v(x)$ represents a small perturbation of the harmonic oscillator if it is smooth and rapidly decaying. This points to the basic deficiency of the choice of HO basis functions: They do not capture the properties of the eigenfunctions.

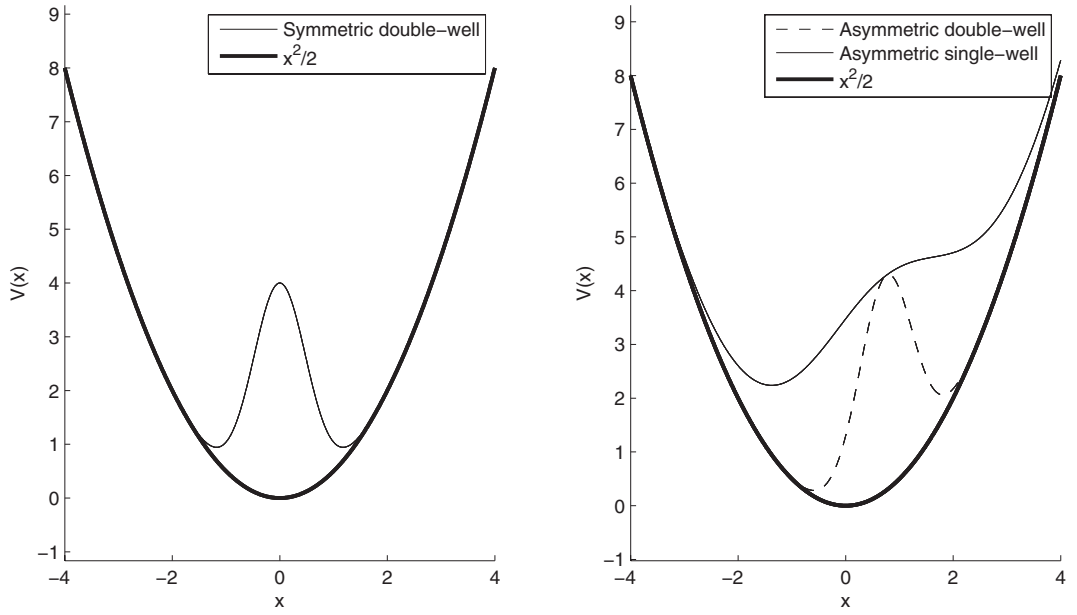

FIG. 3. (Left) Symmetric double-well potential created with the Gaussian perturbation $A\exp[-C(x-\mu)^2]$, with $A=4$, $\mu=0$, and $C=2$. (Right) Asymmetric double-well potential created with the Gaussian perturbation with $A=4$, $\mu=0.75$, and $C=2$, and single-well potential using $C=0.25$.

We could overcome this problem by choosing a different set of basis functions for the Hilbert space, and thus, a different model space $\mathcal{P}$ altogether. However, the symmetries of the HO lets us treat the interaction potential with ease by explicitly performing the center-of-mass transformation, a significant advantage in many-body calculations. In our one-dimensional case, we could replace $U(x_1-x_2)$ by a smooth potential, after all, U is just an approximation somewhat randomly chosen. We would then obtain much better results with the CI method. However, we are not willing to trade the bare Coulomb interaction in two (or even three) dimensions for an approximation. After all, we know that the singular and long-range nature of the interaction is essential.

We, therefore, propose to use *effective interaction theory* known from many-body physics to improve the accuracy of CI calculations for quantum dots. This replaces the matrix in the HO basis of the interaction term with an approximation, giving exact eigenvalues in the case of no trap perturbation $v(x)$, regardless of the energy cut parameter $N_{\max}$. We cannot hope to gain spectral convergence; the eigenfunctions are still nonsmooth. However, we can increase the algebraic convergence considerably by modifying the interaction matrix for the given model space. This is explained in detail in the next section.

IV. EFFECTIVE HAMILTONIAN THEORY

A. Similarity transformation approach

The theories of effective interactions have been, and still are, vital ingredients in many-body physics, from quantum chemistry to nuclear physics.[1,2,47–50] In fields like nuclear physics, due to the complicated nature of the nuclear interactions, no exact spatial potential exists for the interactions between nucleons. Computation of the matrix elements of the many-body Hamiltonian then amounts to computing, for example, successively complicated Feynman diagrams,[48,49] motivating realistic yet tractable approximations such as effective two-body interactions. These effective interactions are, in turn, used as starting points for diagonalization calculations in selected model spaces.[2,22–24] Alternatively, they can be used as starting point for the resummation of selected many-body correlations such as in coupled-cluster theories.[1] In our case, it is the so-called curse of dimensionality that makes a direct approach unfeasible: The number of HO states needed to generate accurate energies and wave functions grows exponentially with the number of particles in the system. Indeed, the dimension of $\mathcal{P}$ grows as $N_{\max}^{Nd}/(Nd)!$

For the derivation of the effective interaction, we consider the Hamiltonian (2) in center-of-mass coordinates, i.e.,

$$\hat{H} = \hat{h}(X) + \hat{h}(x) + v[(X+x)/\sqrt{2}] + v[(X-x)/\sqrt{2}] + U(\sqrt{2}x;\lambda,\delta).$$

For $v(x)\neq 0$, the Hamiltonian is clearly not separable. The idea is then to treat $v(x_j)$ as perturbations of a system separable in center-of-mass coordinates; after all, the trap potential is assumed to be smooth. This new unperturbed Hamiltonian reads

$$\hat{H} = \hat{h}(X) + \hat{h}(x) + \hat{V},$$

where $\hat{V}=U(\sqrt{2}x;\lambda,\delta)$, or any other interaction in a more general setting. We wish to replace the CI matrix of $\hat{H}'$ with a different matrix $\hat{H}'_{\text{eff}}$, having the exact eigenvalues of , but necessarily only approximate eigenvectors.

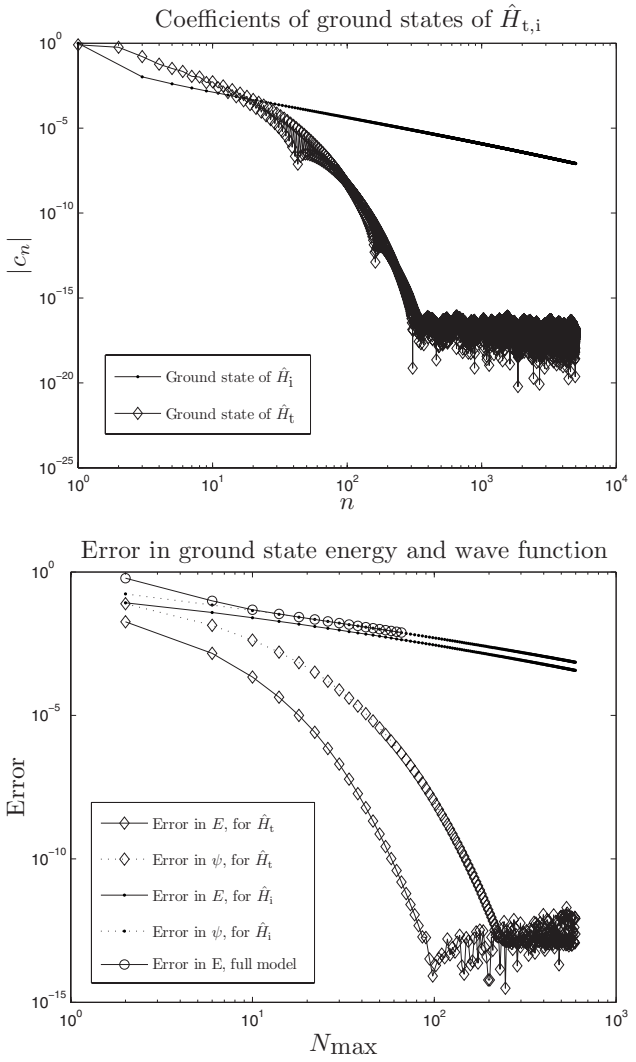

FIG. 4. (Top) Coefficients of the exact ground states of the Hamiltonians $\hat{H}_{t,i}$. For $\hat{H}_i$, only even-numbered coefficients are nonzero and, thus, displayed. The almost straight line indicates approximately $o(n^{-1.57})$ decay of the coefficients around $n=600$, and $o(n^{-1.73})$ around $n=5000$ (cf. Fig. 2). For the $\hat{H}_t$ ground state, we clearly have spectral convergence. (Bottom) The error in the ground state energies and wave functions when using the CI method. For $\hat{H}_i$, we have $o(n^{-1.24})$ decay for the energy error, and $o(n^{-1.20})$ decay for the wave function error, both evaluated at $n=600$. For $\hat{H}_t$, we clearly have spectral convergence. A full two-particle CI calculation is superimposed, showing that the error in the interaction part of the Hamiltonian (2) completely dominates. Here, the error in the energy is $o(N_{\max}^{-1.02})$ at $n=70$, while for $\hat{H}_i$ alone, we have $o(N_{\max}^{-1.01})$.

The effective Hamiltonian $\hat{H}'_{\mathrm{eff}}$ can be viewed as an operator acting in the model space while embodying information about the original interaction in the *complete* space $\mathcal{H}$. We know that this otherwise neglected part of the Hilbert space is very important if $\hat{V}$ is not small. Thus, the first ingredient is the splitting of the Hilbert space into the model space $\mathcal{P}=P\mathcal{H}$ and the *excluded space* $\mathcal{Q}=Q\mathcal{H}=(1-P)\mathcal{H}$. Here, P is the orthogonal projector onto the model space.

In the following, we let N be the dimension of the model space $\mathcal{P}$. There should be no danger of confusion with the number of particles, $N=2$, as this is now fixed. Moreover, we let $\{\Phi_n\}_{n=1}^{N}$ be an orthonormal basis for $\mathcal{P}$, and $\{\Phi_n\}_{n=N+1}^{\infty}$ be an orthonormal basis for $\mathcal{Q}$.

The second ingredient is a *decoupling operator* ω. It is an operator defined by the properties

$$P\omega = \omega Q = 0,$$

which essentially means that ω is a mapping from the model space to the excluded space. Indeed,

$$\omega = (P+Q)\omega(P+Q) = P\omega P + P\omega Q + Q\omega P + Q\omega Q = Q\omega P,$$

which shows that the kernel of ω includes $\mathcal{Q}$, while the range of ω excludes $\mathcal{P}$, i.e., that ω acts only on states in $\mathcal{P}$ and yields only states in $\mathcal{Q}$.

The effective Hamiltonian $\hat{H}_{\mathrm{eff}}=P[\hat{h}(x)+\hat{h}(X)]P+\hat{V}_{\mathrm{eff}}$, where $\hat{V}_{\mathrm{eff}}$ is the effective interaction, is given by the similarity transformation[28]

$$\hat{H}_{\mathrm{eff}} = Pe^{-z}\hat{H}e^{z}P,$$

where $z=\mathrm{artanh}(\omega-\omega^{\dagger})$. The key point is that e^z is a unitary operator with $(e^z)^{-1}=e^{-z}$, so that the N eigenvalues of $\hat{H}'_{\mathrm{eff}}$ are actually eigenvalues of $\hat{H}'$.

In order to generate a well-defined effective Hamiltonian, we must define $\omega=Q\omega P$ properly. The approach of Suzuki and Okamoto[25–28] is simple: Select an orthonormal set of vectors $\{\chi_n\}_{n=1}^{N}$. These can be some eigenvectors of $\hat{H}'$ we wish to include. Assume that $\{P\chi_n\}_{n=1}^{N}$ is a basis for the model space, i.e., that for any $n\leqslant N$, we can write

$$\Phi_n = \sum_{m=1}^{N} a_{n,m} P\chi_m$$

for some constants $a_{n,m}$. We then define ω by

$$\omega P\chi_n := Q\chi_n, \quad n=1,\ldots,N.$$

Observe that ω defined in this way is an operator that reconstructs the excluded space components of χ_n given its model space components, thereby, indeed, embodying information about the Hamiltonian acting on the excluded space.

Using the decoupling properties of ω, we quickly calculate

$$\omega\Phi_n = Q\omega P\Phi_n = Q\omega\sum_{m=1}^{N} a_{n,m}\chi_m, \quad n=1,\ldots,N,$$

and hence, for any $n'>N$, we have

$$\langle\Phi_{n'},\omega\Phi_n\rangle = \sum_{m=1}^{N} a_{n,m}\langle\Phi_{n'},\chi_m\rangle,$$

yielding all the nonzero matrix elements of ω.

As for the vectors χ_n, we do not know *a priori* the exact eigenfunctions of $\hat{H}'$, of course. Hence, we cannot find $\hat{H}'_{\mathrm{eff}}$ exactly. The usual way to find the eigenvalues is to solve a much larger problem with $N'>N$ and then assume that these

eigenvalues are exact. The reason why this is possible at all is that our Hamiltonian $\hat{H}'$ is separable, and therefore, easier to solve. However, we have seen that this is a bad method: Indeed, one needs a matrix dimension of about 10^{10} to obtain about ten significant digits. Therefore, we instead reuse the aforementioned constant reference potential method to obtain eigenfunctions and eigenvectors accurate to machine precision.

Which eigenvectors of $\hat{H}'$ do we wish to include? Intuitively, the first choice would be the lowest N eigenvectors. However, simply ordering the eigenvalues "by value" is not what we want here. Observe that $\hat{H}'$ is block diagonal and that the model space contains $N_{\max}+1$ blocks of sizes 1 through $N_{\max}+1$. If we look at the exact eigenvalues, we know that they have the structure

$$E_{n,m} = (n + 1/2) + \epsilon_m,$$

where n is the block number and ϵ_m are the eigenvalues of $\hat{H}_i$ [see Eq. (4)]. However, it is easy to see that the large-scale diagonalization eigenvalues do *not* have this structure—we only obtain this in the limit $N_{\max} \to \infty$. Therefore, we choose the eigenvectors corresponding to the N eigenvalues $E_{n,m}$, $n+m \leqslant N_{\max}$, thereby achieving this structure in the eigenvalues of $\hat{H}'_{\text{eff}}$.

In general, we wish to incorporate the symmetries of $\hat{H}'$ into the effective Hamiltonian $\hat{H}'_{\text{eff}}$. In this case, it was the separability and even eigenvalue spacing we wished to reproduce. In Sec. V, we treat the two-dimensional Coulomb problem similarly.

B. Numerical experiments with effective interactions

The eigenvectors of the Hamiltonian $\hat{H}'$ differ from those of the effective Hamiltonian $\hat{H}'_{\text{eff}}$. In this section, we first make a qualitative comparison between the ground states of each Hamiltonian. We then turn to a numerical study of the error in the CI method when using the effective interaction in the model problem.

Recall that the ground state eigenvectors are of the form

$$\Psi(X,x) = \phi_0(X)\psi(x) = \phi_0(X)\sum_{n=0}^{\infty} c_n \phi_n(x).$$

For $\hat{H}'_{\text{eff}}$, $c_n=0$ for all $n>N_{\max}$, so that the excluded space part of the error coincides with the excluded space part of the exact ground state. In Fig. 5, the coefficients c_n for both $\hat{H}'$ and $\hat{H}'_{\text{eff}}$ are displayed. The pointwise error is also plotted, and the largest values are seen to be around $x=0$. This is expected since $U(\sqrt{2}x;\lambda,\delta)$ and the exact ground state is nonsmooth there. Notice the slow spatial decay of the error, intuitively explained by the slow decay of the Coulomb interaction.

We now turn to a simulation of the full two-particle Hamiltonian (2) and compare the decay of the ground state energy error with and without the effective interaction. Thus, we perform two simulations with Hamiltonians

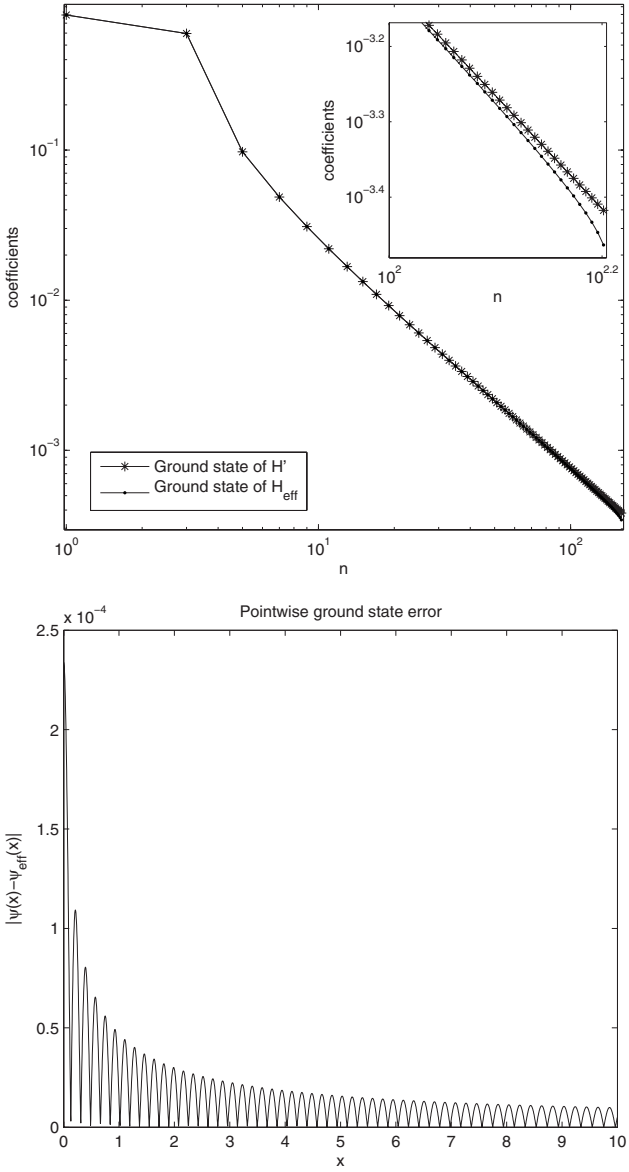

FIG. 5. (Top) Plot of ground state coefficients of $\hat{H}'$ and $\hat{H}_{\text{eff}}$. (Bottom) Pointwise error (in relative coordinate x) of effective Hamiltonian ground state $\psi_{\text{eff}}(x)$.

$$\hat{H} = \hat{H}' + v(x_1) + v(x_2) = \hat{h}(x_1) + \hat{h}(x_2) + v(x_1) + v(x_2) + \hat{T}\hat{V}\hat{T}^{\dagger}$$

and

$$\hat{H}_{\text{eff}} = \hat{H}'_{\text{eff}} + v(x_1) + v(x_2) = \hat{h}(x_1) + \hat{h}(x_2) + v(x_1) + v(x_2) + \hat{T}\hat{V}_{\text{eff}}\hat{T}^{\dagger},$$

respectively, where $\hat{T}$ is the center-of-mass transformation [cf. Eq. (7)].

We remark that the new Hamiltonian matrix has the *same structure* as the original matrix. It is only the values of the interaction matrix elements that are changed. Hence, the new scheme has the same complexity as the CI method if we

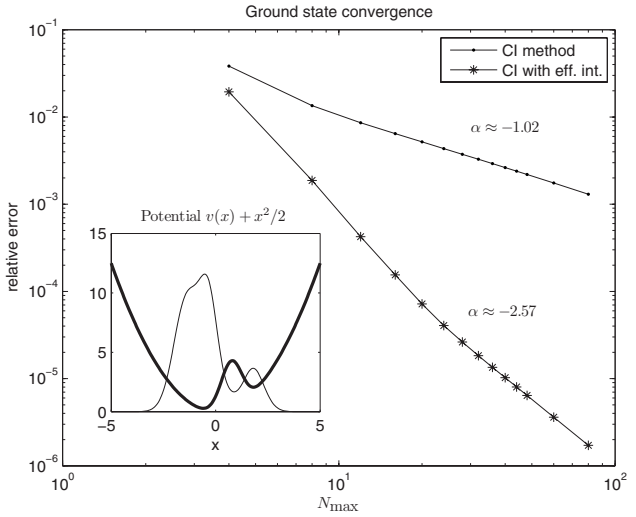

FIG. 6. Ground state energy relative error for a two-particle simulation using the confinement potential $V(x)=x^2/2+4\exp[-2(x-0.75)^2]$. For the CI method without effective interactions, we obtain $\alpha \approx -1.02$, while the effective interactions give $\alpha \approx -2.57$. The electron density is superimposed on the potential plot.

disregard the computation of $\hat{V}_{\text{eff}}$, which is a one-time calculation of low complexity.

The results are striking: In Fig. 6, we see that the ground state error decays as $O(N_{\max}^{-2.57})$, compared to $O(N_{\max}^{-0.95})$ for the original CI method. For $N_{\max}=40$, the CI relative error is $\Delta E/E_0 \approx 2.6\times 10^{-3}$, while for the effective interaction approach $\Delta E/E_0 \approx 1.0\times 10^{-5}$, a considerable gain.

The ground state energy E_0 used for computing the errors were computed using extrapolation of the results.

We comment that $N_{\max} \sim 40$ is the practical limit on a single desktop computer for a two-dimensional two-particle simulation. Adding more particles further restricts this limit, emphasizing the importance of the gain achieved in the relative error.

In a more systematical treatment, we computed the error decay coefficient α for a range of trap potentials $x^2+A\exp[-2(x-\mu)^2]$, where we vary A and μ to create single- and double-well potentials. In most cases, we could estimate α successfully. For low values of μ, i.e., near-symmetric wells, the parameter estimation was difficult in the effective interaction case due to very quick convergence of the energy. The CI calculations also converged quicker in this case. Intuitively this is so because the two electrons are far apart in this configuration.

The results indicate that at $N_{\max}=60$, we have

$$\alpha = -0.96 \pm 0.04 \quad \text{for } \hat{H}$$

and

$$\alpha = -2.6 \pm 0.2 \quad \text{for } \hat{H}_{\text{eff}}$$

for the chosen model. Here, $0.6 \leqslant \mu \leqslant 1.8$ and $2.9 \leqslant A \leqslant 4.7$, and all the fits were successful. In Fig. 7, contour plots of the

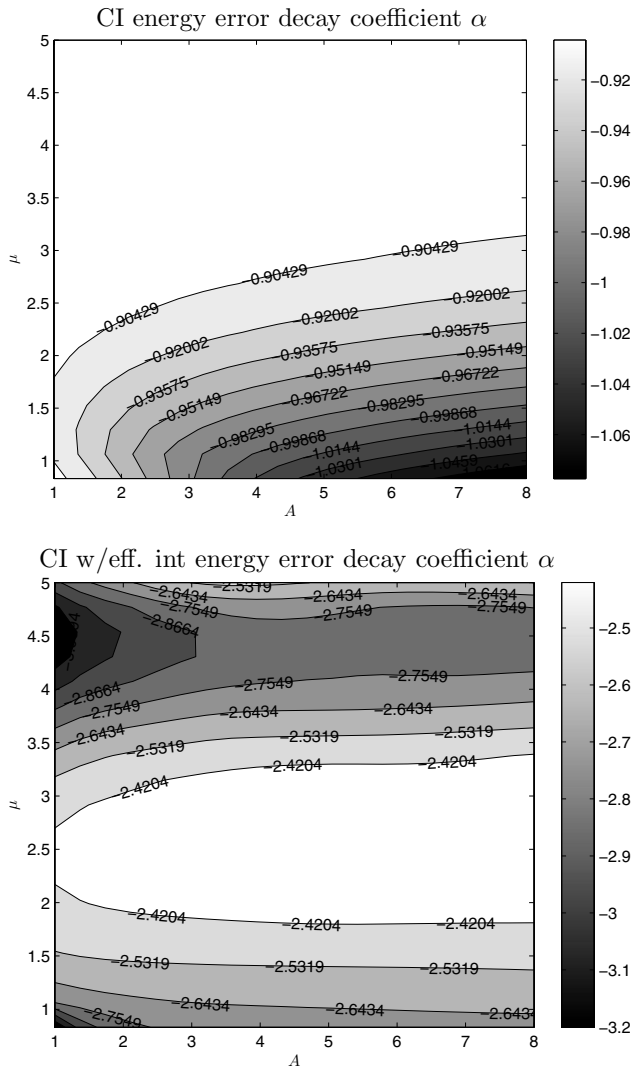

FIG. 7. Estimates of α for CI calculations with (bottom) and without (top) effective interactions.

obtained results are shown. For the range shown, results were unambiguous.

These numerical results clearly indicate that the effective interaction approach will gain valuable numerical precision over the original CI method in general; in fact, we have gained nearly 2 orders of magnitude in the decay rate of the error.

V. DISCUSSION AND OUTLOOK

A. Generalizations

One-dimensional quantum dot models are of limited value in themselves. However, as claimed in Sec. I, the analysis and experiments performed in this article are valid also in higher-dimensional systems.

Consider two particles in two dimensions. Let $\hat{h}(\vec{r})$ be the two-dimensional harmonic oscillator Hamiltonian [we omit the superscript in Eq. (5) for brevity], and let the quantum dot Hamiltonian be given by

$$\hat{H} = \hat{H}' + v(\vec{r}_1) + v(\vec{r}_2),$$

where

$$\hat{H}' = \hat{h}(\vec{r}_1) + \hat{h}(\vec{r}_2) + \frac{\lambda}{\|\vec{r}_1 - \vec{r}_2\|}.$$

The normalized center-of-mass and relative coordinates are defined by

$$\vec{R} = \frac{\vec{r}_1 + \vec{r}_2}{\sqrt{2}} \quad \text{and} \quad \vec{r} = \frac{\vec{r}_1 - \vec{r}_2}{\sqrt{2}},$$

respectively, which gives

$$\hat{H}' = \hat{h}(\vec{R}) + \hat{h}(\vec{r}) + \frac{\lambda}{\sqrt{2}\|\vec{r}}.$$

The HO eigenfunctions in polar coordinates are given by[9]

$$\Phi_{n,m}(r,\theta) \propto e^{im\theta} r^{|m|} L_n^{|m|}(r^2) e^{-r^2/2},$$

and the corresponding eigenvalues are $2n+|m|+1$. Now, $\hat{H}'$ is further separable in polar coordinates, yielding a single radial eigenvalue equation to solve, analogous to the single one-dimensional eigenvalue equation of $\hat{H}_i$ in Eq. (4). This equation, in fact, has analytical solutions for a countable infinite set of λ values, first derived in Ref. 51.

The eigenvalues of $\hat{H}'$ have the structure

$$E_{n',m',n,m} = 2n' + |m'| + 1 + \epsilon_{n,m},$$

where (n',m') and (n,m) are the center-of-mass and relative coordinate quantum numbers, respectively. Again, the degeneracy structure and even spacing of the eigenvalues are destroyed in the CI approach, and we wish to regain it with the effective interaction. We then choose the eigenvectors corresponding to the quantum numbers

$$2n' + |m'| + 2n + m \leq N_{\max}$$

to build our effective Hamiltonian $\hat{H}'_{\text{eff}}$.

Let us also mention that the exact eigenvectors $\Psi_{n',m',n,m}$ are nonsmooth due to the $1/r$ singularity of the Coulomb interaction. The approximation properties of the Hermite functions are then directly applicable as before, when we expand the eigenfunctions in HO basis functions. Hence, the configuration-interaction method will converge slowly also in the two-dimensional case. It is good reason to believe that effective interaction experiments will yield similarly positive results with respect to convergence improvement.

Clearly, the above procedure is applicable to three-dimensional problems as well. The operator $\hat{H}'$ is separable and we obtain a single nontrivial radial equation, and thus, we may apply our effective Hamiltonian procedure. The exact eigenvalues will have the structure

$$E_{n',l',m',n,l,m} = 2n' + l' + \frac{3}{2} + \epsilon_{n,l,m},$$

on which we base the choice of the effective Hamiltonian eigenvectors as before.

The effective interaction approach to the configuration-interaction calculations is easily extended to a many-particle problem, whose Hamiltonian is given by Eq. (1). The form of the Hamiltonian contains only interactions between pairs of particles, and $\hat{V}_{\text{eff}}$ as defined in Sec. IV can simply replace these terms.

B. Outlook

A theoretical understanding of the behavior of many-body systems is a great challenge and provides fundamental insights into quantum mechanical studies, as well as offers potential areas of applications. However, apart from some analytically solvable problems, the typical absence of an exactly solvable contribution to the many-particle Hamiltonian means that we need reliable numerical many-body methods. These methods should allow for controlled expansions and provide a calculational scheme which accounts for successive many-body corrections in a systematic way. Typical examples of popular many-body methods are coupled-cluster methods,[1,52,53] various types of Monte Carlo methods,[54–56] perturbative expansions,[47,48] Green's function methods,[49,50] the density-matrix renormalization group,[57,58] and large-scale diagonalization methods such as the CI method considered here.

In a forthcoming article, we will apply the similarity transformed effective interaction theory to a two-dimensional system and also extend the results to many-body situations. Application of other methods, such as coupled-cluster calculations, is also an interesting approach and can give further refinements on the convergence as well as insight into the behavior of the numerical methods in general.

The study of this effective Hamiltonian is interesting from a many-body point of view: The effective two-body force is built from a two-particle system. The effective two-body interaction derived from an N-body system, however, is not necessarily the same. Intuitively, one can think of the former approach as neglecting interactions and scattering between three or more two particles at a time. In nuclear physics, such three-body correlations are non-negligible and improve the convergence in terms of the number of harmonic oscillator shells.[59] Our hope is that such interactions are much less important for Coulomb systems.

Moreover, as mentioned in Sec. I, accurate determination of eigenvalues is essential for simulations of quantum dots in the time domain. Armed with the accuracy provided by the effective interactions, we may commence interesting studies of quantum dots interacting with their environment.

C. Conclusion

We have mathematically and numerically investigated the properties of the configuration-interaction method, or "exact diagonalization method," by using results from the theory of Hermite series. The importance of the properties of the trap and interaction potentials is stressed: Nonsmooth potentials severely hampers the numerical properties of the method, while smooth potentials yield exact results with reasonable computing resources. On the other hand, the HO basis is

very well suited due to the symmetries under orthogonal coordinate changes.

In our numerical experiments, we have demonstrated that for a simple one-dimensional quantum dot with a smooth trap, the use of similarity transformed effective interactions can significantly reduce the error in the configuration-interaction calculations due to the nonsmooth interaction, while not increasing the complexity of the algorithm. This error reduction can be crucial for many-body simulations, for which the number of harmonic oscillator shells is very modest.

ACKNOWLEDGMENT

This work was supported by the Norwegian Research Council.

*simen.kvaal@cma.uio.no

[1] T. Helgaker, P. Jørgensen, and J. Olsen, *Molecular Electronic Structure Theory: Energy and Wave Functions* (Wiley, New York, 2000).
[2] E. Caurier, G. Martinez-Pinedo, F. Nowacki, A. Poves, and A. P. Zuker, Rev. Mod. Phys. **77**, 427 (2005).
[3] T. Ezaki, N. Mori, and C. Hamaguchi, Phys. Rev. B **56**, 6428 (1997).
[4] P. Maksym, Physica B **249**, 233 (1998).
[5] N. A. Bruce and P. A. Maksym, Phys. Rev. B **61**, 4718 (2000).
[6] C. E. Creffield, W. Häusler, J. H. Jefferson, and S. Sarkar, Phys. Rev. B **59**, 10719 (1999).
[7] W. Häusler and B. Kramer, Phys. Rev. B **47**, 16353 (1993).
[8] S. M. Reimann, M. Koskinen, and M. Manninen, Phys. Rev. B **62**, 8108 (2000).
[9] M. Rontani, C. Cavazzoni, D. Belucci, and G. Goldoni, J. Chem. Phys. **124**, 124102 (2006).
[10] O. Ciftja and M. G. Faruk, J. Phys.: Condens. Matter **18**, 2623 (2006).
[11] K. Jauregui, W. Hausler, and B. Kramer, Europhys. Lett. **24**, 581 (1993).
[12] H. Imamura, P. A. Maksym, and H. Aoki, Phys. Rev. B **59**, 5817 (1999).
[13] S. A. Mikhailov, Phys. Rev. B **65**, 115312 (2002); **66**, 153313 (2002).
[14] M. B. Tavernier, E. Anisimovas, F. M. Peeters, B. Szafran, J. Adamowski, and S. Bednarek, Phys. Rev. B **68**, 205305 (2003).
[15] A. Wensauer, M. Korkusinski, and P. Hawrylak, Solid State Commun. **130**, 115 (2004).
[16] M. Helle, A. Harju, and R. M. Nieminen, Phys. Rev. B **72**, 205329 (2005).
[17] W. Xie, Phys. Rev. B **74**, 115305 (2006).
[18] M. B. Tavernier, E. Anisimovas, and F. M. Peeters, Phys. Rev. B **74**, 125305 (2006).
[19] S. S. Gylfadottir, A. Harju, T. Jouttenus, and C. Webb, New J. Phys. **8**, 211 (2006).
[20] S. Gould, *Variational Methods for Eigenvalue Problems: An Introduction to the Methods of Rayleigh, Ritz, Weinstein, and Aronszajn* (Dover, New York, 1995).
[21] T. Tang, SIAM J. Sci. Comput. (USA) **14**, 594 (1993).
[22] P. Navrátil and B. R. Barrett, Phys. Rev. C **57**, 562 (1998).
[23] P. Navrátil, J. P. Vary, and B. R. Barrett, Phys. Rev. Lett. **84**, 5728 (2000).
[24] P. Navrátil, G. P. Kamuntavicius, and B. R. Barrett, Phys. Rev. C **61**, 044001 (2000).
[25] K. Suzuki, Prog. Theor. Phys. **68**, 246 (1982).
[26] K. Suzuki, Prog. Theor. Phys. **68**, 1627 (1982); K. Suzuki and R. Okamoto, *ibid.* **75**, 1388 (1986); **76**, 127 (1986).
[27] K. Suzuki and R. Okamoto, Prog. Theor. Phys. **93**, 905 (1995).
[28] K. Suzuki and R. Okamoto, Prog. Theor. Phys. **92**, 1045 (1994).
[29] H. Kamada *et al.*, Phys. Rev. C **64**, 044001 (2001).
[30] K. Varga, P. Navrátil, J. Usukura, and Y. Suzuki, Phys. Rev. B **63**, 205308 (2001).
[31] D. Loss and D. P. DiVincenzo, Phys. Rev. A **57**, 120 (1998).
[32] J. Boyd, J. Comput. Phys. **54**, 382 (1984).
[33] E. Hille, Duke Math. J. **5**, 875 (1939).
[34] A. Kumar, S. E. Laux, and F. Stern, Phys. Rev. B **42**, 5166 (1990).
[35] M. Macucci, K. Hess, and G. J. Iafrate, Phys. Rev. B **55**, R4879 (1997).
[36] P. A. Maksym and N. A. Bruce, Physica E (Amsterdam) **1**, 211 (1997).
[37] A. Wensauer, M. Korkusinski, and P. Hawrylak, Phys. Rev. B **67**, 035325 (2003).
[38] P. Kurasov, J. Phys. A **29**, 1767 (1996).
[39] F. Gesztesy, J. Phys. A **13**, 867 (1980).
[40] A. Tveito and R. Winther, *Introduction to Partial Differential Equations* (Springer, Berlin, 2002).
[41] R. Mota, V. D. Granados, A. Queijiro, and J. Garcia, J. Phys. A **36**, 2979 (2002).
[42] A. Wensauer, O. Steffens, M. Suhrke, and U. Rössler, Phys. Rev. B **62**, 2605 (2000).
[43] A. Harju, S. Siljamaki, and R. M. Nieminen, Phys. Rev. Lett. **88**, 226804 (2002).
[44] M. Førre, J. P. Hansen, V. Popsueva, and A. Dubois, Phys. Rev. B **74**, 165304 (2006).
[45] V. Ledoux, M. Van Daele, and G. Vanden Berghe, Comput. Phys. Commun. **162**, 151 (2004).
[46] V. Ledoux, M. Van Daele, and G. Vanden Berghe, ACM Trans. Math. Softw. **31**, 532 (2005).
[47] I. Lindgren and J. Morrison, *Atomic Many-Body Theory* (Springer, Berlin, 1985).
[48] M. Hjorth-Jensen, T. T. S. Kuo, and E. Osnes, Phys. Rep. **261**, 125 (1995).
[49] W. H. Dickhoff and D. V. Neck, *Many-Body Theory Exposed!* (World Scientific, New Jersey, 2005).
[50] J. P. Blaizot and G. Ripka, *Quantum Theory of Finite Systems* (MIT, Cambridge, 1986).
[51] M. Taut, J. Phys. A **27**, 1045 (1994).
[52] R. J. Bartlett, Annu. Rev. Phys. Chem. **32**, 359 (1981).
[53] M. Wloch, D. J. Dean, J. R. Gour, M. Hjorth-Jensen, K. Kowalski, T. Papenbrock, and P. Piecuch, Phys. Rev. Lett. **94**, 212501 (2005).
[54] B. S. Pudliner, V. R. Pandharipande, J. Carlson, S. C. Pieper, and

R. B. Wiringa, Phys. Rev. C **56**, 1720 (1997).
[55] D. M. Ceperley, Rev. Mod. Phys. **67**, 279 (1995).
[56] S. E. Koonin, D. J. Dean, and K. Langanke, Phys. Rep. **278**, 1 (1997); T. Otsuka, M. Homna, T. Mizusaki, N. Shimizu, and Y. Utsuno, Prog. Part. Nucl. Phys. **47**, 319 (2001).
[57] S. R. White, Phys. Rev. Lett. **69**, 2863 (1992).
[58] U. Schollwock, Rev. Mod. Phys. **77**, 259 (2005).
[59] P. Navrátil and W. E. Ormand, Phys. Rev. C **68**, 034305 (2003).

2 Harmonic oscillator eigenfunction expansions, quantum dots, and effective interactions

This paper is submitted to Physical Review B.

Harmonic oscillator eigenfunction expansions, quantum dots, and effective interactions

Simen Kvaal[1,*]

[1]*Centre of Mathematics for Applications, University of Oslo, N-0316 Oslo, Norway*

(Dated: November 1, 2008)

We present a mathematical analysis of the approximation properties of the harmonic oscillator eigenfunctions widely used as basis for configuration-interaction calculations of harmonically confined quantum dots, as well as other physical systems. We further give *a priori* error estimates for the diagonalization methods, that, for example, can be used to estimate the computational parameters needed to give a desired accuracy. We show, that in general the method converges slowly for the quantum dot problem. In order to overcome this, we propose to use an effective two-body interaction well-known from nuclear physics, and demonstrate a significant improvement on the convergence by performing numerical simulations.

I. INTRODUCTION

The harmonic oscillator (HO) is ubiquitous in quantum physics. It is the basis for extremely diverse many-body calculations in nuclear physics,[1] quantum chemistry,[2] and quantum dot calculations in solid state physics.[3] In these calculations, one typically seeks a few of the lowest eigenenergies E_k of the system Hamiltonian H, and their corresponding eigenvectors ψ_k, viz,

$$H\psi_k = E_k\psi_k, \quad k = 1, \cdots, k_{\max}.$$

In all cases, the many-body wave function is expanded in a basis of eigenfunctions of the HO, and then necessarily truncated to give an approximation. In fact, the so-called curse of dimensionality implies that the number of degrees of freedom per particle available is severely limited. It is clear, that an understanding of the properties of such expansions, giving *a priori* error estimates on many-body calculations, is very important. Unfortunately, this is a neglected topic in the physics literature. In this article, we give a thorough mathematical and numerical analysis and give practical convergence estimates of HO basis expansions. It generalizes and refines the findings of a recent study of one-dimensional systems.[4]

The HO eigenfunctions are popular for several reasons. Many quantum systems, such as the quantum dot model considered here, are perturbed harmonic oscillators *per se*, so that the true eigenstates should be perturbations of the HO states. Moreover, the HO has many beautiful properties, such as separability, invariance under orthogonal coordinate changes, and easily computed eigenfunctions, so that computing matrix elements of relevant operators becomes relatively simple. The HO eigenfunctions are defined on the *whole* of $\mathbb{R}^d$ in which the particles live, so that truncation of the domain is unnecessary. Indeed, this is one of the main problems with methods such as finite difference or finite element methods.[5]

The HO eigenfunctions for a many-body system are closely related to the so-called Hermite functions, and their d-dimensional generalizations. We will derive approximation properties of the Hermite functions in arbitrary dimensions using techniques based on the ladder operators for the HO, as well as simple techniques from the abstract Sobolev space theory of partial differential equations.[6] By approximation properties, we mean estimates on the error $\|\psi - P\psi\|$, where ψ is any wave function and P projects onto a finite subspace of HO eigenfunctions. Here, $P\psi$ is in fact the best approximation in the norm. The estimates will depend on analytic properties of ψ, i.e., if it is differentiable, and whether it falls of sufficiently fast at infinity. To our knowledge, these results are not previously published.

The results are crucial for obtaining *a priori* error bounds and rates of convergence for both eigenvalues and wave functions with respect to basis size of commonly used methods such as the full configuration interaction method (CI), also known as "exact diagonalization", and coupled cluster methods.[7]

We apply the obtained results to the CI method for a widely-used model quantum dot, namely that of N interacting electrons trapped in a HO potential in $d = 2$ dimensions, and derive convergence estimates of the method as function of the basis size. The main results are somewhat discouraging. The coefficients for typical eigenfunctions of the system are shown to decay very slowly, limiting the accuracy of *any* practical method using HO basis functions. We illustrate the results by standard numerical calculations paralleling that of many other published works, see for example Refs. 8–13.

Finally, we propose to use an effective two-body interaction to overcome, at least partially, the slow convergence rate. This is routinely used in nuclear physics[1] (see for example Ref. 14) where the interparticle forces are of a completely different, and basically unknown, nature. For electronic systems, however, the interaction is well-known and easy to analyze, but effective interactions of the present kind have not been applied, at least to the author's knowledge. We present results for $N = 3, 4$ and 5 electrons using the full configuration interaction method with effective interactions, demonstrating the usefulness of this approach. The modified method is seen to have convergence rates of at least one order of magnitude higher than the original CI method.

In fact, this remedy should be applicable to most systems of interacting electrons, independent of the confining trap potential, and thereby quite universal. An important point here is that the complexity of the CI calculations is not altered, as no extra non-zero matrix elements are introduced. All one needs is a relatively simple one-time calculation to produce the effective interaction matrix elements.

The article is organized as follows. In Sec. II we discuss the N-body harmonic oscillator in d dimensions and its eigenfunctions, in order to identify the relationship with Hermite

functions in $n = Nd$ dimensions. We also briefly discuss the parabolic quantum dot model. In Sec. III, we give results for the approximation properties of the Hermite functions in n dimensions, and thus also of many-body HO eigenfunctions. In Sec. IV, we briefly discuss the full configuration interaction method, using the results obtained in Sec. III to obtain convergence estimates of the method as function of the model space size. We also briefly discuss the effective interaction utilized in the numerical simulations for $d =$ and $N \leq 5$, which are presented in Sec. V. We conclude with a discussion of the results, its consequences, and an outlook on further directions of research in Sec. VI.

We have also included appendices with the most important facts and definitions from functional analysis and Sobolev space theory that we will use, in addition to multi-indices for ease of notation.

II. MANY-BODY STATES OF THE HARMONIC OSCILLATOR

A. The Harmonic Oscillator

For completeness, we begin with a quick review of the harmonic oscillator in $\mathbb{R}^d$ and establish some notation and units in which we work. A spinless particle of mass m in an isotropic harmonic potential has Hamiltonian

$$H_{\text{HO}} = -\frac{\hbar^2}{2m}\nabla^2 + \frac{1}{2}m\omega^2\|\vec{r}\|^2,$$

where $\vec{r} \in \mathbb{R}^d$ is the particle's coordinates. By choosing proper energy and length units, i.e., $\hbar\omega$ and $\sqrt{\hbar/m\omega}$, respectively, the Hamiltonian becomes

$$H_{\text{HO}} = -\frac{1}{2}\nabla^2 + \frac{1}{2}\|\vec{r}\|^2.$$

This is the set of units in which we work.

H_{HO} can be written as a sum over d one-dimensional harmonic oscillators, viz,

$$H_{\text{HO}} = \sum_{k=1}^{d}\left(-\frac{1}{2}\frac{\partial^2}{\partial r_k^2} + \frac{1}{2}r_k^2\right),$$

so that a complete specification of the HO eigenfunctions is given by

$$\Phi_{\alpha_1,\alpha_2,\ldots,\alpha_d}(\vec{r}) = \phi_{\alpha_1}(r_1)\phi_{\alpha_2}(r_2)\cdots\phi_{\alpha_d}(r_d), \tag{1}$$

where $\phi_{\alpha_i}(x)$, $\alpha_i = 0,1,\ldots$ are one-dimensional HO eigenfunctions, also called Hermite functions. These are defined by

$$\phi_n(x) = (2^n n!\pi^{1/2})^{-1/2}H_n(x)e^{-x^2/2}, \quad n = 0,1,\ldots, \tag{2}$$

where the Hermite polynomials $H_n(x)$ are given by

$$H_n(x) = (-1)^n e^{x^2}\frac{\partial^n}{\partial x^n}e^{-x^2}.$$

The Hermite polynomials also obey the recurrence formula

$$H_{n+1}(x) = 2xH_n(x) - 2nH_{n-1}(x), \tag{3}$$

with $H_0(x) = 1$ and $H_1(x) = 2x$. The Hermite polynomial $H_n(x)$ has n zeroes, and the Gaussian factor will eventually subvert the $H_n(x)$ for large $|x|$. Thus, qualitatively, the Hermite functions can be described as localized oscillations with n nodes with a Gaussian "tail" as x approaches $\pm\infty$. One can easily compute the quantum mechanical variance

$$(\Delta x)^2 := \int_{-\infty}^{\infty} x^2\phi_n(x)^2\mathrm{d}x = n + \frac{1}{2},$$

showing that, loosely speaking, the width of the oscillatory region increases as $(n+1/2)^{1/2}$.

The functions $\Phi_{\alpha_1,\cdots,\alpha_d}$ defined in Eqn. (1) are called d-dimensional Hermite functions. In the sequel, we will write $\alpha = (\alpha_1,\cdots,\alpha_d) \in \mathscr{I}_d$ for a tuple of non-negative integers, also called a multi-index, see Appendix A for definitions and notation. Using multi-indices, we may write

$$\Phi_\alpha(\vec{r}) = \left(2^{|\alpha|}\alpha!\pi^{d/2}\right)^{-1/2}H_{\alpha_1}(r_1)\cdots H_{\alpha_d}(r_d)e^{-\|\vec{r}\|^2/2}. \tag{4}$$

The eigenvalue of $\phi_n(x)$ is $n+1/2$, so that the eigenvalue of $\Phi_\alpha(\vec{r})$ is

$$\epsilon_\alpha = \frac{d}{2} + |\alpha|,$$

i.e., a zero-point energy $d/2$ plus a non-negative integer. We denote by $|\alpha|$ the *shell number* of Φ_α, and the eigenspace $\mathscr{S}_r(\mathbb{R}^d)$ corresponding to the eigenvalue $d/2+r$ a *shell*. We define the *shell-truncated Hilbert space* $\mathscr{P}_R(\mathbb{R}^d) \subset L^2(\mathbb{R}^d)$ as

$$\mathscr{P}_R(\mathbb{R}^d) := \operatorname{span}\{\Phi_\alpha(\vec{r}) \mid |\alpha| \leq R\} = \bigoplus_{r=0}^{R}\mathscr{S}_r(\mathbb{R}^d),$$

i.e., the subspace spanned by all Hermite functions with shell number less than or equal to R, or, equivalently, the direct sum of the shells up to and including R.

Since the Hermite functions constitute an orthonormal basis for $L^2(\mathbb{R}^d)$ (a basic result from spectral theory[15]) $\mathscr{P}_R(\mathbb{R}^d) \to L^2(\mathbb{R}^d)$, in the sense that for every $\psi \in L^2(\mathbb{R}^d)$, $\lim_{R\to\infty}\|\psi - P\psi\| = 0$, where P is the orthogonal projector on $\mathscr{P}_R(\mathbb{R}^d)$. Strictly speaking, we should use a symbol like P_R or even $P_R(\mathbb{R}^d)$ for the projector. However, R and d will always be clear from the context, so we are deliberately sloppy to obtain a concise formulation. For the same reason, we will sometimes simply write $\mathscr{P}$ or $\mathscr{P}_R$ for the space $\mathscr{P}_R(\mathbb{R}^d)$.

An important fact is that since H_{HO} is invariant under rigid spatial transformations (i.e., they conserve energy), so is each individual shell. That is, each shell $\mathscr{S}_r(\mathbb{R}^d)$, and thus $\mathscr{P}_R(\mathbb{R}^d)$, is independent of the spatial coordinates chosen.

For the case $d = 1$ each shell r is spanned by a single eigenfunction, namely $\phi_r(x)$. For $d = 2$, each shell r has degeneracy $r+1$, with eigenfunctions

$$\Phi_{(s,r-s)}(\vec{r}) = \phi_s(r_1)\phi_{r-s}(r_2), \quad 0 \leq s \leq r.$$

The usual HO eigenfunctions used to construct many-body wave functions are not the Hermite functions $\Phi_{\alpha_1,\cdots,\alpha_d}$, however, but rather those obtained by utilizing the spherical symmetry of the HO. This gives a many-body basis diagonal in angular momentum, cf. Sec. II B. For $d = 2$ we obtain the so-called Fock-Darwin orbitals given by

$$\Phi^{\mathrm{FD}}_{n,m}(r,\theta) = \left[\frac{2n!}{(n+|m|)!}\right]^{1/2} \frac{e^{im\theta}}{\sqrt{2\pi}} L_n^{|m|}(r^2) e^{-r^2/2}. \quad (5)$$

Here, $n \geq 0$ is the nodal quantum number, counting the nodes of the radial part, and m is the azimuthal quantum number. The eigenvalues are

$$\epsilon_{n,m} = 2n + |m| + 1.$$

Thus, $R = 2n + |m|$ is the shell number. By construction, the Fock-Darwin orbitals are eigenfunctions of the angular momentum operator $L_z = -i\partial/\partial_\theta$ with eigenvalue m. Of course, we may write $\Phi^{\mathrm{FD}}_{n,m}$ as a linear combination of the Hermite functions $\Phi_{(s,R-s)}$, where $0 \leq s \leq R = 2n + |m|$, and vice versa. The actual choice of form of eigenfunctions is immaterial, as long as we may identify those belonging to a given shell.

The space $\mathscr{P}_{R=4}(\mathbb{R}^2)$ is illustrated in Fig. 1 using both Hermite functions and Fock-Darwin orbitals.

B. Many-body wave functions

We now discuss N-body eigenfunctions of the HO in d dimensions, including spin. This enables us to identify the expansion of a many-body wave function with expansions in Hermite functions for $n = Nd$ dimensions.

Each particle $k = 1,\ldots,N$ has both spatial degrees of freedom $\vec{r}_k \in \mathbb{R}^d$ and a spin coordinate $\tau_k \in \{\pm 1\}$, corresponding to the z-projection $S_z = \pm\frac{\hbar}{2}$ of the electron spin. The configuration space can thus be taken as two copies X of $\mathbb{R}^d$; one for each spin value, i.e., $X = \mathbb{R}^d \times \{\pm 1\}$ and $x_k = (\vec{r}_k, \tau_k) \in X$ are the particle coordinates. Due to the Pauli exclusion principle, the many-body Hilbert space $\mathscr{H}(X,N)$ now consists of the part of $L^2(X^N)$ anti-symmetric with respect to exchanges of any two particles' coordinates, viz,

$$\mathscr{H}(X,N) = \bigwedge_{k=1}^{N} L^2(X) = P_{\mathrm{AS}} L^2(X^N),$$

where P_{AS} is the orthogonal projector onto the totally anti-symmetric functions. An identity is

$$L^2(X^N) \equiv L^2(\mathbb{R}^{Nd}) \otimes (\mathbb{C}^2)^N,$$

i.e., each $\psi \in L^2(X^N)$ is equivalent to 2^N component functions $\psi^{(\sigma)} \in L^2(\mathbb{R}^{Nd})$, $\sigma \in \{\pm 1\}^N$. Thus,

$$\psi(x_1,\cdots,x_N) = \sum_\sigma \psi^{(\sigma)}(\vec{r}_1,\cdots,\vec{r}_N)\chi_\sigma(\tau),$$

where $\tau = (\tau_1,\cdots,\tau_N)$, and where $\chi_\sigma(\tau) = \delta_{\sigma,\tau}$ are basis functions for the N-spinor space $(\mathbb{C}^2)^N$, being eigenfunctions for S_z, viz,

$$S_z\chi_\sigma = \frac{\hbar}{2}\sum_{k=1}^{N}\sigma_k.$$

Now, consider the Nd-dimensional HO as the sum of N HOs in d dimensions, viz,

$$H_{\mathrm{HO}}(\xi) = \sum_{k=1}^{N} H_{\mathrm{HO}}(\vec{r}_k) = -\frac{1}{2}\nabla_\xi^2 + \frac{1}{2}\|\xi\|^2,$$

where $\xi = (\vec{r}_1,\cdots,\vec{r}_N) \in \mathbb{R}^{Nd}$. One easily sees, that if $\alpha^k \in \mathscr{I}_d$, runs over all multi-indices, $k = 1,\cdots,N$, then

$$\beta := (\alpha^1,\cdots,\alpha^N) \in \mathscr{I}_{Nd}$$

is also an arbitrary multi-index. Moreover,

$$\Phi_\beta(\xi) \equiv \Phi_{\alpha^1}(\vec{r}_1)\cdots\Phi_{\alpha^N}(\vec{r}_N)$$

covers all possible Hermite functions in Nd dimensions.

Since functions on the form $\psi_{(\alpha,\sigma)}(\vec{r},\tau) = \Phi_\alpha(\vec{r})\chi^1_\sigma(\tau)$ (where χ^1_σ are basis functions for the single-particle spinor space $\mathbb{C}^2$) constitute a basis for $L^2(X)$, we construct a basis for $L^2(X^N)$ by taking direct products, viz,

$$\tilde{\Psi}_{\alpha^1,\cdots,\alpha^N,\sigma_1,\cdots,\sigma_N}(x_1,\cdots,x_N) = \Phi_\beta(\xi)\chi_\sigma(\tau)$$

which identifies the σ-component as the Hermite function $\Phi_\beta(\xi)$.

A basis of Slater determinants for $\mathscr{H}(X,N)$ is now constructed by anti-symmetrizing the basis for $L^2(X^N)$, see for example Ref. 16. To this end, we introduce a generalized single-particle index $i = i(\alpha,\sigma) \in \mathbb{N}$, so that an ordering on the single-particle basis functions $\Phi_\alpha\chi^1_\sigma$ is apparent. We also let $i_k := i(\alpha^k,\sigma_k)$. A Slater determinant $\Psi_{i_1,\cdots,i_k}(x_1,\cdots,x_N)$ is now defined by

$$\begin{aligned}\Psi_{i_1,\cdots,i_N} &:= \mathscr{A}\tilde{\Psi}_{i_1,\cdots,i_N}(x_1,\cdots,x_N)\\ &:= \sum_{p\in S_N}\mathrm{sgn}(p)\hat{p}\tilde{\Psi}_{i_1,\cdots,i_N}(x_1,\cdots,x_N).\end{aligned}$$

where $p \in S_N$ is a permutation of N symbols and $\mathscr{A}$ is the anti-symmetrization operator. The operator $\hat{p}$ permutes the arguments of the function on which it acts. We obtain

$$\begin{aligned}\hat{p}\tilde{\Psi}_{i_1,\cdots,i_N}(x_1,\cdots,x_N) &= \hat{p}\Phi_\beta(\xi)\chi_\sigma(\tau)\\ &= \Phi_{\beta'}(\xi)\chi_{\sigma'}(\tau),\end{aligned}$$

where

$$\beta' = (\alpha^{q(1)},\cdots,\alpha^{q(N)}), \quad \sigma' = (\sigma_{q(1)},\cdots,\sigma_{q(N)}),$$

where q is the inverse permutation of p. Hence, $\hat{p}\tilde{\Psi}_{i_1,\cdots,i_N}$ is simply a different Hermite function *within the same shell*, i.e., $|\beta'| = |\beta|$, with a different spin configuration.

It is now clear, that the Slater determinant $\Psi_{i_1,\cdots,i_N}$ will have spin components that are linear combinations of Hermite functions within a single shell $|\beta|$, i.e.,

$$\Psi^{(\sigma)}_{i_1,\cdots,i_N} \in \mathscr{S}_{|\beta|}(\mathbb{R}^{Nd}).$$

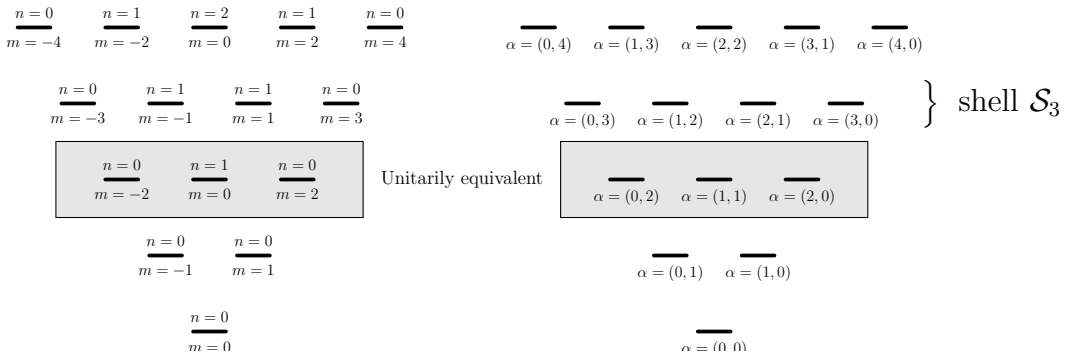

FIG. 1: Illustration of $\mathscr{P}_{R=4}(\mathbb{R}^2)$: (Left) Fock-Darwin orbitals. (Right) Hermite functions. Basis functions with equal HO energy are shown at same line.

Moreover, if we define the shell-truncated Hilbert space

$$\begin{aligned}\mathscr{P}_R(X^N) &:= P_R L^2(X^N) \\ &:= \text{span}\left\{\tilde{\Psi}_{i_1,\cdots,i_N} \,:\, |\beta| = \sum_k |\alpha^k| \leq R\right\} \\ &= \mathscr{P}_R(\mathbb{R}^{Nd}) \otimes (\mathbb{C}^2)^N,\end{aligned}$$

then it is easy to see that

$$\begin{aligned}P_{\text{AS}}\mathscr{P}_R(X^N) &= P_{\text{AS}} P_R L^2(X^N) \\ &= P_R P_{\text{AS}} L^2(X^N) = P_R \mathscr{H}(X,N),\end{aligned}$$

and that a basis for $P_{\text{AS}}\mathscr{P}_R(X^N)$ is given by

$$\left\{\Psi_{i_1,\cdots,i_N} \,:\, i_1 = i < \cdots < i_N,\, \sum_k |\alpha^k| \leq R\right\},$$

where $i_k = i_k(\alpha^k, \sigma_k)$, i.e., the Slater determinants with total single-particle shell number not greater than R. Notice the ordering on i_j, which is necessary to select only linearly independent Slater determinants.

We stress, that, $P_{\text{AS}}\mathscr{P}_R(X^N)$ is independent of the actual one-body HO eigenfunctions used. In actual computations, it may be more convenient to choose the Fock-Darwin orbitals as basis, for example.

As should be clear now, studying approximation of Hermite functions in arbitrary dimensions automatically gives us the corresponding many-body HO approximation theory, since the many-body eigenfunctions can be seen as 2^N component functions, and since the shell-truncated Hilbert space transfers to a many-body setting in a natural way, due to the separable nature of the many-dimensional harmonic oscillator.

C. Parabolic quantum dots

We consider N electrons confined in a harmonic oscillator in d dimensions. This is a very common model for a quantum dot, i.e., a device in which a number of interacting electrons are confined in a quasi-zero dimensional area using semi-conductor techniques, and are interesting due to their possible use as components of future quantum computing technologies.[3,17] We comment, that modelling the quantum dot geometry by a perturbed harmonic oscillator is justified by self-consistent calculations,[18–20] and is a widely adopted assumption.[8,12,13,21–23]

The Hamiltonian of the quantum dot is given by

$$H := T + U, \tag{6}$$

where T is the many-body HO Hamiltonian, and U is the inter-electron Coulomb interactions. Thus, in dimensionless units,

$$U := \sum_{i<j}^{N} C(i,j) = \sum_{i<j}^{N} \frac{\lambda}{\|\vec{r}_i - \vec{r}_j\|}.$$

The parameter λ measures the strength of the interaction over the confinement of the HO, viz,

$$\lambda := \frac{1}{\hbar\omega}\left(\frac{e^2}{4\pi\epsilon_0\epsilon}\right),$$

where we recall that $\sqrt{\hbar/m\omega}$ is the length unit. Typical values for GaAs semiconductors are close to $\lambda = 2$, see for example Ref. 23. Increasing the trap size leads to a larger λ, and the quantum dot then approaches the classical regime.[3]

D. Exact solution for two electrons

We are shortly prepared for the analysis of the approximation properties of the HO eigenfunctions. However, it is instructive to consider the very simplest example of a two-electron parabolic quantum dot, since this case admits analytical solutions for special values of λ.[24,25] Here, we consider $d = 2$ dimensions only, but the $d = 3$ case is similar. We note, that for $N = 2$ it is enough to study the spatial wave function, since it must be either symmetric (for the singlet $S = 0$ spin state) or anti-symmetric (for the triplet $S = 1$ spin states). The Hamiltonian (6) becomes

$$H = -\frac{1}{2}(\nabla_1^2 + \nabla_2^2) + \frac{1}{2}(r_1^2 + r_2^2) + \frac{\lambda}{r_{12}}, \tag{7}$$

where $r_{12} = \|\vec{r}_1 - \vec{r}_2\|$ and $r_j = \|\vec{r}_j\|$. Introduce a set of scaled centre of mass coordinates given by $\vec{R} = (\vec{r}_1 + \vec{r}_2)/\sqrt{2}$ and $\vec{r} = (\vec{r}_1 - \vec{r}_2)/\sqrt{2}$. This coordinate change is orthogonal and symmetric in $\mathbb{R}^4$. This leads to the manifestly separable Hamiltonian

$$\begin{aligned} H &= -\frac{1}{2}(\nabla_r^2 + \nabla_R^2) + \frac{1}{2}(\|\vec{r}\|^2 + \|\vec{R}\|^2) + \frac{\lambda}{\sqrt{2}\|\vec{r}\|} \\ &= H_{\rm HO}(\vec{R}) + H_{\rm rel}(\vec{r}). \end{aligned}$$

A complete set of eigenfunctions of H can now be written on product form, viz,

$$\Psi(\vec{R},\vec{r}) = \Phi^{\rm FD}_{n',m'}(\vec{R})\psi(\vec{r}).$$

The relative coordinate wave function $\psi(\vec{r})$ is an eigenfunction of the relative coordinate Hamiltonian given by

$$H_{\rm rel} = -\frac{1}{2}\nabla_r^2 + \frac{1}{2}r^2 + \frac{\lambda}{\sqrt{2}r}, \tag{8}$$

where $r = \|\vec{r}\|$. This Hamiltonian can be further separated using polar coordinates, yielding eigenfunctions on the form

$$\psi_{m,n}(r,\theta) = \frac{e^{im\theta}}{\sqrt{2\pi}}u_{n,m}(r),$$

where $|m| \geq 0$ is an integer and $u_{n,m}$ is an eigenfunction of the radial Hamiltonian given by

$$H_r = -\frac{1}{2r}\frac{\partial}{\partial r}r\frac{\partial}{\partial r} + \frac{|m|^2}{2r^2} + \frac{1}{2}r^2 + \frac{\lambda}{\sqrt{2}r}.$$

By convention, n counts the nodes away from $r = 0$ of $u_{n,m}(r)$. Moreover, odd (even) m gives anti-symmetric (symmetric) wave function $\Psi(\vec{r}_1,\vec{r}_2)$. For any given $|m|$, it is quite easy to deduce that the special value $\lambda = \sqrt{2|m|+1}$ yields the eigenfunction

$$u_{0,m} = Dr^{|m|}(a+r)e^{-r^2/2},$$

where D and a are constants. The corresponding eigenvalue of H_r is $E_r = |m| + 2$, and $E = 2n' + |m'| + 1 + E_r$. Thus, the ground state (having $m = m' = 0$, $n = n' = 0$) for $\lambda = 1$ is given by

$$\begin{aligned} \Psi_0(\vec{R},\vec{r}) &= D(r+a)e^{-(r^2+R^2)/2} \\ &= \frac{D}{\sqrt{2}}(r_{12} + \sqrt{2}a)e^{-(r_1^2+r_2^2)/2}, \end{aligned}$$

with D being a (new) normalization constant.

Observe that this function has a cusp at $r = 0$, i.e., at the origin $x = y = 0$ (where we have introduced Cartesian coordinates $\vec{r} = (x,y)$ for the relative coordinate). Indeed, the partial derivatives $\partial_x\psi_0$ and $\partial_y\psi_0$ are not continuous there, and Ψ_0 has no partial derivatives (in the distributional sense, see Appendix B) of second order. The cusp stems from the famous "cusp condition" which simply states that, for a non-vanishing wave function at $r_{12} = 0$, the Coulomb divergence must be compensated by a similar divergence in the Laplacian.[26,27] This is only possible if the wave function has a cusp.

On the other hand, the non-smooth function $\Psi_{0,0}(\vec{R},\vec{r})$ is to be expanded in the HO eigenfunctions, e.g., Fock-Darwin orbitals. (Recall, that the particular representation for the HO eigenfunctions are immaterial – also whether we use lab coordinates $\vec{r}_{1,2}$ or centre-of-mass coordinates $\vec{R}$ and $\vec{r}$, since the coordinate change is orthogonal.) For $m = 0$, we have

$$\Phi^{\rm FD}_{n,0}(r) = \sqrt{\frac{2}{\pi}}L_n(r^2)e^{-r^2/2},$$

using the fact that these are independent of θ. Thus,

$$\Psi_0(\vec{r}) = \Phi^{\rm FD}_{0,0}(R)u_{0,0}(r) = \Phi^{\rm FD}_{0,0}(R)\sum_{n=0}^{\infty} c_n\Phi^{\rm FD}_{n,0}(r), \tag{9}$$

The functions $\Phi^{\rm FD}_{n,0}(r)$ are very smooth, as is seen by noting that $L_n(r^2) = L_n(x^2+y^2)$ is a polynomial in x and y, while $u_{0,0}(r) = u_{0,0}(\sqrt{x^2+y^2})$, so Eqn. (9) is basically approximating a square root with a polynomial.

Consider then a truncated expansion $\Psi_{0,R} \in \mathscr{P}_R(\mathbb{R}^2)$, such as the one obtained with the CI or coupled cluster method.[7] In general, this is different from $P_R\Psi_0$, which is the best approximation of the wave function in $\mathscr{P}_R(\mathbb{R}^2)$. In any case, this expansion, consisting of the $R+1$ terms like those of Eqn. (9) is a very smooth function. Therefore, the cusp at $r = 0$ cannot be well approximated.

In Section III C, we will show that the smoothness properties of the wave function Ψ is equivalent to a certain decay rate of the coefficients c_n in Eqn. (9) as $n \to \infty$. In this case, we will show that

$$\sum_{n=0}^{\infty} n^k|c_n|^2 < +\infty,$$

so that

$$|c_n| = o(n^{-(k+1+\epsilon)/2}). \tag{10}$$

Here, k is the number of times Ψ may be differentiated weakly, i.e., $\Psi \in H^k(\mathbb{R}^2)$, and $\epsilon \in [0,1)$ is a constant. For the function Ψ_0 we have $k = 1$. This kind of estimate directly tells us that an approximation using only a few HO eigenfunctions necessarily will give an error depending directly on the smoothness k.

We comment, that for higher $|m|$ the eigenstates will still have cusps, albeit in the higher derivatives.[27] Indeed, we have weak derivatives of order $|m|+1$, as can easily be deduced by operating on $\psi_{0,m}$ with ∂_x and ∂_y. Moreover, recall that $|m| = 1$ is the $S = 1$ ground state, which then will have coefficients decaying faster than the $S = 0$ ground state. Moreover, there will be excited states, i.e., states with $|m| > 1$, that also have more quickly decaying coefficients $|c_n|$. This will be demonstrated numerically in Sec. V.

In fact, Hoffmann-Ostenhof *et al.*[27] have shown that near $r_{12} = 0$, for arbitrary λ *any* local solution Ψ of $(H-E)\Psi = 0$ has the form

$$\Psi(\xi) = \|\xi\|^m P\left(\frac{\xi}{\|\xi\|}\right)(1 + a\|\xi\|) + O(\|\xi\|^{m+1}),$$

where $\xi = (\vec{r}_1, \vec{r}_2) \in \mathbb{R}^4$, and where P, $\deg(P) = m$, is a hyperspherical harmonic (on S^3), and where a is a constant. This also generalizes to arbitrary N, cf. Sec. III D. From this representation, it is manifest, that $\Psi \in H^{m+1}(\mathbb{R}^4)$, i.e., Ψ has weak derivatives of order $m+1$. We discuss these results further in Sec. III D.

III. APPROXIMATION PROPERTIES OF HERMITE SERIES

A. Hermite functions in one dimension

We will now derive approximation properties for the Hermite functions, cf. Eqns. (1) and (4). We first consider the one-dimensional case, and then turn to the general case in Sec. III B. The multidimensional approach has, to the author's knowledge, not been published previously. The treatment for one-dimensional Hermite functions is similar, but not equivalent to, that given by Boyd[28] and Hille.[29] See Appendix B for definitions of L^2-spaces, weak derivatives and the Sobolev spaces H^k, used extensively throughout this section.

Recall that the Hermite functions $\phi_n \in L^2(\mathbb{R})$, where $n \in \mathbb{N}_0$ is a non-negative integer, are defined by

$$\phi_n(x) = (2^n n! \sqrt{\pi})^{-1/2} H_n(x) e^{-x^2/2}, \tag{11}$$

where $H_n(x)$ is the usual Hermite polynomial.

A well-known method for finding the eigenfunctions of H_{HO} in one dimension involves writing

$$H_{\mathrm{HO}} = a^\dagger a + \frac{1}{2},$$

where the ladder operator a is given by

$$a := \frac{1}{\sqrt{2}}(x + \partial_x),$$

with Hermitian adjoint $a^\dagger$ given by

$$a^\dagger := \frac{1}{\sqrt{2}}(x - \partial_x).$$

The name "ladder operator" comes from the important formulas

$$a\phi_n(x) = \sqrt{n}\phi_{n-1}(x) \tag{12}$$
$$a^\dagger\phi_n(x) = \sqrt{n+1}\phi_{n+1}(x), \tag{13}$$

valid for all n. This can easily be proved by using the recurrence relation (3). By repeatedly acting on ϕ_0 with $a^\dagger$ we generate every Hermite function, viz,

$$\phi_n(x) = n!^{-1/2}(a^\dagger)^n \phi_0(x). \tag{14}$$

As Hermite functions constitute a complete, orthonormal sequence in $L^2(\mathbb{R})$, any $\psi \in L^2(\mathbb{R})$ can be written as a series in Hermite functions, viz,

$$\psi(x) = \sum_{n=0}^{\infty} c_n \phi_n(x),$$

where the coefficients c_n are uniquely determined by $c_n = \langle \phi_n, \psi \rangle$.

An interesting fact is that the Hermite functions are also eigenfunctions of the Fourier transform with eigenvalues $(-i)^n$, as can easily be proved by induction by observing firstly that the Fourier transform of $\phi_0(x)$ is $\phi_0(k)$ itself, and secondly that the Fourier transform of $a^\dagger$ is $-ia^\dagger$ (acting on the variable y). It follows from completeness of the Hermite functions, that the Fourier transform defines a unitary operator on $L^2(\mathbb{R})$.

We now make a simple observation, namely that

$$(a^\dagger)^k \phi_n(x) = P_k(n)^{1/2} \phi_{n+k}(x), \tag{15}$$

where $P_k(n) = (n+k)!/n! > 0$ is a polynomial of degree k for $n \geq 0$. Moreover $P_k(n+1) > P_k(n)$ and $P_{k+1}(n) > P_k(n)$.

We now prove the following proposition:

Proposition 1 (Hermite series in one dimension) *Let $\psi \in L^2(\mathbb{R})$. Then*

1. *$a^\dagger\psi \in L^2(\mathbb{R})$ if and only if $a\psi \in L^2(\mathbb{R})$ if and only if $\sum_{n=0}^{\infty} n|c_n|^2 < +\infty$, where $c_n = \langle \phi_n, \psi \rangle$*
2. *$a^\dagger\psi \in L^2(\mathbb{R})$ if and only if $x\psi, \partial_x\psi \in L^2(\mathbb{R})$*
3. *$(a^\dagger)^{k+1}\psi \in L^2(\mathbb{R})$ implies $(a^\dagger)^k\psi \in L^2(\mathbb{R})$*
4. *$(a^\dagger)^k\psi \in L^2(\mathbb{R})$ if and only if*

$$\sum_{n=0}^{\infty} n^k |c_n|^2 < +\infty. \tag{16}$$

5. *$(a^\dagger)^k\psi \in L^2(\mathbb{R})$ if and only if $x^j\partial_x^{k-j}\psi \in L^2(\mathbb{R})$ for $0 \leq j \leq k$*

Proof: We have

$$\|a^\dagger\psi\|^2 = \sum_{n=0}^{\infty} (n+1)|c_n|^2 = \|\psi^2\| + \|a\psi\|^2,$$

from which statement 1 follows. Statement 2 follows from the definition of $a^\dagger$, and that $a^\dagger\psi \in L^2$ implies $a\psi \in L^2$ (since $\|a\psi\| \leq \|a^\dagger\psi\|$), which again implies $x\psi, \partial_x\psi \in L^2$. Statement 3 follows from the monotone behaviour of $P_k(n)$ as function of k. Statement 4 then follows. By iterating statement 2 and using $[\partial_x, x] = 1$ and statement 3, statement 5 follows. $\diamondsuit$

The significance of the condition $a^\dagger\psi \in L^2(\mathbb{R})$ is that the coefficients c_n of ψ must decay faster than for a completely arbitrary wave function in $L^2(\mathbb{R})$. Moreover, $a^\dagger\psi \in L^2(\mathbb{R})$ is the same as requiring $\partial_x\psi \in L^2(\mathbb{R})$, and $x\psi \in L^2(\mathbb{R})$. Proposition 1 also generalizes this fact for $(a^\dagger)^k\psi \in L^2(\mathbb{R})$, giving successfully quicker decay of the coefficients. In all cases, the decay is expressed in an average sense, through a growing weight function in a sum, as in Eqn. (16). Since the terms in the sum must converge to zero, this implies a pointwise faster decay, as stated in Eqn. (17) below.

We comment here, that the partial derivatives must be understood in the weak, or distributional, sense: Even though ψ may not be everywhere differentiable in the ordinary sense,

it may have a weak derivative. For example, if the classical derivative exists everywhere except for a countable set (and if it is in L^2), this is the weak derivative. Moreover, if this derivative has a jump discontinuity, there are no higher order weak derivatives. See Appendix B for a further discussion.

Loosely speaking, since $x\psi(x) \in L^2 \Leftrightarrow \partial_y \hat{\psi}(y) \in L^2$, where $\hat{\psi}(y)$ is the Fourier transform, point 2 of Prop. 1 is a combined smoothness condition on $\psi(x)$ and $\hat{\psi}(y)$. Point 5 is a generalization to higher derivatives, but is difficult to check in general for an arbitrary ψ. On the other hand, it is well-known that the eigenfunctions of many Hamiltonians of interest, such as the quantum dot Hamiltonian (6), decay exponentially fast as $\|\vec{r}\| \to \infty$. For such exponentially decaying functions over $\mathbb{R}^1$, $x^k\psi \in L^2(\mathbb{R})$ for all $k \geq 0$, i.e., $\hat{\psi}(y)$ is infinitely differentiable. We then have the following proposition:

Proposition 2 (Exponential decay in 1D)
Assume that $x^k\psi \in L^2(\mathbb{R})$ for all $k \geq 0$. Then a sufficient criterion for $(a^\dagger)^m\psi \in L^2(\mathbb{R})$ is $\partial_x^m\psi \in L^2(\mathbb{R})$, i.e., $\psi \in H^m(\mathbb{R})$. In fact, $x^k\partial_x^{m'}\psi \in L^2$ for all $m' < m$ and all $k \geq 0$.

Proof: We prove the Proposition inductively. We note that, since $\partial_x^m\psi \in L^2$ implies $\partial_x^{m-1}\psi \in L^2$, the proposition holds for $m-1$ if it holds for a given m. Moreover, it holds trivially for $m = 1$.

Assume then, that it holds for a given m, i.e., that $\psi \in H^m$ implies $x^k\partial_x^{m-j}\psi \in L^2$ for $1 \leq j \leq m$ and for all k (so that, in particular, $(a^\dagger)^m\psi \in L^2$). It remains to prove, that $\psi \in H^{m+1}$ implies $x^k\partial_x^m\psi \in L^2$, since then $(a^\dagger)^{m+1}\psi \in L^2$ by statement 5 of Proposition 1. We compute the norm and use integration by parts, viz,

$$\begin{aligned}\|x^k\partial_x^m\psi\|^2 &= \int_{\mathbb{R}} x^{2k}\partial_x^k\psi^*(x)\partial_x^k\psi(x) \\ &= -2k\langle\partial_x^m\psi, x^{2k-1}\partial_x^{m-1}\psi\rangle \\ &\quad -\langle\partial_x^{m+1}\psi, x^{2k}\partial_x^{m-1}\psi\rangle < +\infty.\end{aligned}$$

The boundary terms vanish. Therefore, $x^k\partial_x^m\psi \in L^2$ for all k, and the proof is complete. $\diamondsuit$

The proposition states that for the subset of $L^2(\mathbb{R})$ consisting of exponentially decaying functions, the approximation properties of the Hermite functions will *only* depend on the smoothness properties of ψ. Moreover, the derivatives up to the penultimate order decay exponentially as well. (The highest order derivative may decay much slower.)

From Prop. 1 and Prop. 2 we extract the following important characterization of the approximating properties of Hermite functions in $d = 1$ dimensions:

Proposition 3 (Approximation in one dimension)
Let $k \geq 0$ be a given integer. Let $\psi \in L^2(\mathbb{R})$ be given by

$$\psi(x) = \sum_{n=0}^{\infty} c_n\phi_n(x).$$

Then $\psi \in H^k(\mathbb{R})$ if and only if

$$\sum_{n=0}^{\infty} n^k|c_n|^2 < \infty.$$

The latter implies that

$$|c_n| = o(n^{-(k+1)/2}). \tag{17}$$

Let $\psi_R = P_R\psi = \sum_{n=0}^{R} c_n\phi_n$. Then

$$\|\psi - \psi_R\| = \left(\sum_{n=R+1}^{\infty} |c_n|^2\right)^{1/2}.$$

This is the central result for Hermite series approximation in $L^2(\mathbb{R}^1)$. Observe that Eqn. (17) implies that the error $\|\psi - \psi_R\|$ can easily be estimated. See also Prop. 6 and comments thereafter.

Now a word on pointwise convergence of the Hermite series. As the Hermite functions are uniformly bounded,[28] viz,

$$|\phi_n(x)| \leq 0.816 \quad \forall\, x \in \mathbb{R},$$

the pointwise error in ψ_R is bounded by

$$|\psi(x) - \psi_R(x)| \leq 0.816 \sum_{n=R+1}^{\infty} |c_n|.$$

Hence, if the sum on the right hand side is finite, the convergence is uniform. If the coefficients c_n decay rapidly enough, both errors can be estimated by the dominating neglected coefficients.

B. Analysis of multidimensional expansions

We now consider expansions of functions in $L^2(\mathbb{R}^n)$. To stress that $\mathbb{R}^n$ may be other than the configuration space of a single particle, we use the notation $x = (x_1, \cdots, x_n) \in \mathbb{R}^n$ instead of the previous $\vec{r} \in \mathbb{R}^d$. For N electrons in d spatial dimensions, $n = Nd$.

Recall that the Hermite functions over $\mathbb{R}^n$ are indexed by multi-indices $\alpha = (\alpha_1, \cdots, \alpha_n) \in \mathscr{I}_n$, and that

$$\Phi_\alpha(x) := \phi_{\alpha_1}(x_1)\cdots\phi_{\alpha_n}(x_n).$$

Now, to each spatial coordinate x_k define the ladder operators $a_k := (x_k + \partial_k)/\sqrt{2}$. These obey $[a_j, a_k] = 0$ and $[a_j, a_k^\dagger] = \delta_{j,k}$, as can easily be verified. Let $\mathbf{a}$ be a formal vector of the ladder operators, viz,

$$\mathbf{a} := (a_1, a_2, \ldots, a_n).$$

For the first Hermite function, we have

$$\Phi_0(x) := \pi^{-n/4}e^{-\|x\|^2/2}.$$

By using Eqn. (14) and Eqn. (A4), we may generate all other Hermite functions, viz,

$$\Phi_\alpha(x) := \alpha!^{-1/2}(\mathbf{a}^\dagger)^\alpha\Phi_0(x). \tag{18}$$

Given two multi-indices α and β, we define the polynomial $P_\alpha(\beta)$ by

$$P_\beta(\alpha) := \frac{(\alpha+\beta)!}{\alpha!} = \prod_{j=1}^{D} P_{\beta_j}(\alpha_j),$$

where P is defined for integers as before.

Since the Hermite functions Φ_α constitute a basis, any $\psi \in L^2(\mathbb{R}^n)$ can be expanded as

$$\psi(x) = \sum_\alpha c_\alpha \Phi_\alpha(x), \quad \|\psi\|^2 = \sum_\alpha |c_\alpha|^2, \tag{19}$$

where the sum is to be taken over all multi-indices $\alpha \in \mathscr{I}_n$. Now, let $\beta \in \mathscr{I}_n$ be arbitrary. By using Eqn. (13) in each spatial direction we compute the action of $(\mathbf{a}^\dagger)^\beta$ on ψ:

$$\begin{aligned}(\mathbf{a}^\dagger)^\beta \psi &= (a_1^\dagger)^{\beta_1} \cdots (a_n^\dagger)^{\beta_n} \sum_\alpha c_\alpha \Phi_\alpha \\ &= \sum_\alpha c_\alpha \prod_{k=1}^n \frac{(\alpha_k+\beta_k)!^{1/2}}{\alpha_k!^{1/2}} \Phi_{\alpha+\beta} \\ &= \sum_\alpha c_\alpha P_\beta(\alpha)^{1/2} \Phi_{\alpha+\beta}.\end{aligned}$$

Similarly, by using Eqn. (12) we obtain

$$\begin{aligned}\mathbf{a}^\beta \psi &= a_1^{\beta_1} \cdots a_n^{\beta_n} \sum_\alpha c_\alpha \Phi_\alpha \\ &= \sum_\alpha c_{\alpha+\beta} \prod_{k=1}^n \frac{(\alpha_k+\beta_k)!^{1/2}}{\alpha_k!^{1/2}} \Phi_\alpha \\ &= \sum_\alpha c_{\alpha+\beta} P_\beta(\alpha)^{1/2} \Phi_\alpha,\end{aligned}$$

Computing the square norm gives

$$\|(\mathbf{a}^\dagger)^\beta \psi\|^2 = \sum_\alpha P_\beta(\alpha) |c_\alpha|^2. \tag{20}$$

and

$$\|\mathbf{a}^\beta \psi\|^2 = \sum_\alpha P_\beta(\alpha) |c_{\alpha+\beta}|^2. \tag{21}$$

The polynomial $P_\beta(\alpha) > 0$ for all $\beta, \alpha \in \mathscr{I}_n$, and $P_\beta(\alpha + \alpha') > P_\beta(\alpha)$ for all non-zero multi-indices $\alpha' \neq 0$. Therefore, if $(\mathbf{a}^\dagger)^\beta \psi \in L^2(\mathbb{R}^n)$ then $\mathbf{a}^\beta \psi \in L^2(\mathbb{R}^n)$. However, the converse is not true for $n > 1$ dimensions, as the norm in Eqn. (21) is independent of infinitely many coefficients c_α, while Eqn. (20) is not. (This should be contrasted with the one-dimensional case, where $a\psi \in L^2(\mathbb{R})$ was *equivalent* to $a^\dagger \psi \in L^2(\mathbb{R})$.) On the other hand, as in the $n = 1$ case, the condition $a_k^\dagger \psi \in L^2(\mathbb{R}^n)$ is equivalent to the conditions $x_k \psi \in L^2(\mathbb{R}^n)$ and $\partial_k \psi \in L^2(\mathbb{R}^n)$.

We are in position to formulate a straightforward generalization of Prop. 1. The proof is easy, so we omit it.

Proposition 4 (General Hermite expansions)
Let $\psi \in L^2(\mathbb{R}^n)$, with coefficients c_α as in Eqn. (19), and let $\beta \in \mathscr{I}_n$ be arbitrary. Assume $(\mathbf{a}^\dagger)^\beta \psi \in L^2(\mathbb{R}^n)$. Then $(\mathbf{a}^\dagger)^{\beta'} \psi \in L^2(\mathbb{R}^n)$ and $\mathbf{a}^{\beta'} \psi \in L^2(\mathbb{R}^n)$ for all $\beta' \leq \beta$. Moreover, the following points are equivalent:

1. *$(\mathbf{a}^\dagger)^\beta \psi \in L^2(\mathbb{R}^n)$*
2. *For all multi-indices $\gamma \leq \beta$, $x^\gamma \partial^{\beta-\gamma} \psi \in L^2(\mathbb{R}^n)$.*
3. *$\sum_\alpha \alpha^\beta |c_\alpha|^2 < +\infty$*

We observe, that as we obtained for $n = 1$, condition 2 is a combined decay and smoothness condition on ψ, and that this can be expressed as a decay-condition on the coefficients of ψ in the Hermite basis by 3.

Exponential decay of $\psi \in L^2(\mathbb{R}^n)$ implies that that $x^\gamma \psi \in L^2(\mathbb{R}^n)$ for all $\gamma \in \mathscr{I}_n$. We now generalize Proposition 2 to the n-dimensional case.

Proposition 5 (Exponentially decaying functions)
Assume that $\psi \in L^2(\mathbb{R}^n)$ is such that for all $\gamma \in \mathscr{I}_n$, $x^\gamma \psi \in L^2(\mathbb{R}^n)$. Then, a sufficient criterion for $(\mathbf{a}^\dagger)^\beta \psi \in L^2(\mathbb{R}^n)$ is $\partial^\beta \psi \in L^2(\mathbb{R}^n)$. Moreover, for all $\mu \leq \beta$, we have $x^\gamma \partial^{\beta-\mu} \psi \in L^2(\mathbb{R}^n)$ for all $\gamma \in \mathscr{I}_n$ such that $\gamma_k = 0$ whenever $\mu_k = 0$, i.e., the partial derivatives of lower order than β decay exponentially in the directions where the differentiation order is lower.

Proof: The proof is a straightforward application of the $n = 1$ case in an inductive proof, together with the following elementary fact concerning weak derivatives: If $1 \leq j < k \leq n$, and if $x_j \psi(x)$ and $\partial_k \psi(x)$ are in $L^2(\mathbb{R}^n)$, then, by the product rule, $\partial_k(x_j \psi(x)) = x_j(\partial_k \psi(x)) \in L^2(\mathbb{R}^n)$. Notice, that Prop. 2 trivially generalizes to a single index in n dimensions, i.e., to $\beta = \beta_k e_k$, since the integration by parts formula used is valid in $\mathbb{R}^n$ as well. Similarly, the present Proposition is valid in $n-1$ dimensions, it is valid for $\bar{\beta} = (0, \beta_2, \cdots, \beta_n)$.

Assume that our statement holds for $n-1$ dimensions. We must prove that it then holds in n dimensions. Assume then, that $\partial^\beta \psi \in L^2(\mathbb{R}^n)$. Let $\phi = \partial^{\bar{\beta}} \psi \in L^2$. Moreover, $\partial_1^{\beta_1} \phi \in L^2$. Since ψ is exponentially decaying, and by the product rule, $x_1^{\gamma_1} \phi \in L^2$ for all $\gamma_1 \geq 0$. By Prop. 2, $x_1^{\gamma_1} \partial_1^{\beta_1 - \mu_1} \phi \in L^2$ for all γ_1 and $0 < \mu_1 \leq \beta_1$. Thus, $x_1^{\gamma_1} \partial^{\beta - e_1 \mu_1} \psi \in L^2$. Thus, the result holds as long as $\mu = e_1 \mu_1$; or equivalently $\mu = e_k \mu_k$ for any k. To apply induction, let $\chi = x_1^{\gamma_1} \partial_1^{\beta_1 - \mu_1} \psi \in L^2$. Note that $\partial^{\bar{\beta}} \chi \in L^2$ and $x^{\bar{\gamma}} \chi \in L^2$ for all $\bar{\gamma} = (0, \gamma_2, \cdots, \gamma_n)$. But by the induction hypothesis, $x^{\bar{\gamma}} \partial^{\bar{\beta} - \bar{\mu}} \chi \in L^2$ for all $\bar{\mu} \leq \bar{\beta}$ and all $\bar{\gamma}$ such that $\bar{\gamma}_k = 0$ if $\bar{\mu}_k = 0$. This yields, using the product rule, that $x^\gamma \partial^{\beta - \mu} \psi \in L^2$ for all $\mu \leq \beta$ and all γ such that $\gamma_k = 0$ if $\mu_k = 0$, which was the hypothesis for n dimensions, and the proof is complete. Notice, that we have proved that $(\mathbf{a}^\dagger)^\beta \psi \in L^2$ as a by-product. $\diamondsuit$

In order to generate a simple and useful result for approximation in n dimensions, we consider the case where ψ decays exponentially, and $\psi \in H^k(\mathbb{R}^n)$, i.e., $\partial^\beta \psi(x) \in L^2(\mathbb{R}^n)$ for all $\beta \in \mathscr{I}_n$ with $|\beta| = k$. In this case, we may also generalize Eqn. (17). For this, we consider the shell-weight $p(r)$ defined by

$$p(r) := \sum_{\alpha \in \mathscr{I}_n,\, |\alpha| = r} |c_\alpha|^2, \tag{22}$$

where $c_\alpha = \langle \Phi_\alpha, \psi \rangle$. Then, $\|\psi\|^2 = \sum_{r=0}^\infty p(r)$. Moreover, if P projects onto the shell-truncated Hilbert space $\mathscr{P}_R(\mathbb{R}^n)$, then

$$\|P\psi\|^2 = \sum_{r=0}^R p(r).$$

Proposition 6 (Approximation in n dimensions)
Let $\psi \in L^2(\mathbb{R}^n)$ be exponentially decaying and given by

$$\psi(x) = \sum_\alpha c_\alpha \Phi_\alpha(x).$$

Then $\psi \in H^k(\mathbb{R}^n)$, $k \geq 0$, if and only if

$$\sum_\alpha |\alpha|^k |c_\alpha|^2 = \sum_{r=0}^{\infty} r^k p(r) < +\infty. \tag{23}$$

The latter implies that

$$p(r) = o(r^{-(k+1)}). \tag{24}$$

Moreover, for the shell-truncated Hilbert space $\mathscr{P}_R$, the approximation error is given by

$$\|(1-P)\psi\| = \left(\sum_{r=R+1}^{\infty} p(r) \right)^{1/2}. \tag{25}$$

Proof: The only non-trivial part of the proof concerns Eqn. (23). Since ψ is exponentially decaying and since $\psi \in H^k$ if and only if $\partial^\beta \psi \in L^2$ for all β, $|\beta| \leq k$, we know that $\sum_\alpha \alpha^\beta |c_\alpha|^2 < +\infty$ for all β, $|\beta| \leq k$. Since $|\alpha|^k$ is a polynomial of order k with terms of type $a_\beta \alpha^\beta$, $a_\beta \geq 0$ and $|\beta| = k$, we have

$$\sum_\alpha |\alpha|^k |c_\alpha|^2 = \sum_{\beta,\,|\beta|=k} a_\beta \sum_\alpha \alpha^\beta |c_\alpha|^2 < +\infty.$$

On the other hand, since $a_\beta \geq 0$ and the sum over β has finitely many terms, $\sum_\alpha |\alpha|^k |c_\alpha| < +\infty$ implies $\sum_\alpha \alpha^\beta |c_\alpha|^2 < +\infty$ for all β, $|\beta| = k$, and thus $\psi \in H^k$ since ψ was exponentially decaying. $\diamondsuit$

In applications, we often observe a decay of non-integral order, i.e., there exists an $\epsilon \in [0,1)$ such that we observe

$$p(r) = o(r^{-(k+1+\epsilon)}). \tag{26}$$

This does not, of course, contradict our analysis. To see this, we observe that if $\psi \in H^k(\mathbb{R}^n)$ but $\psi \notin H^{k+1}(\mathbb{R}^n)$, then $p(r)$ must decay at least as fast as $o(r^{-(k+1)})$ but as fast as $o(r^{-k+2})$. Thus, the decay exponent can be anything inside the interval $[k+1, k+2)$.

Consider also the case where $\psi \in H^k(\mathbb{R}^n)$ for every k, i.e., we can differentiate it (weakly) as many times we like. Then $p(r)$ decays faster than $r^{-(k+1)}$, for any $k \geq 0$, giving so-called exponential convergence of the Hermite series. Hence, functions that are best approximated by Hermite series are rapidly decaying *and* very smooth functions ψ.

C. Two electrons revisited

To clarify how the preceding discussion can be applied, we return to the exact solutions of the two-electron quantum dot considered in Sec. II D. Recall, that the wave functions were on the form

$$\psi(r,\theta) = e^{im\theta} f(r),$$

where $f(r)$ decayed exponentially fast as $r \to \infty$. Assume now, that $\psi \in H^k(\mathbb{R}^2)$, i.e., that all partial derivatives of ψ of order k exists in the weak sense, viz,

$$\partial_x^j \partial_y^{k-j} \psi \in L^2(\mathbb{R}^2), \quad 0 \leq j \leq k,$$

where $x = r\cos(\theta)$ and $y = r\sin(\theta)$. Then, by Proposition 5, $(a_x^\dagger)^j (a_y^\dagger)^{k-j} \psi \in L^2(\mathbb{R}^2)$ for $0 \leq j \leq k$ as well.

The function $\psi(r,\theta)$ was expanded in Fock-Darwin orbitals, viz,

$$\psi(r,\theta) = \sum_{n=0}^{\infty} c_n \Phi_{n,m}^{\mathrm{FD}}(r,\theta).$$

Recall, that the shell number N for $\Phi_{n,m}^{\mathrm{FD}}$ was given by $N = 2n + |m|$. Thus, the shell-weight $p(N)$ is in this case simply

$$p(N) = |c_{(N-|m|)/2}|^2, \quad N \geq |m|,$$

and $p(N) = 0$ otherwise. From Prop. 6, we have

$$\sum_{N=|m|}^{\infty} N^k p(N) < +\infty,$$

which yields

$$|c_n| = o(n^{-(k+1+\epsilon)/2}), \quad 0 \leq \epsilon < 1,$$

as claimed in Sec. II D.

D. The analytic properties of many-electron wave functions

As we now have established the impact of weak regularity of the eigenfunctions on the approximation properties of the HO eigenfunctions for arbitrary number of particles N and spatial dimensions d, we mention some results, mainly due to Hoffmann-Ostenhof *et al.*,[27,30] concerning smoothness of many-electron wave functions. Strictly speaking, their results are valid only in $d = 3$ spatial dimensions, since the Coulomb interaction in $d = 2$ dimensions fails to be a Kato potential, the definition of which is quite subtle and out of the scope for this article. See, however, Ref. 30. On the other hand, it is reasonable to assume that the results will still hold true, since the analytical results of the $N = 2$ case is very similar in the $d = 2$ and $d = 3$ cases: The eigenfunctions decay exponentially with the same cusp singularities at the origin.[24,25]

Consider the Schrödinger equation $(H-E)\psi(\xi) = 0$, where $\xi = (\xi_1, \cdots, \xi_{Nd}) = (\vec{r}_1, \cdots, \vec{r}_N) \in \mathbb{R}^{Nd}$, and where $\psi(\xi)$ is assumed only to be a solution locally, i.e., it may fail to satisfy the boundary conditions. (A proper solution is of course also a local solution.) Recall, that ψ has 2^N spin-components. Define a coalesce point ξ_{CP} as a point where at least two particles coincide, i.e., $\vec{r}_j = \vec{r}_\ell$, $j \neq \ell$. Away from the set of such points, $\psi(\xi)$ is real analytic, since the interaction is real analytic there. Near a ξ_{CP}, the wave function has the form

$$\psi(\xi + \xi_{\mathrm{CP}}) = r^k P(\xi/r)(1 + ar) + O(r^{k+1}),$$

where $r = \|\xi\|$, P is a hyper-spherical harmonic (on the sphere S^{Nd-1}) of degree $k = k(\xi_{\rm CP})$, and where a is a constant. It is immediately clear, that $\psi(\xi)$ is $k+1$ times weakly differentiable in a neighborhood of $\xi_{\rm CP}$. However, at K-electron coalesce points, i.e., at points $\xi_{\rm CP}$ where K different electrons coincide, the integer k may differ. Using exponential decay of a proper eigenfunction, we have $\psi \in H^{\min(k)+1}(\mathbb{R}^{Nd})$. Hoffmann-Ostenhof *et al.* also showed, that symmetry restrictions on the spin-components due to the Pauli principle induces an increasing degree k of the hyper-spherical harmonic P, generating even higher order of smoothness. A general feature, is that the smoothness increases with the number of particles.

However, their results in this direction are not general enough to ascertain the *minimum* of the values for k for a given wave function, although we feel rather sure that such an analysis is possible. This is, however, left for future work. Suffice it to say, that the results are clearly visible in the numerical calculations in Sec. V.

Another interesting direction of research has been undertaken by Yserentant,[31] who showed that there are some very high order mixed partial derivatives at coalesce points. It seems unclear, though, if this can be exploited to improve the CI calculations further.

IV. THE CONFIGURATION INTERACTION METHOD

A. Convergence analysis using HO eigenfunction basis

The basic problem is to determine a few eigenvalues and eigenfunctions of the Hamiltonian H in Eqn. (6), i.e.,

$$H\psi_k = E_k\psi_k, \quad k = 1, \cdots, k_{\max}.$$

The CI method consists of approximating eigenvalues of H with those obtained by projecting the problem onto a finite-dimensional subspace $\mathscr{H}_h \subset \mathscr{H}(X,N)$, where $X = \mathbb{R}^d \times \{\pm 1\}$ as in Sec. II B. Thus, it is identical to the Ritz-Galerkin variational method.[15,32,33] We comment, that the convergence of the Ritz-Galerkin method is *not* simply a consequence of the completeness of the basis functions.[15] We will analyze the CI method when the model space is given by

$$\begin{aligned}\mathscr{H}_h &= P_R\mathscr{H}(X,N) = \mathscr{P}_R(N)\\ &= \text{span}\left\{\Psi_{i_1,\cdots,i_N} \,:\, \sum_k |\alpha^k| \le R\right\},\end{aligned}$$

used in Refs. 11,34, for example, although other spaces also are common. The space $\mathscr{P}_R(N)$ given by

$$\mathscr{M}_R(N) := \text{span}\left\{\Psi_{i_1,\cdots,i_N} \,:\, \forall k,\ |\alpha^k| \le R\right\},$$

i.e., a cut in the single-particle shell numbers instead of the global shell number is also common.[9,12] For obvious reasons, $\mathscr{P}_R(N)$ is often referred to as an "energy cut space", while $\mathscr{M}_R(N)$ is referred to as a "direct product space". See also Ref. 4 for a further discussion.

As in Sec. III B, P_R is the orthogonal projector onto the model space $\mathscr{P}_R(N)$. We also define $Q_R = 1 - P_R$ as the projector onto the excluded space $\mathscr{H}_h^{\perp}$. The discrete eigenvalue problem is then

$$(P_RHP_R)\psi_{h,k} = E_{h,k}\psi_{h,k}, \quad k = 1, \cdots, k_{\max}.$$

Recall from Sec. II B, that each $\psi \in \mathscr{H}(N)$ can be viewed as 2^N component wave functions $\psi^{(\sigma)}$, each σ corresponding to a different configuration of the N spin projections. In terms of Hermite functions in $n = Nd$ dimensions, we write

$$\psi^{(\sigma)}(\vec{r}_1, \cdots, \vec{r}_N) := \sum_\alpha c_\alpha^{(\sigma)} \Phi_\alpha(\vec{r}_1, \cdots, \vec{r}_N)$$

with corresponding shell-weights $p(r)^{(\sigma)}$, viz,

$$p(r)^{(\sigma)} := \sum_{\alpha;\, |\alpha| = r} |c_\alpha^{(\sigma)}|.$$

The CI method becomes, in principle, exact as $R \to \infty$. Indeed, a widely-used name for the CI method is "exact diagonalization." This is somewhat a misnomer in light of the analysis presented here and the fact that only a very limited number of degrees of freedom per particle is achievable.

It is clear that

$$\mathscr{P}_R(N) \subset \mathscr{M}_R(N) \subset \mathscr{P}_{NR}(N), \tag{27}$$

so that studying the convergence in terms of $\mathscr{P}_R(N)$ is sufficient. In our numerical experiments we focus on the energy cut model space. A comparison between the convergence of the two spaces is, on the other hand, an interesting topic for future research.

Using the results in Refs. 15,35 for non-degenerate eigenvalues, we obtain an estimate for the error in the numerical eigenvalue E_h as

$$E_h - E \le [1 + \nu(R)](1 + K\lambda)\langle\psi, Q_RT\psi\rangle, \tag{28}$$

where K is a constant, and where $\nu(R) \to 0$ as $R \to \infty$. Using $T\Phi_\alpha = (Nd/2 + |\alpha|)\Phi_\alpha$ and Eqn. (23), we obtain

$$\langle\psi, Q_RT\psi\rangle = \sum_{r=R+1}^{\infty} \left(\frac{Nd}{2} + r\right) \sum_\sigma p^{(\sigma)}(r).$$

Assume now, that $\psi^{(\sigma)} \in H^k(\mathbb{R}^{Nd})$ for all σ, so that according to Prop. 6, we will have

$$\sum_{r=0}^{\infty} r^k p^{(\sigma)}(r) < +\infty$$

for all 2^N values σ, implying that $rp^{(\sigma)}(r) = o(r^{-k})$. We then obtain, for $k > 1$,

$$\langle\psi, (1 - P_R)T\psi\rangle = o(R^{-(k-1)}) + o(R^{-k}).$$

For $k = 1$ (which is the worst case), we merely obtain $\langle\psi, (1-P_R)T\psi\rangle \to 0$ as $R \to \infty$. We assume, that R is sufficiently large, so that the $o(R^{-k})$ term can be neglected.

Again, we may observe a slight deviation from the decay, confer discussion after Prop. 6. Thus, we expect to observe eigenvalue errors on the form

$$E_h - E \sim (1+K\lambda)R^{-(k-1+\epsilon)}, \tag{29}$$

where $0 \leq \epsilon < 1$.

As for the eigenvector error $\|\psi_h - \psi\|$ (recall that $\psi_h \neq P_R\psi$), we mention that

$$\|\psi_h - \psi\| \leq [1+\eta(R)]\left[(1+K\lambda)\langle\psi, (1-P_R)T\psi\rangle\right]^{1/2},$$

where $\eta(R) \to 0$ as $R \to \infty$.

B. Effective interaction scheme

Effective interactions have a long tradition in nuclear physics, where the bare nuclear interaction is basically unknown and highly singular, and where it must be renormalized and fitted to experimental data.[1] In quantum chemistry and atomic physics, the Coulomb interaction is well-known so there is no intrinsic need to formulate an effective interaction. However, in lieu of the in general low order of convergence implied by Eqn. (29), we believe that HO-based calculations of the CI and coupled cluster type in general may benefit from the use of effective interactions.

A complete account of the effective interaction scheme outlined here is out of scope for the present article, but we refer to Refs. 4,14,36,37 for details as well as numerical algorithms.

Recall, that the interaction is given by

$$U = \sum_{i<j}^{N} C(i,j) = \sum_{i<j}^{N} \frac{\lambda}{\|\vec{r}_i - \vec{r}_j\|},$$

a sum of fundamental two-body interactions. For the $N = 2$ problem we have, in principle, the exact solution, since the Hamiltonian (7) can be reduced to a one-dimensional radial equation, e.g., the eigenproblem of H_r defined in Eqn. (8). This equation may be solved to arbitrarily high precision using various methods, for example using a basis expansion in generalized half-range Hermite functions.[38] In nuclear physics, a common approach is to take the best two-body CI calculations available, where $R = O(10^3)$, as "exact" for this purpose.

We now define the effective Hamiltonian for $N = 2$ as a Hermitian operator H_{eff} defined only within $\mathscr{P}_R(N=2)$ that gives $K = \dim[\mathscr{P}_R(N=2)]$ *exact* eigenvalues E_k of H, and K approximate eigenvectors $\psi_{\text{eff},k}$. Of course, there are infinitely many choices for the K eigenpairs, but by treating $U = \lambda/r_{12}$ as a perturbation, and "following" the unperturbed HO eigenpairs ($\lambda = 0$) through increasing values of λ, one makes the eigenvalues unique.[4,39] The approximate eigenvectors $\psi_{\text{eff},k} \in \mathscr{P}_R(N=2)$ are chosen by minimizing the distance to the exact eigenvectors $\psi_k \in \mathscr{H}(N=2)$ while retaining orthonormality.[36] This uniquely defines H_{eff} for the two-body system. In terms of matrices, we have

$$H_{\text{eff}} = \tilde{U}\,\text{diag}(E_1, \cdots, E_K)\tilde{U}^\dagger, \tag{30}$$

where X and Y are unitary matrices defined as follows. Let U be the $K \times K$ matrix whose k'th column is the coefficients of $P_R\psi_k$. Then the singular value decomposition of U can be written

$$U = X\Sigma Y^\dagger,$$

where Σ is diagonal. Then,

$$\tilde{U} := XY^\dagger.$$

The columns of $\tilde{U}$ are the projections $P_R\psi_k$ "straightened out" to an orthonormal set. Eqn. (30) is simply the spectral decomposition of H_{eff}. Although different in form than most implementations in the literature (e.g., Ref. 14), it is equivalent.

The effective two-body interaction $C_{\text{eff}}(i,j)$ is now given by

$$C_{\text{eff}}(1,2) := H_{\text{eff}} - P_R T P_R,$$

which is defined only within $\mathscr{P}_R(N=2)$.

The N-body effective Hamiltonian is defined by

$$H_{\text{eff}} := P_R T P_R + \sum_{i<j}^{N} C_{\text{eff}}(i,j), \tag{31}$$

where P_R projects onto $\mathscr{P}_R(N)$, and thus H_{eff} is defined *only* within $\mathscr{P}_R(N)$. The diagonalization of $H_{\text{eff}}(N)$ is equivalent to a perturbation technique where a certain class of diagrams is summed to infinite order in the full problem.[37]

Rigorous mathematical treatment of the convergence properties of the effective interaction is, to the author's knowledge, not available. Effective interactions have, however, enjoyed great success in the nuclear physics community, and we strongly believe that we soon will see sufficient proof of the improved accuracy with this method. Indeed, in Sec. V we see clear evidence of the accuracy boost when using an effective interaction.

V. NUMERICAL RESULTS

A. Code description

We now present numerical results using the full configuration-interaction method for $N = 2$–5 electrons in $d = 2$ dimensions. We will use both the "bare" Hamiltonian $H = T + U$ and the effective Hamiltonian (31).

Since the Hamiltonian commutes with angular momentum L_z, the latter taking on eigenvalues $M \in \mathbb{Z}$, the Hamiltonian matrix is block diagonal. (Recall, that the Fock-Darwin orbitals $\Phi^{\text{FD}}_{n,m}$ are eigenstates of L_z with eigenvalue m, so each Slater determinant has eigenvalue $M = \sum_{k=1}^{N} m_k$.) Moreover, the calculations are done in a basis of joint eigenfunctions for total electron spin S^2 and its projection S_z, as opposed to the Slater determinant basis used for convergence analysis. Such basis functions are simply linear combinations of Slater determinants within the same shell, and further reduce the dimensionality of the Hamiltonian matrix.[12] The eigenfunctions of

H are thus labeled with the total spin $S = 0, 1, \cdots, \frac{N}{2}$ for even N and $S = \frac{1}{2}, \frac{3}{2}, \cdots, \frac{N}{2}$ for odd N, as well as the total angular momentum $M = 0, 1, \cdots$. ($-M$ produce the same eigenvalues as M, by symmetry.) We thus split $\mathscr{P}_R(N)$ (or $\mathscr{M}_R(N)$) into invariant subspaces $\mathscr{P}_R(N,M,S)$ ($\mathscr{M}_R(N,M,S)$) and perform computations solely within these, viz,

$$\mathscr{P}_R(N) = \bigoplus_{M,S} \mathscr{P}_R(N,M,S).$$

The calculations were carried out with a code similar to that described by Rontani *et al.* in Ref. 12. Table I shows comparisons of the present code with that of Table IV of Ref. 12 for various parameters using the model space $\mathscr{M}_R(N,M,S)$. Table I also shows the case $\lambda = 1$, $N = 2$, $M = 0$, and $S = 0$, whose exact lowest eigenvalue is $E_0 = 3$, cf. Sec. II D. We note that there are some discrepancies between the results in the last digits of the results of Ref. 12. The spaces $\mathscr{M}_R(N)$ were identical in the two approaches, i.e., the number of basis functions and the number of non-zero matrix elements produced are cross-checked and identical.

We have checked that the code also reproduces the results of Refs. 11,13,40, using the $\mathscr{P}_R(N,M,S)$ spaces. Our code will be published and described in detail elsewhere,[41] where it will also be demonstrated that it reproduces the eigenvalues of an analytically solvable N-particle system[42] to machine precision.

B. Experiments

For the remainder, we only use the energy cut spaces $\mathscr{P}_R(N,M,S)$. Figure 2 shows the development of the lowest eigenvalue $E_0 = E_0(N,M,S)$ for $N = 4$, $M = 0, 1, 2$ and $S = 0$ as function of the shell truncation parameter R, using both Hamiltonians H and H_{eff}. Apparently, the effective interaction eigenvalues provide estimates for the ground state eigenvalues that are better than the bare interaction eigenvalues. This effect is attenuated with higher N, due to the fact that the two-electron effective Coulomb interaction does not take into account three- and many-body effects which become substantial for higher N.

We take the H_{eff}-eigenvalues as "exact" and graph the relative error in $E_0(N,M,S)$ as function of R on a logarithmic scale in Fig. 3, in anticipation of the relation

$$\ln(E_h - E) \approx C + \alpha \ln R, \quad \alpha = -(k - 1 + \epsilon). \tag{32}$$

The graphs show straight lines for large R, while for small R there is a transient region of non-straight lines. For $N = 5$, however, $\lambda = 2$ is too large a value to reach the linear regime for the range of R available, so in this case we chose to plot the corresponding error for the very small value $\lambda = 0.2$, showing clear straight lines in the error. The slopes are more or less independent of λ, as observed in different calculations.

In Fig. 4 we show the corresponding graphs when using the effective Hamiltonian H_{eff}. We estimate the relative error as before, leading to artifacts for the largest values of R due to the fact that there is a finite error in the best estimates for

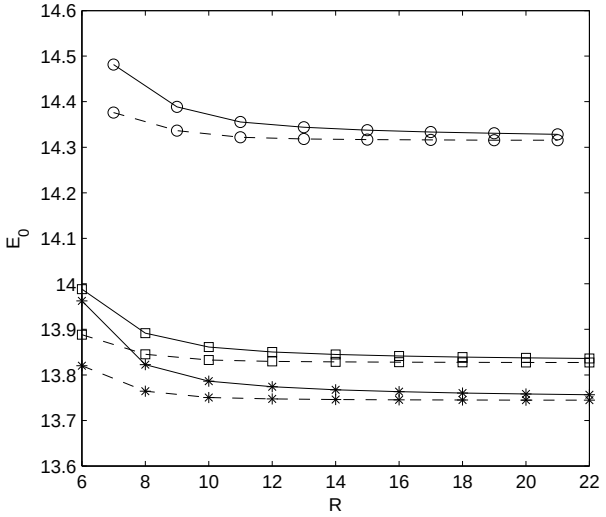

FIG. 2: Eigenvalues for $N = 4$, $S = 0$, $\lambda = 2$ as function of R for H (solid) and H_{eff} (dashed). $M = 0, 1$ and 2 are represented by squares, circles and stars, resp.

the eigenvalues. However, in all cases there are clear, linear regions, in which we estimate the slope α. In all cases, the slope can be seen to decrease by at least $\Delta\alpha \approx -1$ compared to Fig. 3, indicating that the effective interaction indeed accelerates the CI convergence by at least an order of magnitude. We also observe, that the relative errors are improved by an order of magnitude or more for the lowest values of R shown, indicating the gain in accuracy when using small model spaces with the effective interaction.

Notice, that for symmetry reasons only even (odd) R for even (odd) M yields increases in basis size $\dim[\mathscr{P}_R(N,M,S)]$, so only these values are included in the plots.

To overcome the limitations of the two-body effective interaction for higher N, an effective three-body interaction could be considered, and is hotly debated in the nuclear physics community. (In nuclear physics, there are also more complicated three-body effective forces that need to be included.[43]) However, this will lead to a huge increase in memory consumption due to extra nonzero matrix elements. At the moment, there are no methods available that can generate the exact three-body effective interaction with sufficient precision.

We stress, that the relative error decreases very slowly in general. It is a common misconception, that if a number of digits of $E_0(N,M,S)$ is unchanged between R and $R+2$, then these digits have converged. This is not the case, as is easily seen from Fig. 3. Take for instance $N = 4$, $M = 0$ and $S = 0$, and $\lambda = 2$. For $R = 14$ and $R = 16$ we have $E_0 = 13.84491$ and $E_0 = 13.84153$, respectively, which would give a relative error estimate of 2.4×10^{-4}, while the correct relative error is 1.3×10^{-3}.

The slopes in Fig. 3 vary greatly, showing that the eigenfunctions indeed have varying global smoothness, as predicted in Sec. III D. For $(N,M,S) = (5,3,5/2)$, for example, $\alpha \approx -4.2$, indicating that $\psi \in H^5(\mathbb{R}^{10})$. It seems, that higher

TABLE I: Comparison of current code and Ref. 12

				$R=5$		$R=6$		$R=7$	
N	λ	M	$2S$	Current	Ref. 12	Current	Ref. 12	Current	Ref. 12
2	1	0	0	3.013626		3.011020		3.009236	
	2	0	0	3.733598	3.7338	3.731057	3.7312	3.729324	3.7295
		1	2	4.143592	4.1437	4.142946	4.1431	4.142581	4.1427
3	2	1	1	8.175035	8.1755	8.169913		8.166708	8.1671
	4	1	1	11.04480	11.046	11.04338		11.04254	11.043
		0	3	11.05428	11.055	11.05325		11.05262	11.053
4	6	0	0	23.68944	23.691	23.65559		23.64832	23.650
		2	4	23.86769	23.870	23.80796		23.80373	23.805
5	2	0	5	21.15093	21.15	21.13414	21.13	21.12992	21.13
	4	0	5	29.43528	29.44	29.30898	29.31	29.30251	29.30

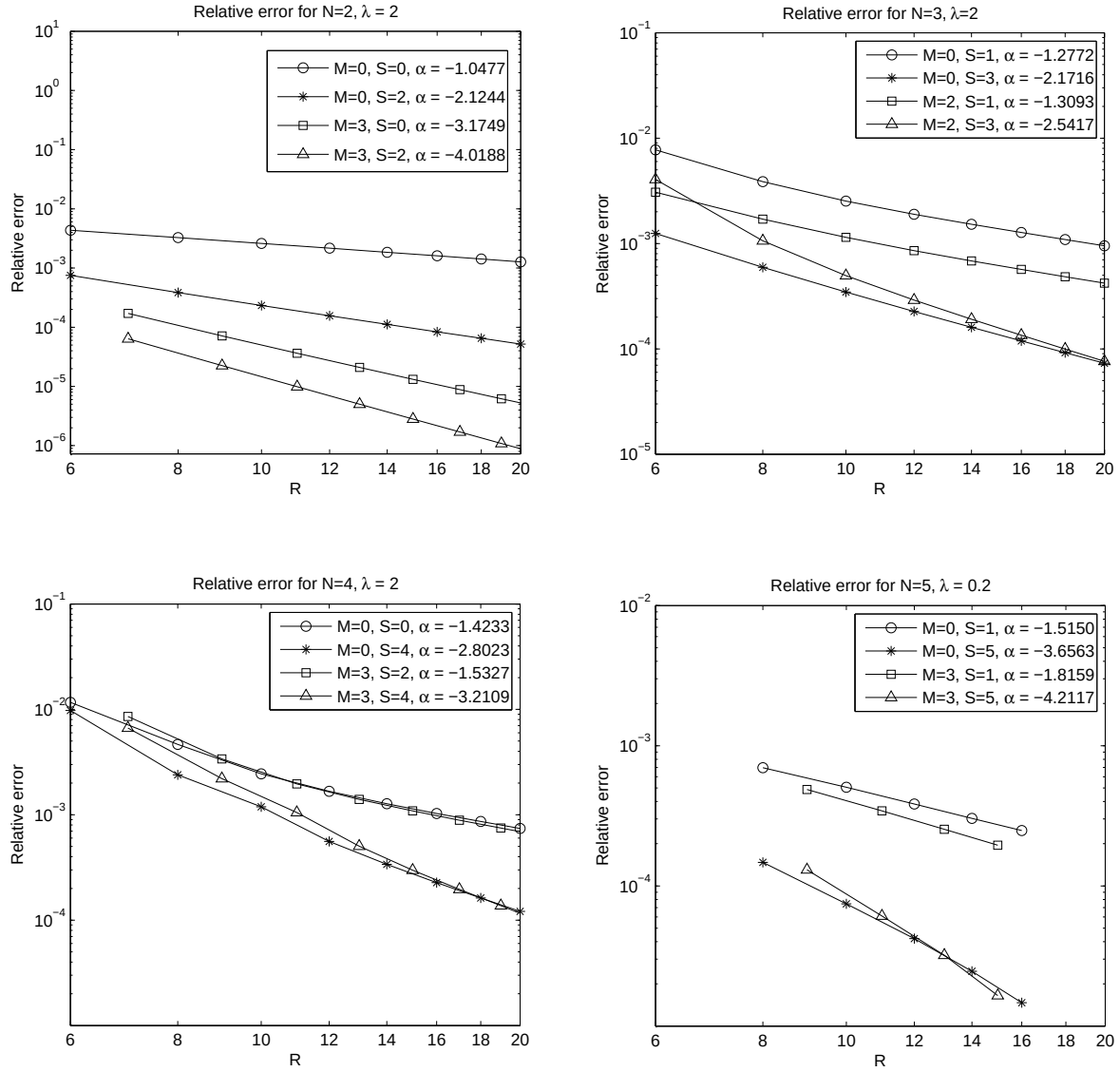

FIG. 3: Plot of relative error using the bare interaction for various N, M and S. Clear $o(R^{\alpha})$ dependence in all cases.

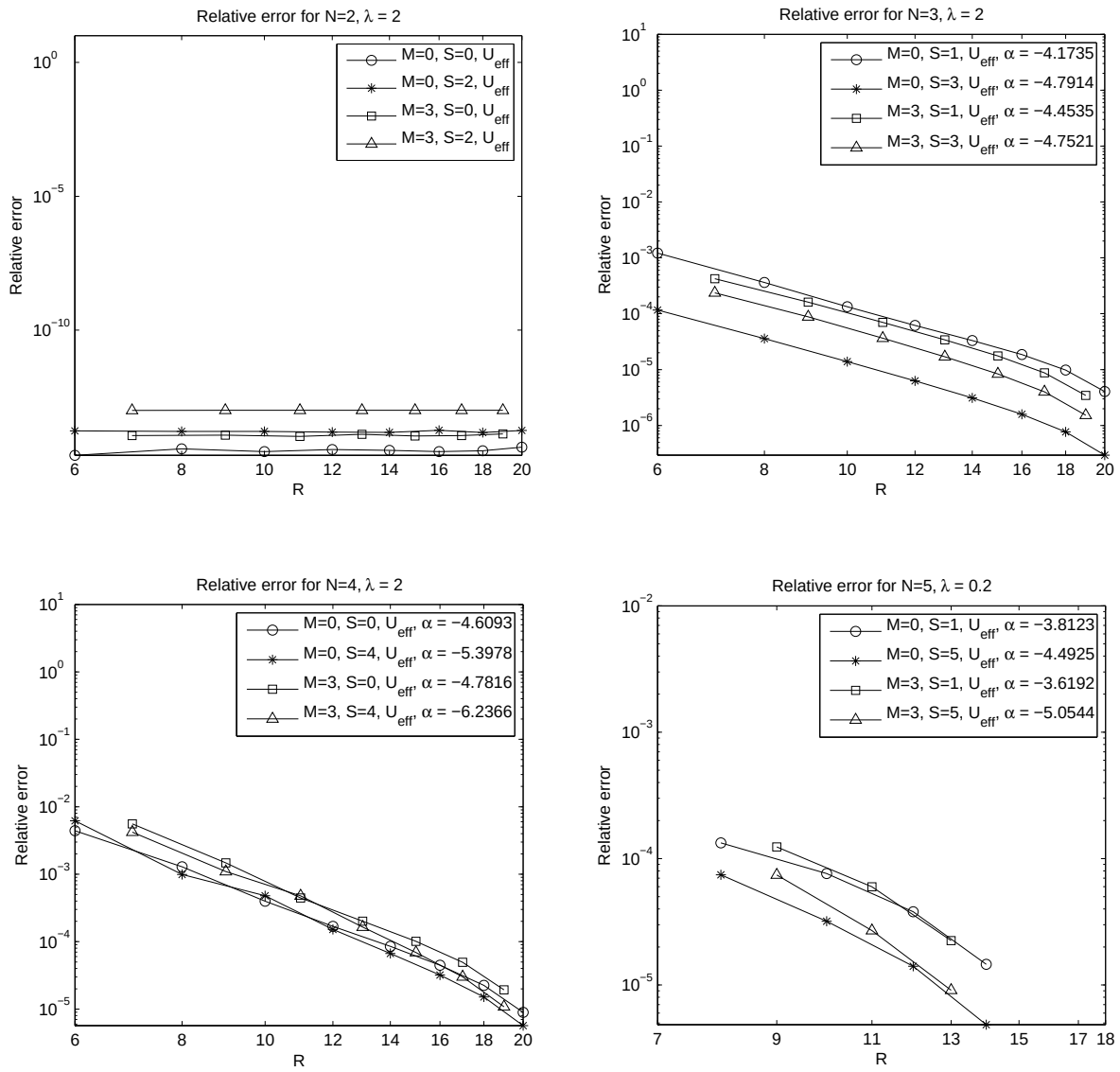

FIG. 4: Plot of relative error using an effective interaction for various N, M and S. Clear $o(R^{\alpha})$ dependence in all cases, but notice artifacts when R is large, due to errors in most correct eigenvalues. The $R = 5$ case does not contain enough data to compute the slopes with sufficient accuracy.

S gives higher k, as a rule of thumb. Intuitively, this is because the Pauli principle forces the wave function to be zero at coalesce points, thereby generating smoothness.

VI. DISCUSSION AND CONCLUSION

We have studied approximation properties of Hermite functions and harmonic oscillator eigenfunctions. This in turn allowed for a detailed convergence analysis of numerical methods such as the CI method for the parabolic quantum dot. Our main conclusion, is, that for wave functions $\psi \in H^k(\mathbb{R}^n)$ falling off exponentially as $\|x\| \to \infty$, the shell-weight function $p(r)$ decays as $p(r) = o(r^{-k-1})$. Applying this to the convergence theory of the Ritz-Galerkin method, we obtained the estimate (28) for the error in the eigenvalues. A complete characterization of the upper bound on the differentiability k, i.e., in $\psi^{(s)} \in H^k$, as well as a study of the constant K in Eqn. (29), would complete our knowledge of the convergence of the CI calculations.

We also demonstrated numerically, that the use of a two-body effective interaction accelerates the convergence by at least an order of magnitude, which shows that such a method *should* be used whenever possible. On the other hand, a rigorous mathematical study of the method is yet to come.

The theory and ideas presented in this article should in prin-

ciple be universally applicable. In fact, Figs. 1–3 of Ref. 14 clearly indicates this, where the eigenvalues of ^{3}He as function of model space size are graphed both for bare and effective interactions, showing some of the features we have discussed.

We would like to point out, that coupled-cluster methods have eigenvalue errors bounded by Eqn. (29) as well.[2] A further study of coupled-cluster calculations using effective interactions for parabolic quantum dots could be a very interesting venture, both with respect to the study of the coupled cluster methods, but also for the effective interactions.

Other interesting future studies would be a direct comparison of the direct product model space $\mathscr{M}_R(N)$ and our energy cut model space $\mathscr{P}_R(N)$. Both techniques are common, but may have different numerical characteristics. Indeed, $\dim[\mathscr{M}_R(N)]$ grows much quicker than $\dim[\mathscr{P}_R(N)]$, while we are uncertain of whether the increased basis size yields a corresponding increased accuracy.

We have focused on the parabolic quantum dot, firstly because it requires relatively small matrices to be stored, due to conservation of angular momentum, but also because it is a widely studied model. Our analysis is, however, general, and applicable to other systems as well, e.g., quantum dots trapped in double-wells, finite wells, and so on. Indeed, by adding a one-body potential V to the Hamiltonian $H = T + U$ we may model other geometries, as well as adding external fields.[44–46] As long as the potential is sufficiently weak, the differentiability of the wave function should not be affected.

APPENDIX A: MULTI-INDICES

A very handy tool for compact and unified notation when the dimension n of the underlying measure space $\mathbb{R}^n$ is a parameter, are multi-indices. The set $\mathscr{I}_n$ of multi-indices are defined as n-tuples of non-negative indices, viz, $\alpha = (\alpha_1, \cdots, \alpha_n)$.

We define several useful operations on multi-indices as follows. Let u be a formal vecor of n symbols. Moreover, let $\phi(\xi) = \phi(\xi_1, \xi_2, \cdots, \xi_n)$ be a function. Then, define

$$|\alpha| := \alpha_1 + \alpha_2 + \cdots + \alpha_n \tag{A1}$$

$$\alpha! := \alpha_1! \alpha_2! \cdots \alpha_n! \tag{A2}$$

$$\alpha \pm \beta := (\alpha_1 \pm \beta_1, \cdots, \alpha_n \pm \beta_n) \tag{A3}$$

$$u^\alpha := u_1^{\alpha_1} u_2^{\alpha_2} \cdots u_n^{\alpha_n}, \tag{A4}$$

$$\partial^\alpha \phi(\xi) := \frac{\partial^{\alpha_1}}{\partial \xi_1^{\alpha_1}} \frac{\partial^{\alpha_1}}{\partial \xi_2^{\alpha_2}} \cdots \frac{\partial^{\alpha_d}}{\partial \xi_d^{\alpha_1}} \phi(\xi) \tag{A5}$$

In Eqn. (A3), the result may not be a multi-index when we subtract two indices, but this will not be an issue for us. Notice, that Eqn. (A5) is a mixed partial derivative of order $|\alpha|$. Moreover, we say that $\alpha < \beta$ if and only if $\alpha_j < \beta_j$ for all j. We define $\alpha = \beta$ similarly. We also define "basis indices" e_j by $(e_j)_{j'} = \delta_{j,j'}$. These relations will be used extensively in Sec. III B. We comment, that we will often use the notation $\partial_x := \frac{\partial}{\partial x}$ and $\partial_k := \frac{\partial}{\partial \xi_k}$ to simplify notation. Thus,

$$\partial^\alpha = (\partial_1^{\alpha_1}, \cdots, \partial_n^{\alpha_n}),$$

consistent with Eqn. (A4).

APPENDIX B: WEAK DERIVATIVES AND SOBOLEV SPACES

We present a quick summary of weak derivatives and related concepts needed. The material is elementary and superficial, but probably unfamiliar to many readers, so we include it here. Many terms will be left undefined; if needed, the reader may consult standard texts, e.g., Refs. 6,47.

The space $L^2(\mathbb{R}^n)$ is defined as

$$L^2(\mathbb{R}^n) := \left\{ \psi : \mathbb{R}^n \to \mathbb{C} \ : \ \int_{\mathbb{R}^n} |\psi(\xi)|^2 \mathrm{d}^n\xi \ < +\infty \right\}, \tag{B1}$$

where the Lebesgue integral is more general than the Riemann "limit-of-small-boxes" integral. It is important that we identify two functions ψ and ψ_1 differing only at a set $Z \in \mathbb{R}^n$ of measure zero. Examples of such sets are points if $n \geq 1$, curves if $n \geq 2$, and so on, and countable unions of such. For example, the rationals constitute a set of measure zero in $\mathbb{R}$. Under this assumption, $L^2(\mathbb{R}^n)$ becomes a Hilbert space with the inner product

$$\langle \psi_1, \psi_2 \rangle := \int_{\mathbb{R}^n} \psi_1(\xi)^* \psi_2(\xi) \mathrm{d}^n\xi,$$

where the asterisk denotes complex conjugation.

The classical derivative is too limited a concept for the abstract theory of partial differential equations, including the Schrödinger equation. Let $\mathscr{C}_0^\infty$ be the set of infinitely differentiable functions which are non-zero only in a ball of finite radius. Of course, $\mathscr{C}_0^\infty \subset L^2(\mathbb{R}^n)$. Let $\psi \in L^2(\mathbb{R}^n)$, and let $\alpha \in \mathscr{I}_n$ be a multi-index. If there exists a $v \in L^2(\mathbb{R}^n)$ such that, for all $\phi \in \mathscr{C}_0^\infty$,

$$\int_{\mathbb{R}^n} (\partial^\alpha \phi(\xi)) \psi(\xi) \mathrm{d}^n\xi = (-1)^{|\alpha|} \int_{\mathbb{R}^n} \phi(\xi) v(\xi) \mathrm{d}^n\xi,$$

then $\partial^\alpha \psi := v \in L^2$ is said to be a *weak derivative*, or distributional derivative, of ψ. In this way, the weak derivative is defined in an average sense, using integration by parts.

The weak derivative is unique (up to redefinition on a set of measure zero), obeys the product rule, chain rule, etc.

It is easily seen, that if ψ has a classical derivative $v \in L^2(\mathbb{R}^n)$ it coincides with the weak derivative. Moreover, if the classical derivative is defined almost everywhere (i.e., everywhere except for a set of measure zero), then ψ has a weak derivative.

The Sobolev space $H^k(\mathbb{R}^n)$ is defined as the subset of $L^2(\mathbb{R}^n)$ given by

$$H^k(\mathbb{R}^n) := \left\{ \psi \in L^2 \ : \ \partial^\alpha \psi \in L^2, \quad \forall \alpha \in \mathscr{I}_n, \ |\alpha| \leq k \right\}. \tag{B2}$$

The Sobolev space is also a Hilbert space with the inner product

$$(\psi_1, \psi_2) := \sum_{\alpha, \, |\alpha| \leq k} \langle \partial^\alpha \psi_1, \partial^\alpha \psi_2 \rangle,$$

and this is the main reason why one obtains a unified theory of PDE using such spaces.

The space $H^k(\mathbb{R}^n)$ for $n > 1$ is a big space – there are some exceptionally ill-behaved functions there, for example there are functions in H^k that are unbounded on arbitrary small regions but still differentiable. (Hermite series for such functions would still converge faster than, e.g., for a function with a jump discontinuity!) For our purposes, it is enough to realize that the Sobolev spaces offer exactly the notion of derivative we need in our analysis of the Hermite function expansions.

ACKNOWLEDGMENTS

The author wishes to thank Prof. M. Hjorth-Jensen (CMA) for useful discussions, suggestions and feedback, and also Dr. G. M. Coclite (University of Bari, Italy) for mathematical discussions. This work was financed by CMA through the Norwegian Research Council.

* Electronic address: simen.kvaal@cma.uio.no

[1] M. Hjorth-Jensen, T. Kuo, and E. Osnes, Phys. Rep. **261**, 125 (1995).
[2] T. Helgaker, P. Jørgensen, and J. Olsen, *Molecular Electronic-Structure Theory* (Wiley, 2002).
[3] S. M. Reimann and M. Manninen, Rev. Mod. Phys **74**, 1283 (2002).
[4] S. Kvaal, M. Hjorth-Jensen, and H.M. Nilsen, Phys. Rev. B. **76**, 085421 (2007).
[5] R. Ram-Mohan, *Finite Element and Boundary Element Applications in Quantum Mechanics* (Oxford University Press, 2002).
[6] L. Evans, *Partial Differential Equations*, vol. 19 of *Graduate Studies in Mathematics* (AMS, 1998).
[7] R. J. Bartlett and M. Musiał, Rev. Mod. Phys. **79**, 291 (pages 62) (2007).
[8] P.A. Maksym and T. Chakraborty, Phys. Rev. Lett. **65**, 108 (1990).
[9] S. M. Reimann, M. Koskinen, and M. Manninen, Phys. Rev. B **62**, 8108 (2000).
[10] N. A. Bruce and P. A. Maksym, Phys. Rev. B **61**, 4718 (2000).
[11] S. A. Mikhailov, Phys. Rev. B **66**, 153313 (2002).
[12] M. Rontani, C. Cavazzoni, D. Belucci, and G. Goldoni, J. Chem. Phys. **124**, 124102 (2006).
[13] A. Wensauer, M. Korkusinski, and P. Hawrylak, Solid State Comm. **130**, 115 (2004).
[14] P. Navrátil, J.P. Vary, and B.R. Barrett, Phys. Rev. C **62**, 054311 (2000).
[15] I. Babuska and J. Osborn, *Handbook of Numerical Analysis: Finite Element Methods*, vol. 2 (North-Holland, 1996).
[16] S. Raimes, *Many-Electron Theory* (North-Holland, 1972).
[17] D. Loss and D. P. DiVincenzo, Phys. Rev. A **57**, 120 (1998).
[18] A. Kumar, S.E. Laux, and F. Stern, Phys. Rev. B **42**, 5166 (1990).
[19] M. Macucci, K. Hess, and G. J. Iafrate, Phys. Rev. B **55**, R4879 (1997).
[20] P. A. Maksym and N. A. Bruce, Physica E **1**, 211 (1997).
[21] T. Ezaki, N. Mori, and C. Hamaguchi, Phys. Rev. B **56**, 6428 (1997).
[22] P. Maksym, Physica B **249**, 233 (1998).
[23] M. B. Tavernier, E. Anisimovas, F. M. Peeters, B. Szafran, J. Adamowski, and S. Bednarek, Phys. Rev. B **68**, 205305 (2003).
[24] M. Taut, Phys. Rev. A **48**, 3561 (1993).
[25] M. Taut, J. Phys. A: Math. Gen. **27**, 1045 (1994).
[26] T. Kato, Commun. Pure Appl. Math. **10**, 151 (1957).
[27] M. Hoffmann-Ostenhof, T. Hoffmann-Ostenhof, and H. Stremnitzer, Phys. Rev. Lett. **68**, 3857 (1992).
[28] J. Boyd, J. Comp. Phys. **54**, 382 (1984).
[29] E. Hille, Duke Math. J. **5**, 875 (1939).
[30] M. Hoffmann-Ostenhof, T. Hoffmann-Ostenhof, and H. Stremnitzer, Comm. Math. Phys. **163**, 185 (1994).
[31] H. Yserentant, Numer. Math. **98**, 731 (2004).
[32] S. Gould, *Variational Methods for Eigenvalue Problems: An Introduction to the Methods of Rayleigh, Ritz, Weinstein, and Aronszajn* (Dover, 1995).
[33] I. Babuska and J. Osborn, SIAM J. Numer. Anal. **24**, 1249 (1987).
[34] M. B. Tavernier, E. Anisimovas, and F. M. Peeters, Phys. Rev. B **74**, 125305 (pages 9) (2006).
[35] I. Babuska and J. Osborn, Math. Comp. **52**, 275 (1989).
[36] S. Kvaal (2008), submitted to Phys. Rev. C, URL http://arxiv.org/abs/0808.1831
[37] D. Klein, J. Chem. Phys. **61**, 786 (1974).
[38] J. S. Ball, SIAM J. Numer. Anal. **40**, 2311 (2003).
[39] T. Schucan and H. Weidenmüller, Ann. Phys. **76**, 483 (1973).
[40] S. A. Mikhailov, Phys. Rev. B **65**, 115312 (2002).
[41] S. Kvaal (2008), in preparation.
[42] N. F. Johnson and M. C. Payne, Phys. Rev. Lett. **67**, 1157 (1991).
[43] E. Caurier, G. Martinez-Pinedo, F. Nowacki, A. Poves, and A. P. Zuker, Rev. Mod. Phys. **77**, 427 (pages 62) (2005).
[44] M. Helle, A. Harju, and R. M. Nieminen, Phys. Rev. B) **72**, 205329 (pages 24) (2005).
[45] M. Braskén, M. Lindberg, D. Sundholm, and J. Olsen, Phys. Rev. B **61**, 7652 (2000).
[46] S. Corni, M. Braskén, M. Lindberg, J. Olsen, and D. Sundholm, Phys. Rev. B **67**, 045313 (2003).
[47] R. Bartle, *The Elements of Integration and Measure* (Wiley, New York, USA, 1995).

3 Geometry of effective Hamiltonians

This paper appeared in volume 78 of Physical Review C, 2008.

PHYSICAL REVIEW C **78**, 044330 (2008)

Geometry of effective Hamiltonians

Simen Kvaal*
Centre of Mathematics for Applications, University of Oslo, N-0316 Oslo, Norway
(Received 13 August 2008; published 31 October 2008)

We give a complete geometrical description of the effective Hamiltonians common in nuclear shell-model calculations. By recasting the theory in a manifestly geometric form, we reinterpret and clarify several points. Some of these results are hitherto unknown or unpublished. In particular, commuting observables and symmetries are discussed in detail. Simple and explicit proofs are given, and numerical algorithms are proposed that improve and stabilize methods commonly used today.

DOI: 10.1103/PhysRevC.78.044330 PACS number(s): 21.30.Fe, 21.60.−n

I. INTRODUCTION

Effective Hamiltonians and interactions are routinely used in shell-model calculations of nuclear spectra [1–3]. The published mathematical theory of the effective Hamiltonian is complicated and usually focuses on perturbation theoretical aspects, diagram expansions, etc. [4–12]. In this article, we recast and reinterpret the basic elements of the theory geometrically. We focus on the geometric relationship between the exact eigenvectors $|\psi_k\rangle$ and the effective eigenvectors $|\psi_k^{\text{eff}}\rangle$, both for the usual non-Hermitian Bloch-Brandow effective Hamiltonian [1,4,5,9] and for the Hermitian effective Hamiltonian [6,11,13,14], which we dub the canonical effective Hamiltonian because of its geometric significance. This results in a clear geometric understanding of the decoupling operator ω (defined in Sec. III C), and a simple proof and characterization of the Hermitian effective Hamiltonian in terms of subspace rotations, in the same way as the non-Hermitian Hamiltonian is characterized by subspace projections.

The goal of effective interaction theory is to devise a Hamiltonian H_{eff} in a model space $\mathcal{P}$ of (much) smaller dimension m than the dimension n of Hilbert space $\mathcal{H}$, with m *exact* eigenvalues of the original Hamiltonian $H = H_0 + H_1$, where H_1 is usually considered as a perturbation. The model space $\mathcal{P}$ is usually taken as the span of a few eigenvectors $|e_k\rangle_{k=1}^m$ of H_0, i.e., the unperturbed Hamiltonian in a perturbational view.

Effective Hamiltonians in A-body systems must invariably be approximated (otherwise there would be no need for H_{eff}), usually by many-body perturbation theory, but since such approaches suffer from bad convergence properties in general [15], a subcluster approximation approach has been proposed and is in wide use today [3,6]. In this case, the exact a-body canonical effective Hamiltonian is computed, where $a < A$. From this, one extracts an effective a-body interaction and applies it to the A-body system. We present a new algorithm for computing the exact effective Hamiltonian, which is useful in the subcluster approach to H_{eff}. It is conceptually and computationally simpler than the usual one, which relies on both matrix inversion and square root [3,11], because the only nontrivial matrix operation is the singular value decomposition (SVD). This algorithm is a simple by-product of the geometric approach to analyzing the effective Hamiltonians. We comment that in the subcluster approach, it is invariably assumed that the a-body Hamiltonian is *exactly diagonizable*, so its exact eigenpairs are available. Thus, algorithms for the subcluster approach to H_{eff} are not perturbative in nature.

The article is organized as follows. In Sec. II we introduce some notation and define the singular value decomposition of linear operators and the principal angles and vectors between two linear spaces. In Sec. III we define and analyze the Bloch-Brandow and canonical effective Hamiltonians. The main part consists of a geometric analysis of the exact eigenvectors and forms the basis for the analysis of the effective Hamiltonians. We also discuss the impact of symmetries of the Hamiltonian, i.e., conservation laws. In Sec. IV we give concrete matrix expressions and algorithms for computing the effective Hamiltonians; and in the canonical case, it is, to the best of our knowledge, previously unknown. In Sec. V we sum up and briefly discuss the results and possible future projects.

II. TOOLS AND NOTATION

A. Linear spaces and operators

We shall use the Dirac notation for vectors, inner products, and operators, in order to make a clear, basis-independent formulation. By $\mathcal{F}, \mathcal{G}$, etc., we denote (finite dimensional) Hilbert spaces, and vectors are denoted by kets, e.g., $|\psi\rangle$, as usual. Our underlying Hilbert space is denoted by $\mathcal{H}$, with $n = \dim(\mathcal{H})$. In general, n is infinite. We shall, however, assume it to be finite. Our results are still valid in the infinite dimensional case if H is assumed to have a discrete spectrum and at least m linearly independent eigenvectors.

We are also given a Hamiltonian H, a linear, Hermitian operator (i.e., $H = H^\dagger$) on $\mathcal{H}$. Its spectral decomposition is defined to be

$$H = \sum_{k=1}^{n} E_k |\psi_k\rangle\langle\psi_k|.$$

Thus, E_k and $|\psi_k\rangle$ are the (real) eigenvalues and (orthonormal) eigenvectors, respectively.

*simen.kvaal@cma.uio.no

We are also given a subspace $\mathcal{P} \subset \mathcal{H}$, called the model space, which in principle is arbitrary. Let $\{|e_k\rangle\}_{k=1}^m$ be an orthonormal basis, for definiteness, viz.,

$$\mathcal{P} := \text{span}\{|e_k\rangle \ : \ k = 1, \ldots, m\}.$$

Let P be its orthogonal projector, i.e.,

$$P : \mathcal{H} \to \mathcal{P}, \quad P = \sum_{j=1}^{m} |e_j\rangle\langle e_j|, \quad m = \dim(\mathcal{P}) \leqslant n.$$

The basis $\{|e_j\rangle\}_{j=1}^m$ is commonly taken to be eigenvectors for H_0.

The orthogonal complement of the model space, $\mathcal{Q} = \mathcal{P}^\perp$, has the orthogonal projector $Q = 1 - P$, and is called the excluded space.

This division of $\mathcal{H}$ into $\mathcal{P}$ and $\mathcal{Q}$ transfers to operators in $\mathcal{H}$. These are in a natural way split into four parts, viz., for an arbitrary operator A,

$$A = (P + Q)A(P + Q) = PAP + PAQ + QAP + QAQ, \tag{1}$$

where PAP maps the model space into itself, QAP maps $\mathcal{P}$ into $\mathcal{Q}$, and so forth. It is convenient to picture this in a block form of A, viz.,

$$A = \begin{bmatrix} PAP & PAQ \\ QAP & QAQ \end{bmatrix}.$$

B. Singular value decomposition

A recurrent tool in this work is the singular value decomposition (SVD) of an operator $A : \mathcal{X} \to \mathcal{Y}$. Here, $p = \dim(\mathcal{X})$ and $q = \dim(\mathcal{Y})$ are arbitrary. Then there exists orthonormal bases $\{|x_k\rangle\}_{k=1}^p$ and $\{|y_k\rangle\}_{k=1}^q$ of $\mathcal{X}$ and $\mathcal{Y}$, respectively, and $r = \min(p, q)$ non-negative real numbers σ_k with $\sigma_k \geqslant \sigma_{k+1}$ for all k, such that

$$A = \sum_{k=1}^{r} \sigma_k |y_k\rangle\langle x_k|.$$

This is the SVD of A, and it always exists. It may happen that some of the basis vectors do not participate in the sum, either if $p \neq q$ or if $\sigma_k = 0$ for some k.

The vectors $|x_k\rangle$ are called right singular vectors, while $|y_k\rangle$ are called left singular vectors. The values σ_k are called singular values, and A is one-to-one and onto (i.e., nonsingular) if and only if $\sigma_k > 0$ for all k, and $p = q$. The inverse is then

$$A^{-1} = \sum_{k=1}^{r} \frac{1}{\sigma_k} |x_k\rangle\langle y_k|,$$

as easily verified.

A recursive variational characterization of the singular values and vectors is the following [16]:

$$\begin{aligned} \sigma_k &= \max_{\substack{|u\rangle \in \mathcal{X}, \ \langle u|u\rangle = 1 \\ \langle u|u_j\rangle = 0, \ j<k}} \ \max_{\substack{|v\rangle \in \mathcal{Y}, \ \langle v|v\rangle = 1 \\ \langle v|v_j\rangle = 0, \ j<k}} \text{Re}\langle v|A|u\rangle \\ &=: \langle v_k|A|u_k\rangle. \end{aligned} \tag{2}$$

The latter equality implicitly states that the maximum is actually real. The SVD is very powerful, as it gives an interpretation and representation of *any* linear operator A as a simple scaling with respect to one orthonormal basis, and then transformation to another. The singular vectors are not unique, but the singular values are.

C. Principal angles and vectors

Important tools for comparing linear subspaces $\mathcal{F}$ and $\mathcal{G}$ of $\mathcal{H}$ are the principal angles and principal vectors [17,18]. The principal angles generalize the notion of angles between vectors to subspaces in a natural way. They are also called canonical angles. Assume that

$$p = \dim(\mathcal{F}) \geqslant q = \dim(\mathcal{G}) \geqslant 1.$$

(If $p < q$, we simply exchange $\mathcal{F}$ and $\mathcal{G}$.) Then, q principal angles $\theta_k \in [0, \pi/2]$, with $\theta_k \leqslant \theta_{k+1}$ for all k, and the left and right principal vectors $|\xi_k\rangle \in \mathcal{F}$ and $|\eta_k\rangle \in \mathcal{G}$ are defined recursively through

$$\begin{aligned} \cos\theta_k &= \max_{\substack{|\xi\rangle \in \mathcal{F}, \ \langle\xi|\xi\rangle = 1 \\ \langle\xi|\xi_j\rangle = 0, \ j<k}} \ \max_{\substack{|\eta\rangle \in \mathcal{G}, \ \langle\eta|\eta\rangle = 1 \\ \langle\eta|\eta_j\rangle = 0, \ j<k}} \text{Re}\langle\xi|\eta\rangle \\ &=: \langle\xi_k|\eta_k\rangle. \end{aligned} \tag{3}$$

Again, the last equality implicitly states that the maximum actually is real. One sees that θ_k is the angle between $|\xi_k\rangle \in \mathcal{F}$ and $|\eta_k\rangle \in \mathcal{G}$.

It is evident from Eqs. (2) and (3) that the principal angles and vectors are closely related to the SVD. Indeed, if we consider the product of the orthogonal projectors $P_\mathcal{F}$ and $P_\mathcal{G}$ and compute the SVD, we obtain

$$P_\mathcal{F} P_\mathcal{G} = \sum_{k=1}^{p} |\xi_k\rangle\langle\xi_k| \sum_{j=1}^{q} |\eta_k\rangle\langle\eta_k| = \sum_{k=1}^{q} \cos\theta_k |\xi_k\rangle\langle\eta_k|,$$

where we extended the orthonormal vectors $\{|\xi_k\rangle\}_{k=1}^q$ with $p - q$ vectors into a basis for $\mathcal{F}$, which is always possible. This equation in particular implies the additional orthogonality relation $\langle\xi_j|\eta_k\rangle = \delta_{j,k}\cos\theta_k$ on the principal vectors.

The principal vectors constitute orthonormal bases that should be rotated into each other if the spaces were to be aligned. Moreover, the rotations are by the smallest angles possible.

III. EFFECTIVE HAMILTONIANS

A. Similarity transforms

The goal of the effective Hamiltonian is to reproduce exactly m of the eigenvalues, and (necessarily) approximately m of the eigenvectors. We shall assume that the first m eigenpairs $(E_k, |\psi_k\rangle)$, $k = 1, \ldots, m$, defines these. We define the space $\mathcal{E}$ as

$$\mathcal{E} := \text{span}\{|\psi_k\rangle \ : \ k = 1, \ldots, m\}.$$

The orthogonal projector P' onto $\mathcal{E}$ is

$$P' = \sum_{k=1}^{m} |\psi_k\rangle\langle\psi_k|. \tag{4}$$

We denote by $(E_k, |\psi_k^{\text{eff}}\rangle)$, $k = 1, \ldots, m$, the effective Hamiltonian eigenvalues and eigenvectors. Of course, the $|\psi_k^{\text{eff}}\rangle \in \mathcal{P}$ must constitute a basis for $\mathcal{P}$, but not necessarily an orthonormal basis. Geometrically, we want $|\psi_k^{\text{eff}}\rangle$ to be as close as possible to $|\psi_k\rangle$, i.e., we want $\mathcal{E}$ to be as close to $\mathcal{P}$ as possible.

Let $|\widetilde{\psi_k^{\text{eff}}}\rangle$ be the bi-orthogonal basis, i.e., $\langle\widetilde{\psi_j^{\text{eff}}}|\psi_k^{\text{eff}}\rangle = \delta_{j,k}$, so that

$$P = \sum_{k=1}^{m} |e_k\rangle\langle e_k| = \sum_{k=1}^{m} |\psi_k^{\text{eff}}\rangle\langle\widetilde{\psi_k^{\text{eff}}}|.$$

The spectral decomposition of H_{eff} becomes

$$H_{\text{eff}} = \sum_{k=1}^{m} E_k |\psi_k^{\text{eff}}\rangle\langle\widetilde{\psi_k^{\text{eff}}}|.$$

Since H_{eff} is to have eigenvalues identical to m of those of H, and since H_{eff} operates only in $\mathcal{P}$, we may relate H_{eff} to H through a similarity transform, viz.,

$$H_{\text{eff}} = P\tilde{H}P = P(e^{-S}He^{S})P, \tag{5}$$

where $\exp(S)\exp(-S) = I$. Any invertible operator has a logarithm, so Eq. (5) is completely general.

Now, $H_{\text{eff}} = P\tilde{H}P$ is an effective Hamiltonian only if the Bloch equation

$$Q\tilde{H}P = Qe^{-S}He^{S}P = 0 \tag{6}$$

is satisfied [8], since $\mathcal{P}$ is then invariant under the action of $\tilde{H}$. The eigenvectors of H_{eff} are now given by

$$|\psi_k^{\text{eff}}\rangle = e^{-S}|\psi_k\rangle \in \mathcal{P}, \quad k = 1, \ldots, m. \tag{7}$$

Thus, an effective Hamiltonian can now be defined for every S such that Eq. (6) holds. It is readily seen that $\tilde{H} = \tilde{H}^{\dagger}$ if and only if S is skew-Hermitian, i.e., that $S^{\dagger} = -S$. There is still much freedom in the choice of exponent S. Indeed, given any invertible operator A in $\mathcal{P}$, $A^{-1}H_{\text{eff}}A$ is a new effective Hamiltonian with the same effective eigenvalues as H_{eff}, and $|\psi^{\text{eff}}\rangle = A^{-1}\exp(-S)|\psi\rangle$.

B. Geometry of the model space

We will benefit from a detailed discussion of the spaces $\mathcal{E}$ and $\mathcal{P}$ before we discuss the Bloch-Brandow and canonical effective Hamiltonians in detail.

Since $\dim(\mathcal{P}) = \dim(\mathcal{E}) = m$, the closeness of the effective and exact eigenvectors can be characterized and measured by the orientation of $\mathcal{E}$ relative to $\mathcal{P}$ in $\mathcal{H}$, using m canonical angles θ_k and principal vectors $|\eta_k\rangle \in \mathcal{E}$ and $|\xi_k\rangle \in \mathcal{P}$. Recall that $\cos\theta_k = \langle\xi_k|\eta_k\rangle$ and that the angles $\theta_k \in [0, \pi/2]$ were the smallest possible such that the principal vectors are the orthonormal bases of $\mathcal{P}$ and $\mathcal{E}$ that are closest to each other.

We now define the unitary operator $Z = \exp(G)$ that rotates $\mathcal{P}$ into $\mathcal{E}$ according to this description, i.e., we should have $Z|\xi_k\rangle = |\eta_k\rangle$. In Fig. 1 the plane spanned by $|\eta_k\rangle$ and $|\xi_k\rangle$ if $\theta_k > 0$ is depicted. Recall that $\langle\xi_j|\eta_k\rangle = \cos\theta_j\delta_{j,k}$. Note that $|\xi_k\rangle = |\eta_k\rangle$ if and only if $\theta_k = 0$, and the plane degenerates into a line. If $\theta_k > 0$, the vector $|\chi_k\rangle$ is defined so that it together

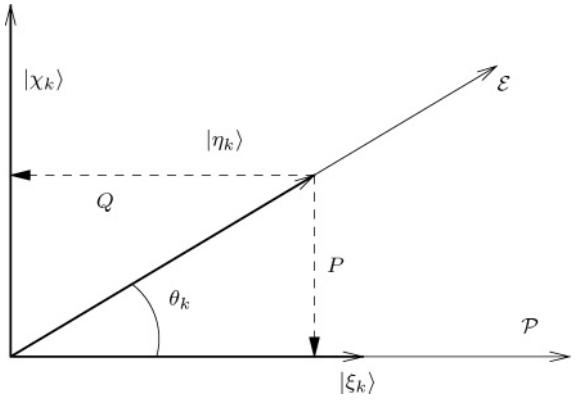

FIG. 1. Plane spanned by $|\xi_k\rangle$ and $|\eta_k\rangle$, and action of projectors P and Q on $|\eta_k\rangle$.

with $|\xi_k\rangle$ is an orthonormal basis for the plane, viz.,

$$|\eta_k\rangle = P|\eta_k\rangle + Q|\eta_k\rangle = \cos(\theta_k)|\xi_k\rangle + \sin(\theta_k)|\chi_k\rangle, \tag{8}$$

where

$$|\chi_k\rangle = \frac{Q|\eta_k\rangle}{\langle\eta_k|Q|\eta_k\rangle^{1/2}}. \tag{9}$$

Thus, $\{|\chi_k\rangle\} \cup \{|\xi_k\rangle\}$ is an orthonormal basis for $\mathcal{P} \oplus \mathcal{E}$, whose dimension is $2m - n_z$, where n_z is the number of $\theta_k = 0$. The set $\{|\chi_k\rangle : \theta_k > 0,\ k = 1, \ldots, m\}$ is an orthonormal basis for $Q\mathcal{E}$ which contains $Q|\psi_k\rangle$ for all $k = 1, \ldots, m$.

The operator Z is now defined as a rotation in $\mathcal{P} \oplus \mathcal{E}$, i.e., by elementary trigonometry,

$$\begin{aligned} Z|\xi_k\rangle &:= |\eta_k\rangle, \\ Z|\eta_k\rangle &:= 2\cos\theta_k|\eta_k\rangle - |\xi_k\rangle. \end{aligned} \tag{10}$$

In terms of the orthonormal basis, we obtain a manifest planar rotation for each k, i.e.,

$$\begin{aligned} Z|\chi_k\rangle &= \cos\theta_k|\chi_k\rangle - \sin\theta_k|\xi_k\rangle, \\ Z|\xi_k\rangle &= \sin\theta_k|\chi_k\rangle + \cos\theta_k|\xi_k\rangle. \end{aligned} \tag{11}$$

On the rest of the Hilbert space, $\mathcal{H} \ominus (\mathcal{P} \oplus \mathcal{E})$, Z is the identity. The operator Z implements the so-called direct rotation [19] of $\mathcal{P}$ into $\mathcal{E}$. From Eq. (11) we obtain

$$\begin{aligned} Z := I &+ \sum_{k=1}^{m} [\cos(\theta_k) - 1](|\chi_k\rangle\langle\chi_k| + |\xi_k\rangle\langle\xi_k|) \\ &+ \sum_{k=1}^{m} \sin(\theta_k)(|\chi_k\rangle\langle\xi_k| - |\xi_k\rangle\langle\chi_k|). \end{aligned} \tag{12}$$

It is instructive to exhibit the Lie algebra element $G \in \mathrm{su}(n)$ such that $Z = \exp(G) \in \mathrm{SU}(n)$. Since we have Eq. (11), it is easy to do this. Indeed, taking the exponential of

$$G = \sum_{k=1}^{m} \theta_k(|\chi_k\rangle\langle\xi_k| - |\xi_k\rangle\langle\chi_k|), \tag{13}$$

by summing the series for $\sin(\theta)$ and $\cos(\theta)$, we readily obtain $Z = \exp(G)$, the desired result. Moreover, observe that the kth term in Eq. (13) commutes with the jth term, so, $\exp(G)$ is exhibited as a sequence of commuting rotations using the canonical angles θ_k.

C. Bloch-Brandow effective Hamiltonian and decoupling operator

For reference, we review some properties of the Bloch-Brandow effective Hamiltonian, which we denote by $H_{\text{eff}}^{\text{BB}}$ [1,4,5,9]. The effective eigenvectors $|\psi_k^{\text{eff}}\rangle$ are defined by

$$\left|\psi_k^{\text{eff}}\right\rangle := P|\psi_k\rangle := |P\psi_k\rangle. \tag{14}$$

Since $|P\psi_k\rangle$ are the orthogonal projections of $|\psi_k\rangle$ onto $\mathcal{P}$, we deduce that the Bloch-Brandow effective eigenvectors are *the closest possible to the exact model space eigenvectors*. In this sense, the Bloch-Brandow effective Hamiltonian is the optimal choice.

It is obvious that $H_{\text{eff}}^{\text{BB}}$ is non-Hermitian, as rejecting the excluded space eigenvector components renders the effective eigenvectors non-orthonormal, i.e.,

$$\left\langle\psi_j^{\text{eff}}|\psi_k^{\text{eff}}\right\rangle = \delta_{j,k} - \langle\psi_j|Q|\psi_k\rangle \neq \delta_{j,k}.$$

In terms of similarity transforms, we obtain $H_{\text{eff}}^{\text{BB}}$ by setting $S = \omega$, the so-called decoupling operator or correlation operator [1,11]. It is defined by $\omega = Q\omega P$ and the equation

$$\omega P|\psi_k\rangle := Q|\psi_k\rangle. \tag{15}$$

Again, for this to be a meaningful definition, $\{|P\psi_k\rangle\}_{k=1}^m$ must be a basis for $\mathcal{P}$.

Since $\omega^2 = 0$, $\exp(\pm\omega) = 1 \pm \omega$, and Eq. (7) becomes

$$e^{-\omega}|\psi_k\rangle = (1-\omega)|\psi_k\rangle = (1-Q)|\psi_k\rangle = |P\psi_k\rangle.$$

For $H_{\text{eff}}^{\text{BB}}$ we thus obtain

$$H_{\text{eff}}^{\text{BB}} = Pe^{-\omega}He^{\omega}P = PH(P+\omega). \tag{16}$$

After this initial review, we now relate ω to the geometry of $\mathcal{E}$ and $\mathcal{P}$. The SVD of ω is readily obtainable by expanding the principal vectors $\{|\eta_k\rangle\}_{j=1}^m$ in the m eigenvectors $\{|\psi_k\rangle\}_{k=1}^m$, sets, which both constitute a basis for $\mathcal{E}$, and inserting into Eq. (15). We have

$$\begin{aligned} Q|\eta_k\rangle &= \sum_{j=1}^m Q|\psi_j\rangle\langle\psi_j|\eta_k\rangle \\ &= \sum_{j=1}^m \omega P|\psi_j\rangle\langle\psi_j|\eta_k\rangle = \omega P|\eta_k\rangle, \end{aligned}$$

that is,

$$\omega\,(\cos\theta_k|\xi_k\rangle) = \sin\theta_k|\chi_j\rangle.$$

The result is

$$\omega = \sum_{k=1}^m \tan\theta_k|\chi_k\rangle\langle\xi_k|, \tag{17}$$

which is the SVD of ω. The operator ω is thus exhibited as an operator intimately related to the principal angles and vectors of $\mathcal{P}$ and $\mathcal{E}$: it transforms the principal vectors of $\mathcal{P}$ into an orthonormal basis for $Q\mathcal{E}$, with coefficients determined by the canonical angles θ_k. Using Eq. (8) we obtain an alternative expression, viz.,

$$\omega + P = \sum_{k=1}^m \frac{1}{\cos\theta_k}|\eta_k\rangle\langle\xi_k|. \tag{18}$$

D. Canonical effective Hamiltonian

Hermitian effective Hamiltonians have independently been introduced by various authors since 1929, when Van Vleck [13,14,20] introduced a unitary transformation $\tilde{H} = \exp(-S)H\exp(S)$ to decouple the model space to second order in the interaction. In 1963, Primas [21] considered an order by order expansion of this $\tilde{H}$ using the Baker-Campbell-Hausdorff formula and commutator functions to determine S, a technique also used in many other settings in which a transformation is in a Lie group, see, e.g., Ref. [22] and references therein. This approach was elaborated by Shavitt and Redmon [7], who were the first to mathematically connect this Hermitian effective Hamiltonian to $H_{\text{eff}}^{\text{BB}}$, as in Eq. (27) below. In the nuclear physics community, Suzuki [23] has been a strong advocate of Hermitian effective interactions and the a-body subcluster approximation to the A-body effective interaction [3,11,23]. Hermiticity in this case is essential.

Even though a Hermitian effective Hamiltonian is not unique because of the non-uniqueness of $S = -S^\dagger$, the various Hermitian effective Hamiltonians put forward in the literature all turn out to be equivalent [6]. In the spirit of Klein and Shavitt [6,7] we employ the term "canonical effective Hamiltonian" since this emphasizes the "natural" and geometric nature of the Hermitian effective Hamiltonian, which we denote by $H_{\text{eff}}^{\text{c}}$.

Recall the spectral decomposition

$$H_{\text{eff}}^{\text{c}} = \sum_{k=1}^m E_k\left|\psi_k^{\text{eff}}\right\rangle\left\langle\psi_k^{\text{eff}}\right|,$$

where the (orthonormal) effective eigenvectors are now defined by the following optimization property: *The effective eigenvectors* $|\psi_k^{\text{eff}}\rangle$ *are the closest possible to the exact eigenvectors* $|\psi_k\rangle$ *while still being orthonormal*. Thus, where the Bloch-Brandow approach *globally* minimizes the distance between the eigenvectors, at the cost of non-orthonormality, the canonical approach has the unitarity constraint on the similarity transformation, rendering $H_{\text{eff}}^{\text{c}}$ Hermitian.

Given a collection $\{\Phi = |\phi_1\rangle, \ldots, |\phi_m\rangle\} \subset \mathcal{P}$ of m vectors, which are candidates for effective eigenvectors, we define the functional $S[\Phi]$ by

$$\begin{aligned} S[\Phi] &:= \sum_{k=1}^m \||\phi_k\rangle - |\psi_k\rangle\|^2 \\ &= \sum_{k=1}^m \|Q|\psi_k\rangle\|^2 + \sum_{k=1}^m \|P|\psi_k\rangle - |\phi_k\rangle\|^2 \\ &= m + \sum_{k=1}^m \||\phi_k\rangle\|^2 - 2\,\mathrm{Re}\sum_{k=1}^m \langle\psi_k|P|\phi_k\rangle. \end{aligned} \tag{19}$$

In the last equality, we have used $\||\psi_k\rangle\| = 1$. The effective eigenvectors are now minimizers of $S[\Phi]$.

The global minimum, when $\Phi \subset \mathcal{P}$ is allowed to vary freely, is seen to be attained for $|\phi_k\rangle = |P\psi_k\rangle$, the Bloch-Brandow effective eigenvectors. However, the canonical effective eigenvectors are determined by minimizing $S[\Phi]$ over all orthonormal sets Φ, which then becomes equivalent to maximizing the last term in Eq. (19), i.e., the overlaps $\sum_k \mathrm{Re}\langle\psi_k|P|\phi_k\rangle$ under the orthonormality constraint.

We will now prove the striking fact that the solution is given by

$$\left|\psi_k^{\text{eff}}\right\rangle = |\phi_k\rangle = e^{-G}|\psi_k\rangle, \tag{20}$$

where the unitary operator $Z := \exp(G) \in \mathrm{SU}(n)$ is the rotation (12). Equation (20) should be compared with Eq. (7). Thus, the exact eigenvectors are simply *the direct rotations of the effective eigenvectors from the model space into* $\mathcal{E}$.

Let us expand $|\psi_k\rangle \in \mathcal{E}$ and $|\phi_k\rangle \in \mathcal{P}$ in the principal vector bases, viz.,

$$|\psi_k\rangle = \sum_{j=1}^{m} |\eta_j\rangle\langle\eta_j|\psi_k\rangle,$$

$$|\phi_k\rangle = \sum_{j=1}^{m} |\xi_j\rangle\langle\xi_j|\phi_k\rangle.$$

Using $\langle\eta_j|\xi_k\rangle = \delta_{j,k}\cos\theta_j$, we compute the sum $A := \sum_{k=1}^{m}\langle\psi_k|P|\phi_k\rangle$ as

$$\begin{aligned} A &= \sum_{k,j,\ell=1}^{m} \langle\psi_k|\eta_j\rangle\langle\eta_j|\xi_\ell\rangle\langle\xi_\ell|\phi_k\rangle \\ &= \sum_{j,k=1}^{m} \cos\theta_j \langle\xi_j|\phi_k\rangle\langle\psi_k|\eta_j\rangle \end{aligned}$$

Now,

$$A = \sum_{j=1}^{m} \cos\theta_j u_{j,j},$$

where $u_{j,k}$ is a unitary matrix, which implies $|u_{j,j}| \leqslant 1$. Moreover, $u_{j,j} = 1$ for all j if and only if $u_{j,k} = \delta_{j,k}$, which then maximizes A, and also $\mathrm{Re}\,A$. Thus,

$$\sum_{k=1}^{m} \langle\xi_j|\phi_k\rangle\langle\psi_k|\eta_\ell\rangle = \delta_{j,\ell},$$

i.e.,

$$\langle\xi_j|\phi_k\rangle = \langle\eta_j|\psi_k\rangle = \langle\xi_j|Z^\dagger|\psi_k\rangle,$$

from which Eq. (20) follows, since $\{|\xi_k\rangle\}_{k=1}^m$ is a basis for $\mathcal{P}$, and the proof is complete.

The similarity transform in Eq. (5) is thus manifest, with $S = G$, viz.,

$$H_{\text{eff}}^{\text{c}} = PZ^\dagger HZP = Pe^{-G}He^{G}P. \tag{21}$$

Moreover, $Q\tilde{H}P = P\tilde{H}Q = 0$, verifying that the direct rotation in fact block-diagonalizes H.

E. Computing $|\psi_k^{\text{eff}}\rangle$

Assume that $|P\psi_k\rangle := P|\psi_k\rangle$, $k = 1, \ldots, m$ are available, as would be the case in the subcluster approach to the effective Hamiltonian. The effective eigenvectors $|\psi_k^{\text{eff}}\rangle$ are then given by a basis change F, i.e., the operator $F : \mathcal{P} \to \mathcal{P}$ defined by

$$F|P\psi_k\rangle := \left|\psi_k^{\text{eff}}\right\rangle.$$

Using the principal vector basis, we obtain

$$\begin{aligned} F|P\psi_k\rangle &= FP\sum_{j=1}^{m} |\eta_j\rangle\langle\eta_j|\psi_k\rangle \\ &= F\sum_{j=1}^{m} \cos\theta_j|\xi_j\rangle\langle\eta_j|\psi_k\rangle \\ &:= \sum_{j=1}^{m} |\xi_j\rangle\langle\xi_j|\psi_k^{\text{eff}}\rangle \\ &= \sum_{j=1}^{m} |\xi_j\rangle\langle\eta_j|\psi_k\rangle, \end{aligned}$$

from which we get the SVD

$$\begin{aligned} F &:= \sum_{k=1}^{m} \frac{1}{\cos\theta_k}|\xi_k\rangle\langle\xi_k| \\ &= (\omega^\dagger\omega + P)^{1/2}, \end{aligned} \tag{22}$$

where we have used Eq. (18). From Eq. (22) we see that F is symmetric and positive definite. Moreover, smaller angles θ_k means F is closer to the identity, consistent with $\mathcal{E}$ being closer to $\mathcal{P}$.

Let $|P\psi_k\rangle$ now be given in the orthonormal "zero order" basis $\{|e_k\rangle\}_{k=1}^m$ for $\mathcal{P}$, i.e., we have the basis change operator $\tilde{U}$ given by

$$\tilde{U} := \sum_{k=1}^{m} |P\psi_k\rangle\langle e_k|, \tag{23}$$

which transforms from the given basis to the Bloch-Brandow effective eigenvectors. In terms of the principal vector basis,

$$\begin{aligned} \tilde{U} &= \sum_{j=1}^{m} \cos\theta_j|\xi_j\rangle\langle\eta_j|\sum_k |\psi_k\rangle\langle e_k| \\ &=: \sum_{j=1}^{m} \cos\theta_j|\xi_j\rangle\langle y_j|, \end{aligned} \tag{24}$$

which is, in fact, the SVD, since the last sum over k is a unitary map from $\mathcal{P}$ to $\mathcal{E}$. In the operator $\tilde{U}\tilde{U}^\dagger$ this basis-dependent factor cancels, viz.,

$$\begin{aligned} \tilde{U}\tilde{U}^\dagger &= \sum_{k=1}^{m} |P\psi_k\rangle\langle P\psi_k| \\ &= \sum_{k=1}^{m} \cos^2\theta_k|\xi_k\rangle\langle\xi_k|, \end{aligned}$$

that is,

$$F = (\tilde{U}\tilde{U}^\dagger)^{-1/2}.$$

If we seek $|\psi_k^{\text{eff}}\rangle$ in the basis $\{|e_k\rangle\}_{k=1}^m$ as well, we let $\tilde{V}$ be the corresponding basis change operator, i.e.,

$$\tilde{V} := F\tilde{U} = (\tilde{U}\tilde{U}^\dagger)^{-1/2}\tilde{U}. \tag{25}$$

Equation (25) shows that $|\psi_k^{\text{eff}}\rangle$ is obtained by "straightening out" $|P\psi_k\rangle$, and that this depends *only* on the latter vectors. This is, in fact, an alternative to the common Gram-Schmidt

orthogonalization used in mathematical constructions and proofs. It was first introduced by Löwdin [24] under the name "symmetric orthogonalization," and the so-called Löwdin bases are widely used in quantum chemistry, where non-orthogonal basis functions are orthogonalized according to Eq. (25). It seemingly requires both inversion and matrix square root but is easily computed using the SVD. Combining Eqs. (22) and (24) gives

$$\tilde{V} = \sum_{k=1}^{m} |\xi_k\rangle\langle y_k|, \tag{26}$$

so that if the SVD (24) is available, $\tilde{V}$ is readily computed. Equation (26) is easily expressed in terms of matrices, but we defer the discussion to Sec. IV.

F. Shavitt's expression for exp(G)

Shavitt and Redmon [7] proved that

$$G = \tanh^{-1}(\omega - \omega^\dagger) \tag{27}$$

gives the Lie algebra element for the unitary operator $Z = \exp(G)$. The quite complicated proof was done using an expansion of the similarity transform using the Baker-Campbell-Hausdorff formula.

It may be clear now that in the present context we obtain the result simply as a by-product of the treatment in Sec. III B and the SVD (17) of ω, given in terms of the principal vectors and angles. We prove this here.

The function $\tanh^{-1}(z)$ is defined by its (complex) Taylor expansion about the origin, i.e.,

$$\tanh^{-1}(z) = \sum_{n=0}^{\infty} \frac{z^{2n+1}}{2n+1}. \tag{28}$$

The series converges for $|z| < 1$. Moreover,

$$\tanh^{-1}(z) = \frac{1}{2}\ln\left(\frac{1+z}{1-z}\right), \tag{29}$$

also valid for $|z| < 1$. For $z := \omega - \omega^\dagger$ we compute

$$z = \sum_{k=1}^{m} \mu_k(|\chi_k\rangle\langle\xi_k| - |\xi_k\rangle\langle\chi_k|), \quad \mu_k := \tan(\theta_k).$$

Using orthogonality relations between $|\xi_k\rangle$ and $|\chi_k\rangle$, we obtain

$$\begin{aligned} z^{2n+1} &= (-1)^n \sum_{k=1}^{m} \mu_k^{2n+1}(|\chi_k\rangle\langle\xi_k| - |\xi_k\rangle\langle\chi_k|) \\ &= i\sum_{k=1}^{m}(-i\mu_k)^{2n+1}(|\chi_k\rangle\langle\xi_k| - |\xi_k\rangle\langle\chi_k|). \end{aligned}$$

Using $i\tanh^{-1}(-iz) = \tan^{-1}(z)$, we sum the series (28) to

$$G = \tanh^{-1}(z) = \sum_{k=1}^{m} \theta_k(|\chi_k\rangle\langle\xi_k| - |\xi_k\rangle\langle\chi_k|),$$

which is identical to Eq. (13). The series does not converge for $\theta_k \geqslant \pi/4$, but the result is trivially analytically continued to arbitrary $0 \leqslant \theta_k \leqslant \pi/2$.

We now turn to the effective Hamiltonian. It is common [2,3,11] to compute $H_{\text{eff}}^{\text{c}}$ in terms of ω directly, using the definition (29) of $\tanh^{-1}(z)$, which implies

$$e^{\pm\tanh^{-1}(z)} = \sqrt{\frac{1\pm z}{1\mp z}} = \frac{1\pm z}{\sqrt{1-z^2}}$$

Upon insertion into $\tilde{H} = \exp(-G)H\exp(G)$, we obtain

$$\tilde{H} = \frac{1-\omega+\omega^\dagger}{\sqrt{1+\omega^\dagger\omega+\omega\omega^\dagger}} H \frac{1+\omega-\omega^\dagger}{\sqrt{1+\omega^\dagger\omega+\omega\omega^\dagger}}.$$

Projecting onto $\mathcal{P}$, the effective Hamiltonian becomes

$$H_{\text{eff}} = (P+\omega^\dagger\omega)^{-1/2}(P+\omega^\dagger)H(P+\omega)(P+\omega^\dagger\omega)^{-1/2}. \tag{30}$$

By using the Bloch equation (6) for the Bloch-Brandow effective Hamiltonian, we may eliminate QHQ from the above expression for H_{eff}, yielding

$$H_{\text{eff}}^{\text{c}} = (P+\omega^\dagger\omega)^{1/2}H(P+\omega)(P+\omega^\dagger\omega)^{-1/2}. \tag{31}$$

This expression is commonly implemented in numerical applications [3,25]. By comparing with Eqs. (22) and (16), we immediately see that

$$H_{\text{eff}}^{\text{c}} = F H_{\text{eff}}^{\text{BB}} F^{-1}, \tag{32}$$

which gives $H_{\text{eff}}^{\text{c}}$ as a similarity transform of $H_{\text{eff}}^{\text{BB}}$. In themselves, Eqs. (31) and (32) are not manifestly Hermitian, stemming from the elimination of QHQ. An implementation would require complicated matrix manipulations, including a matrix square root. It is therefore better to compute $H_{\text{eff}}^{\text{c}}$ using

$$H_{\text{eff}}^{\text{c}} = \sum_k E_k |\psi_k^{\text{eff}}\rangle\langle\psi_k^{\text{eff}}|,$$

together with Eq. (26), where the most complicated operation is the SVD of the operator $\tilde{U}$ given by Eq. (23). In Sec. IV we give a concrete matrix expression for $H_{\text{eff}}^{\text{c}}$.

G. Commuting observables

Great simplifications arise in the general quantum problem if continuous symmetries of the Hamiltonian can be identified, i.e., if one can find one or more observables S such that $[H, S] = 0$. Here, we discuss the impact of such symmetries of H on the effective Hamiltonian H_{eff}; both in the Bloch-Brandow and the canonical case. We point out the importance of choosing a model space that is an invariant of S as well, i.e., $[S, P] = 0$. In fact, we prove that this is the case if and only if $[H_{\text{eff}}, S] = 0$, i.e., H_{eff} has the same continuous symmetry.

Let $S = S^\dagger$ be an observable such that $[H, S] = 0$, i.e., H and S have a common basis of eigenvectors. We shall assume that $\{|\psi_k\rangle\}_{k=1}^n$ is such a basis, viz.,

$$\begin{aligned} H|\psi_k\rangle &= E_k|\psi_k\rangle, \\ S|\psi_k\rangle &= s_k|\psi_k\rangle. \end{aligned} \tag{33}$$

In general, there will be degeneracies in both E_k and s_k.

We now make the important assumption that

$$[S, P] = 0, \tag{34}$$

which is equivalent to

$$S = PSP + QSQ.$$

Under the assumption (34), we have

$$S|P\psi_k\rangle = PS|\psi_k\rangle = s_k|P\psi_k\rangle,$$

so that the Bloch-Brandow effective eigenvectors are still eigenvectors of S with the same eigenvalue s_k. Moreover, as we assume that $\{|P\psi_k\rangle\}_{k=1}^m$ is a (non-orthonormal) basis for $\mathcal{P}$, this not possible if $[S, P] \neq 0$. Thus, $[H_{\text{eff}}^{\text{BB}}, S] = 0$ if and only if $[S, P] = 0$ [in addition to the assumption (33).]

The assumption (34) also implies that $[S, \omega] = 0$, where $\omega = Q\omega P$ is the decoupling operator. We prove this by checking that it holds for *all* $|\psi_k\rangle$. For $k \leqslant m$,

$$\omega S|\psi_k\rangle = s_k Q|\psi_k\rangle = SQ|\psi_k\rangle = S\omega|\psi_k\rangle, \tag{35}$$

while for $k > m$ we need to expand $P|\psi_k\rangle$ in $|P\psi_j\rangle$, $j \leqslant m$, viz.,

$$P|\psi_k\rangle = \sum_{j=1}^{m} |P\psi_j\rangle\langle\widetilde{P\psi}_j|P|\psi_k\rangle, \quad k > m,$$

and use Eq. (35). Furthermore, $[S, \omega^\dagger]^\dagger = [\omega^\dagger, S] = 0$. It follows that

$$[S, (\omega - \omega^\dagger)^n] = 0, \quad n = 0, 1, \ldots,$$

and, by Eq. (28), that

$$[S, e^G] = [S, e^{-G}] = 0.$$

This gives

$$S\big|\psi_k^{\text{eff}}\big\rangle = Se^{-G}|\psi_k\rangle = s_k\big|\psi_k^{\text{eff}}\big\rangle.$$

Again, since $\{|\psi_k^{\text{eff}}\rangle\}_{k=1}^m$ is a basis for $\mathcal{P}$, this holds if and only if $[S, P] = 0$. Accordingly, $[H_{\text{eff}}^{\text{c}}, S] = 0$ if and only if $[S, P] = 0$ [and the assumption (33).]

The importance of this fact is obvious. If one starts with a Hamiltonian that conserves, say, angular momentum, and computes the effective interaction using a model space that is *not* an invariant for the angular momentum operator, i.e., not rotationally symmetric, then the final Hamiltonian will not have angular momentum as a good quantum number.

One possible remedy if $[P, S] \neq 0$ is to define the effective observable $S_{\text{eff}} := P\exp(-G)S\exp(G)P$ (which in the commuting case is equal to PSP) which obviously commutes with H_{eff} and satisfies

$$S_{\text{eff}}\big|\psi_k^{\text{eff}}\big\rangle = s_k\big|\psi_k^{\text{eff}}\big\rangle.$$

This amounts to modifying the concept of rotational symmetry in the above example.

The assumptions (33) and (34) have consequences also for the structure of the principal vectors $|\xi_k\rangle \in \mathcal{P}$ and $|\eta_k\rangle \in \mathcal{E}$. Indeed, we write

$$\mathcal{E} = \bigoplus_s \mathcal{E}_s,$$

$$\mathcal{P} = \bigoplus_s \mathcal{P}_s,$$

where the sum runs over all distinct eigenvalues $s_k, k = 1, \ldots, m$ of S, and where $\mathcal{E}_s$ ($\mathcal{P}_s$) is the corresponding eigenspace, i.e.,

$$\mathcal{E}_s := \text{span}\{|\psi_k\rangle : S|\psi_k\rangle = s|\psi_k\rangle\},$$
$$\mathcal{P}_s := \text{span}\big\{\big|\psi_k^{\text{eff}}\big\rangle : S\big|\psi_k^{\text{eff}}\big\rangle = s\big|\psi_k^{\text{eff}}\big\rangle\big\}.$$

The eigenspaces are all mutually orthogonal, viz., $\mathcal{E}_s \perp \mathcal{E}_{s'}$, $\mathcal{P}_s \perp \mathcal{P}_{s'}$, and $\mathcal{E}_s \perp \mathcal{P}_{s'}$, for $s \neq s'$. The definition (3) of the principal vectors and angles can then be written

$$\cos(\theta_k) = \max_s \max_{\substack{|\xi\rangle\in\mathcal{P}_s,\ \langle\xi|\xi\rangle=1 \\ \langle\xi_j|\xi\rangle=0,\ j<k}} \max_{\substack{|\eta\rangle\in\mathcal{E}_s,\ \langle\eta|\eta\rangle=1 \\ \langle\eta_j|\eta\rangle=0,\ j<k}} Re\langle\xi|\eta\rangle$$
$$=: \langle\xi_k|\eta_k\rangle.$$

Thus, for each k, there is an eigenvalue s of S such that

$$S|\xi_k\rangle = s|\xi_k\rangle,$$
$$S|\eta_k\rangle = s|\eta_k\rangle,$$

showing that the principal vectors are eigenvectors of S if and only if $[S, P] = 0$, $[S, H] = 0$, and the assumption (33).

The present symmetry considerations imply that model spaces obeying as many symmetries as possible should be favored over less symmetric model spaces, since these other model spaces become less "natural" or "less effective" in the sense that their geometry is less similar to the original Hilbert space. This is most easily seen from the fact that principal vectors are eigenvectors for the conserved observable S. This may well have great consequences for the widely used subcluster approximation to the effective Hamiltonian in no-core shell model calculations [3,6,26], where one constructs the effective Hamiltonian for a system of a particles in order to obtain an approximation to the $A > a$-body effective Hamiltonian. The model space in this case is constructed in different ways in different implementations. Some of these model spaces may therefore be better than others due to different symmetry properties.

IV. MATRIX FORMULATIONS

A. Preliminaries

Since computer calculations are invariably done using matrices for operators, we here present matrix expressions for $H_{\text{eff}}^{\text{c}}$ and compare them to those usually programed in the literature, as well as expressions for $H_{\text{eff}}^{\text{BB}}$ and ω.

Recall the standard basis $\{|e_k\rangle\}_{k=1}^n$ of $\mathcal{H}$, where the $\{|e_k\rangle\}_{k=1}^m$ constitute a basis for $\mathcal{P}$. These are usually eigenvectors of the unperturbed "zero order" Hamiltonian H_0, but we will not use this assumption. As previously, we also assume without loss that the eigenpairs we wish to approximate in H_{eff} are $\{(E_k, |\psi_k\rangle)\}_{k=1}^m$.

An operator $A : \mathcal{H} \to \mathcal{H}$ has a matrix $\mathsf{A} \in \mathbb{C}^{n\times n}$ associated with it. The matrix elements are given by $\mathsf{A}_{jk} = \langle e_j|A|e_k\rangle$ such that

$$A = \sum_{j,k=1}^{n} |e_j\rangle\langle e_j A|e_k\rangle\langle e_k|| = \sum_{j,k=1}^{n} |e_j\rangle\mathsf{A}_{jk}\langle e_k|.$$

Similarly, any vector $|\phi\rangle \in \mathcal{H}$ has a column vector $\vec{\phi} \in \mathbb{C}^n$ associated with it, with $\vec{\phi}_j = \langle e_j|\phi\rangle$. We will also view dual vectors, e.g., $\langle\psi|$, as row vectors.

The model space $\mathcal{P}$ and the excluded space $\mathcal{Q}$ are conveniently identified with $\mathbb{C}^m$ and $\mathbb{C}^{n-m}$, respectively. Also note that PAP, PAQ, etc., are identified with the upper left $m \times m$, upper right $m \times (n-m)$, etc., blocks of A as in Eq. (1). We use a notation inspired by FORTRAN and MATLAB and write

$$\mathsf{PAP} = \mathsf{A}(1:m, 1:m), \quad \mathsf{PAQ} = \mathsf{A}(1:m, m+1:n),$$

and so forth.

We introduce the unitary operator U as

$$U = \sum_{k=1}^{n} |\psi_k\rangle\langle e_k|,$$

i.e., a basis change from the chosen standard basis to the eigenvector basis. The columns of U are the eigenvector components in the standard basis, i.e.,

$$\mathsf{U}_{jk} = \vec{\psi}_{k,j} = \langle e_j|\psi_k\rangle,$$

and are typically the eigenvectors returned from a computer implementation of the spectral decomposition, viz.,

$$\mathsf{H} = \mathsf{UEU}^\dagger, \quad \mathsf{E} = \mathrm{diag}(E_1, \ldots, E_n). \tag{36}$$

The SVD is similarly transformed to matrix form. The SVD defined in Sec. II B is then formulated as follows: for any matrix $\mathsf{A} \in \mathbb{C}^{q\times r}$ there exist matrices $\mathsf{X} \in \mathbb{C}^{q\times p}[p = \min(q, r)]$ and $\mathsf{Y} \in \mathbb{C}^{r\times p}$, such that $\mathsf{X}^\dagger\mathsf{X} = \mathsf{Y}^\dagger\mathsf{Y} = I_p$ (the identity matrix $\mathbb{C}^{p\times p}$), and a non-negative diagonal matrix $\Sigma \in \mathbb{R}^{p\times p}$ such that

$$\mathsf{A} = \mathsf{X}\Sigma\mathsf{Y}^\dagger.$$

Here, $\Sigma = \mathrm{diag}(\sigma_1, \ldots, \sigma_p)$, σ_k being the singular values.

The columns of X are the left singular vectors' components, i.e., $\mathsf{X}_{j,k} = \langle e_j|x_k\rangle$, and similarly for Y and the right singular vectors. The difference between the two SVD formulations is then purely geometric, as the matrix formulation favors the standard bases in $\mathcal{X}$ and $\mathcal{Y}$.

The present version of the matrix SVD is often referred to as the "economic" SVD, since the matrices X and Y may be extended to unitary matrices over $\mathbb{C}^q$ and $\mathbb{C}^r$, respectively, by adding singular values $\sigma_k = 0$, $k > m$. The matrix Σ is then a $q \times r$ matrix with "diagonal" given by σ_k. This is the "full" SVD, equivalent to our basis-free definition.

B. Algorithms

Let the m eigenvectors $|\psi_k\rangle$ be calculated and arranged in a matrix U, i.e., $\psi_k = \mathsf{U}(1:n, k)$ (where the subscript does *not* pick a single component). Consider the operator $\tilde{U}$ defined in Eq. (23), whose matrix columns are the Bloch-Brandow effective eigenvectors $|P\psi_k\rangle$ in the standard basis, viz.,

$$\tilde{\mathsf{U}} = \mathsf{U}(1:m, 1:m).$$

The columns of the matrix of $\tilde{V} = (\tilde{U}\tilde{U}^\dagger)^{-1/2}\tilde{U}$ are the canonical effective eigenvectors $\vec{\tilde{\psi}}_k^{\mathrm{eff}}$. The SVD (24) can be written as

$$\tilde{\mathsf{U}} = \mathsf{X}\Sigma\mathsf{Y}^\dagger,$$

which gives

$$\tilde{\mathsf{U}}\tilde{\mathsf{U}}^\dagger = \mathsf{X}\Sigma^2\mathsf{X}^\dagger.$$

Since $\Sigma_{kk} = \cos\theta_k > 0$, we obtain

$$(\tilde{\mathsf{U}}\tilde{\mathsf{U}}^\dagger)^{-1/2} = \mathsf{X}\Sigma^{-1}\mathsf{X}^\dagger,$$

which gives, when applied to $\tilde{\mathsf{U}}$,

$$\tilde{\mathsf{V}} = (\tilde{\mathsf{U}}\tilde{\mathsf{U}}^\dagger)^{-1/2}\tilde{\mathsf{U}} = \mathsf{XY}^\dagger.$$

Thus, we obtain the canonical effective eigenvectors by taking the matrix SVD of $\tilde{\mathsf{U}} = \mathsf{U}(1:m, 1:m)$ and multiplying together the matrices of singular vectors. As efficient and robust SVD implementations are almost universally available, e.g., in the LAPACK library, this makes the canonical effective interaction much easier to compute than that in Eq. (31), viz.,

$$\mathsf{H}^{\mathrm{c}}_{\mathrm{eff}} = \tilde{\mathsf{V}}\mathsf{E}(1:m, 1:m)\tilde{\mathsf{V}}^\dagger.$$

This version requires one SVD computation and three matrix multiplications, all with $m \times m$ matrices, one of which is diagonal. Equation (31) requires, on the other hand, several more matrix multiplications, inversions, and the square root computation. The Bloch-Brandow effective Hamiltonian is simply calculated by

$$\mathsf{H}^{\mathrm{BB}}_{\mathrm{eff}} = \tilde{\mathsf{U}}\mathsf{E}(1:m, 1:m)\tilde{\mathsf{U}}^{-1}.$$

For the record, the matrix of ω is given by

$$\boldsymbol{\omega} = \mathsf{U}(m+1:n, 1:m)\tilde{\mathsf{U}}^{-1},$$

although we have no use for it when using the SVD-based algorithm. It may be useful, though, to be able to compute the principal vectors for $\mathcal{P}$ and $\mathcal{E}$. For this, one may compute the SVD of ω or of $\mathsf{PP}' = \tilde{\mathsf{U}}\mathsf{U}(1:n, 1:m)^\dagger$; the latter gives $\cos\theta_k$, $|\xi_k\rangle$, and $|\eta_k\rangle$ directly in the standard basis as singular values and vectors, respectively.

V. DISCUSSION AND OUTLOOK

We have characterized the effective Hamiltonians commonly used in nuclear shell-model calculations in terms of geometric properties of the spaces $\mathcal{P}$ and $\mathcal{E}$. The SVD and the principal angles and vectors were central in the investigation. While the Bloch-Brandow effective Hamiltonian is obtained by orthogonally projecting $\mathcal{E}$ onto $\mathcal{P}$, thereby *globally* minimizing the norm-error of the effective eigenvectors, the canonical effective Hamiltonian is obtained by rotating $\mathcal{E}$ into $\mathcal{P}$ using $\exp(-G)$, which minimizes the norm-error while retaining orthonormality of the effective eigenvectors. Moreover, we obtained a complete description of the decoupling operator ω in terms of the principal angles and vectors defining $\exp(G)$.

An important question is whether the present treatment generalizes to infinite dimensional Hilbert spaces. Our analysis fits into the general assumptions in the literature, being that $n = \dim(\mathcal{H})$ is large but finite, or at least that the spectrum of H is purely discrete. A minimal requirement is that H has m eigenvalues, so that $\mathcal{E}$ can be constructed. In particular, the SVD generalizes to finite rank operators in the infinite dimensional case and is thus valid for all the operators considered here even when $n = \infty$.

Unfortunately, H has almost never a purely discrete spectrum. It is well known that the spectrum in general

has continuous parts and resonances embedded in these, and a proper theory should treat these cases as well as the discrete part. In fact, the treatments of H_{eff} in the literature invariably glosses over this. It is an interesting future project to develop a geometric theory for the effective Hamiltonians that incorporates resonances and continuous spectra.

The geometrical view simplified and unified the available treatments in the literature somewhat and offered further insights into the effective Hamiltonians. Moreover, the symmetry considerations in Sec. III G may have significant bearing on the analysis of perturbation expansions and the properties of subcluster approximations to $H^{\text{c}}_{\text{eff}}$.

Indeed, it is easy to see that if we have a *complete* set of commuting observables (CSCO) [27] for H_0, and the same set of observables form a CSCO for H_1, all eigenvalues and eigenfunctions of $H(z) = H_0 + zH_1$ are analytic in $z \in \mathbb{C}$, implying that the Rayleigh-Schrödinger perturbation series for $H = H_0 + H_1$ converges (i.e., at $z = 1$) [15]. Intuitively, the fewer commuting observables we are able to identify, the more likely it is that there are singularities in $H_{\text{eff}}(z)$, the so-called intruder states. The Rayleigh-Schrödinger series diverges outside the singularity closest to $z = 0$ [15]; and in nuclear systems, this singularity is indeed likely to be close to $z = 0$. On the other hand, resummation of the series can be convergent and yield an analytic continuation of H_{eff} outside the region of convergence [28]. To the best of our knowledge, there is no systematic treatment of this phenomenon in the literature, except for some iterative procedures [29,30] and attempts at using Padé approximants [31]. On the contrary, to be able to do such a resummation consistently is sort of the "holy grail" of many-body perturbation theory. A geometric study of the present kind to many-body perturbation theory and diagram expansions may yield a step closer to this goal, as we have clearly identified the impact of commuting observables on the principal vectors of $\mathcal{E}$ and $\mathcal{P}$.

We have also discussed a compact algorithm in terms of matrices to compute $H^{\text{c}}_{\text{eff}}$, relying on the SVD. This algorithm, useful in the subcluster approach to the effective Hamiltonian, is, to the best of our knowledge, previously unpublished. Since robust and fast SVD implementations are readily available, e.g., in the LAPACK library, and since few other matrix manipulations are needed, it should be preferred in computer implementations.

As stressed in the Introduction, the algorithms presented are really only useful if we compute the *exact* effective Hamiltonian, as opposed to a many-body perturbation theoretical calculation, and if we know what exact eigenpairs to use, such as in a subcluster approximation. In this case, one should analyze the error in the approximation, i.e., the error in neglecting the many-body correlations in $H^{\text{c}}_{\text{eff}}$. In the perturbative regime, some results exist [6]. We believe that the geometric description may facilitate a deeper analysis, and this is an interesting idea for future work.

ACKNOWLEDGMENTS

The author wishes to thank Prof. M. Hjorth-Jensen, CMA, for helpful discussions. This work was funded by CMA through the Norwegian Research Council.

[1] D. Dean, T. Engeland, M. Hjorth-Jensen, M. Kartamyshev, and E. Osnes, Prog. Part. Nucl. Phys. **53**, 419 (2004).
[2] E. Caurier, G. Martinez-Pinedo, F. Nowacki, A. Poves, and A. P. Zuker, Rev. Mod. Phys. **77**, 427 (2005).
[3] P. Navrátil, J. P. Vary, and B. R. Barrett, Phys. Rev. C **62**, 054311 (2000).
[4] C. Bloch, Nucl. Phys. **6**, 329 (1958).
[5] B. Brandow, Rev. Mod. Phys. **39**, 771 (1967).
[6] D. Klein, J. Chem. Phys. **61**, 786 (1974).
[7] I. Shavitt and L. T. Redmon, J. Chem. Phys. **73**, 5711 (1980).
[8] I. Lindgren, J. Phys. B **7**, 2441 (1974).
[9] P. Ellis and E. Osnes, Rev. Mod. Phys. **49**, 777 (1977).
[10] I. Lindgren and J. Morrison, *Atomic Many-Body Theory* (Springer, New York, 1982).
[11] K. Suzuki, Prog. Theor. Phys. **68**, 246 (1982).
[12] T. Kuo, Springer Lect. Notes Phys. **144**, 248 (1981).
[13] J. Van Vleck, Phys. Rev. **33**, 467 (1929).
[14] Kemble, *The Fundamental Principles of Quantum Mechanics with Elementary Applications* (McGraw-Hill, New York, 1937).
[15] T. Schucan and H. Weidenmüller, Ann. Phys. (NY) **76**, 483 (1973).
[16] A. Björck and G. Golub, Math. Comput. **27**, 579 (1973).
[17] A. Knyazev and M. Argentati, SIAM J. Sci. Comput. **23**, 2008 (2002).
[18] G. Golub and C. van Loan, *Matrix Computations* (Johns Hopkins, Baltimore, MD, 1989).
[19] C. Davis and W. M. Kahan, SIAM J. Numer. Anal. **7**, 1 (1970).
[20] O. Jordahl, Phys. Rev. **45**, 87 (1934).
[21] H. Primas, Rev. Mod. Phys. **35**, 710 (1963).
[22] S. Blanes, F. Casas, J. Oteo, and J. Ros, J. Phys. A: Math. Theor. **31**, 259 (1998).
[23] K. Suzuki, Prog. Theor. Phys. **68**, 1627 (1982).
[24] P.-O. Löwdin, J. Chem. Phys. **18**, 365 (1950).
[25] G. Hagen, M. Hjorth-Jensen, and N. Michel, Phys. Rev. C **73**, 064307 (2006).
[26] J. Da Providencia and C. Shakin, Ann. Phys. (NY) **30**, 95 (1964).
[27] A. Messiah, *Quantum Mechanics* (Dover, New York, 1999).
[28] P. Schaefer, Ann. Phys. (NY) **87**, 375 (1974).
[29] F. Andreozzi, Phys. Rev. C **54**, 684 (1996).
[30] K. Suzuki and S. Lee, Prog. Theor. Phys. **64**, 2091 (1980).
[31] H. M. Hofmann, Ann. Phys. (NY) **113**, 400 (1978).

4 Open source FCI code for quantum dots and effective interactions

This paper is submitted to Physical Review E.

Open source FCI code for quantum dots and effective interactions

Simen Kvaal[1,*]

[1]*Centre of Mathematics for Applications, University of Oslo, N-0316 Oslo, Norway*

(Dated: October 15. 2008)

We describe OPENFCI, an open source implementation of the full configuration-interaction method (FCI) for two-dimensional quantum dots with optional use of effective renormalized interactions. The code is written in C++ and is available under the Gnu General Public License. The code and core libraries are well documented and structured in a way such that customizations and generalizations to other systems and numerical methods are easy tasks. As examples we provide a matrix element tabulation program and an implementation of a simple model from nuclear physics, in addition to the quantum dot application itself.

PACS numbers: 02.60.-x, 95.75.Pq, 73.21.La, 24.10.Cn
Keywords: full configuration interaction; open source; C++; quantum dots; effective interactions

I. INTRODUCTION

Quantum dots, nanometre-scale semiconductor devices confining a varying number of electrons, have been studied intensely in the last two decades. Quantum dots are fabricated using essentially macroscopic tools, for example etching techniques, but the resulting confinement allows for quantum mechanical behaviour of the electrons. Many of the parameters are directly controllable, thereby justifying the term "artificial atoms" or "designer atoms". These considerations explain the immense research activity on these systems. For a general introduction, see Ref. [1] and references therein.

A very common model is that of a parabolic quantum dot, in which N electrons are confined in an isotropic harmonic oscillator potential in d spatial dimensions, where d is determined by the semi-conductor environment. Electronic structure calculations on the parabolic dot and similar systems are often carried out using the full configuration-interaction method (FCI), also called exact diagonalization [1]. The Hamiltonian is then projected onto a finite-dimensional subspace of the N-electron Hilbert space and diagonalized. Care is taken in order to exploit dynamical and discrete symmetries of the exact problem, such as conservation of angular momentum and total electron spin, in order to block-diagonalize the Hamiltonian matrix and reduce the computational complexity.

In this article, we describe OPENFCI, a recently developed open source C++ code implementing the FCI method for quantum dots [2]. The code has a generic framework in the shape of library functions, thereby allowing easy customization and extension to other systems and methods, e.g., three-dimensional quantum dots or the nuclear no-core shell model.

OPENFCI implements a renormalization of the two-body interactions, a technique widely used in nuclear no-core shell model calculations. This allows for accelerated convergence with respect to Slater determinant basis size [3, 4]. To the author's knowledge, no other available code provides such effective interactions for quantum dot systems. The code can be easily modified to create effective interactions for almost many-body problem using a harmonic oscillator basis.

The code is developed in a Linux environment using Gnu C++, and is readily portable to other environments and compilers. The Fortran 77 libraries LAPACK and ARPACK are required, but as these are available on a wide range of platforms, portability should not be affected. OPENFCI is released under the Gnu General Public License (Gnu GPL) [5] and is documented using Doxygen [6]. As an open source project, the code can freely be used and modified.

The article is organized as follows: In Section II, the FCI method is introduced in the context of the parabolic quantum dot, where we also discuss the reduction of the Hamiltonian matrix by means of commuting operators and configurational state functions. In Section III we discuss the effective two-body interaction. As the technique is likely to be unfamiliar to most readers outside the nuclear physics community, this is done in some detail. In Section IV we discuss the organization and use of OPENFCI. We also give some results from example runs, and in particular an analytically solvable non-trivial model due to Johnson and Payne is considered [7], where the only modification of the parabolic quantum dot is the interaction. Finally, we conclude our article in Section V.

Two appendices have been provided, Appendix A detailing the heavily-used centre-of-mass transformation and Appendix B discussing the exact numerical solution of the two-electron quantum dot needed for the effective interaction scheme.

II. FCI METHOD

A. Hamiltonian in occupation number formalism

We consider N electrons trapped in an isotropic harmonic oscillator potential in d spatial dimensions. The electrons interact via the Coulomb potential given by $U(r_{ij}) = \lambda/r_{ij}$, where $r_{ij} = \|\vec{r}_i - \vec{r}_j\|$ is the inter-particle distance and λ is a constant. The quantum dot Hamiltonian then reads

$$H := \sum_{i=1}^{N} H_0(i) + \sum_{i<j}^{N} U(r_{ij}), \tag{1}$$

*Electronic address: simen.kvaal@cma.uio.no

where the second sum runs over all pairs $1 \le i < j \le N$, and where $H_0(i)$ is the one-body Hamiltonian defined by

$$H_0(i) := -\frac{1}{2}\nabla_i^2 + \frac{1}{2}\|\vec{r}_i\|^2.$$

The interaction strength λ is given by

$$\lambda = \sqrt{\frac{m^*}{\omega\hbar^3}}\frac{1}{\epsilon}\frac{e^2}{4\pi\epsilon_0}, \tag{2}$$

where ϵ is the dielectric constant of the semiconductor bulk, $e^2/4\pi\epsilon_0 \approx 1.440$ eV·nm, and $\omega = \hbar/m^*a^2$, a being the trap size and length unit, and m^* being the effective electron mass. Typical values for GaAs quantum dots are $\epsilon = 12.3$, $m^* = 0.067$ electron masses, and $a = 20$ nm, yielding $\lambda = 2.059$. The energy unit is $\hbar\omega$, in this case $\hbar\omega = 2.84$ meV.

Choosing a complete set $\{\phi_\alpha(x)\}_{\alpha\in A}$ of single-particle orbitals (where $x = (\vec{r}, s)$ denotes both spatial and spin degrees of freedom, and $\alpha = (a,\sigma)$ denotes both generic spatial quantum numbers a and spin projection quantum numbers $\sigma = \pm 1$), H can be written in occupation number form as

$$H = \sum_{a,b}\sum_{\sigma} h_b^a a_{a,\sigma}^\dagger a_{b,\sigma} + \frac{1}{2}\sum_{abcd}\sum_{\sigma\tau} u_{cd}^{ab} a_{a,\sigma}^\dagger a_{b,\tau}^\dagger a_{d,\tau} a_{c,\sigma}, \tag{3}$$

where $a_\alpha^\dagger$ (a_α) creates (destroys) a particle in the orbital $\phi_\alpha(x)$. These operators obey the usual anti-commutation relations

$$\{a_\alpha, a_\beta^\dagger\} = \delta_{\alpha,\beta}, \quad \{a_\alpha, a_\beta\} = 0. \tag{4}$$

For a review of second quantization and occupation number formalism, see for example Ref. [8]. The single-particle orbitals are chosen on the form

$$\phi_{(a,\sigma)}(x) := \varphi_a(\vec{r})\chi_\sigma(s),$$

where $\{\varphi_a(\vec{r})\}$ are spinless orbitals and $\chi_\sigma(s) = \delta_{\sigma,s}$ are spinor basis functions corresponding to the eigenstates of the spin-projection operator S_z with eigenvalues $\sigma/2$.

It is important, that since the single-particle orbitals $\{\varphi_a(\vec{r})\}_{a\in A}$ are denumerable, we may choose an ordering on the set A, such that A can in fact be identified with a range of integers, $A \approxeq \{0,1,2,\cdots,L/2\}$. In most *ab initio* systems L is infinite, since the Hilbert space is infinite-dimensional. Similarly, $\alpha = (a,+1)$ is identified with even integers, and $\alpha = (a,-1)$ with odd integers, creating an ordering of the single-particle orbitals $\phi_\alpha(x)$, and α is identified with an integer $0 \le I(\alpha) \le L$.

The single-particle matrix elements h_b^a and the two-particle elements u_{cd}^{ab} are defined by

$$h_b^a := \langle\varphi_a|H_0|\varphi_b\rangle = \int \overline{\varphi_a(\vec{r})} H_0 \varphi_b(\vec{r})\, \mathrm{d}^d r,$$

and

$$\begin{aligned} u_{cd}^{ab} &:= \langle\varphi_a\varphi_b|U(\vec{r}_{12})|\varphi_c\varphi_d\rangle \\ &= \lambda\int \overline{\varphi_a(\vec{r}_1)\varphi_b(\vec{r}_2)}\frac{1}{r_{12}}\varphi_c(\vec{r}_1)\varphi_d(\vec{r}_2)\, \mathrm{d}^d r_1 \mathrm{d}^d r_2, \end{aligned} \tag{5}$$

respectively.

The spatial orbitals $\varphi_a(\vec{r})$ are usually chosen as eigenfunctions of H_0, so that $h_b^a = \delta_{a,b}\epsilon_a$.

The basis functions for N-particle Hilbert space are Slater determinants $|\Phi_{\alpha_1,\alpha_2,\cdots,\alpha_N}\rangle$ defined by

$$|\Phi_{\alpha_1,\cdots\alpha_N}\rangle := a_{\alpha_1}^\dagger a_{\alpha_2}^\dagger \cdots a_{\alpha_N}^\dagger |-\rangle,$$

where $|-\rangle$ is the zero-particle vacuum. In terms of single-particle orbitals, the spatial representation is

$$\Phi_{\alpha_1,\cdots,\alpha_N}(x_1,\cdots,x_N) = \frac{1}{\sqrt{N!}}\sum_{p\in S_N}(-)^{|p|}\prod_{i=1}^N \phi_{\alpha_{p(i)}}(x_i),$$

where S_N is the group of permutations of N symbols. The Slater determinants are anti-symmetric with respect to permutations of both x_i and α_i, so that the orbital numbers α_i must all be distinct to give a nonzero function. Each orbital is then occupied by at most one particle. Moreover, for a given set $\{\alpha_i\}_{i=1}^N$ of orbitals, one can create $N!$ distinct Slater determinants that are linearly dependent. In order to remove this ambiguity, we choose only orbital numbers such that $I(\alpha_i) < I(\alpha_j)$ whenever $i < j$.

It follows, that there is a natural one-to-one correspondence between Slater determinants with N particles and integers b whose binary representations have N bits set. (If $|A| = L < \infty$, the integers are limited to $0 \le b < 2^L$.) Each bit position k corresponds to an orbital $\phi_\alpha(x)$ through $k = I(\alpha)$, and the bit is set if the orbital is occupied. Creating and destroying particles in $|\Phi_{\alpha_1,\cdots,\alpha_N}\rangle$ simply amounts to setting or clearing bits (possibly obtaining the zero-vector if a particle is destroyed or created twice in the same orbital), keeping track of the possible sign change arising from bringing the set $\{\alpha_i\}$ on ordered form using Eqn. (4). Note that the vacuum $|-\rangle$ corresponds to $b = 0$, which is *not* the zero vector, but the single state with zero particles.

B. Model spaces

The FCI calculations are done in a finite-dimensional subspace $\mathscr{P}$ of the N-particle Hilbert space, called the model space. The model space has a basis $\mathscr{B}$ of Slater determinants, and $\mathscr{P}$ has the orthogonal projector P given by

$$P := \sum_{|\Phi_b\rangle\in\mathscr{B}} |\Phi_b\rangle\langle\Phi_b|. \tag{6}$$

The configuration-interaction method in general now amounts to diagonalizing (in the sense of finding a few of the lowest eigenvalues of) the, in general, large and sparse matrix PHP. The only approximation we have made is the truncation of the N-particle Hilbert space.

The model space $\mathscr{P}$ is seen to be a function of the single particle orbitals $\varphi_a(\vec{r})$, whom we choose to be the eigenfunctions of H_0, i.e., harmonic oscillator eigenfunctions. These may be given on several equivalent forms, but it is convenient to utilize rotational symmetry of H_0 to create eigenfunctions

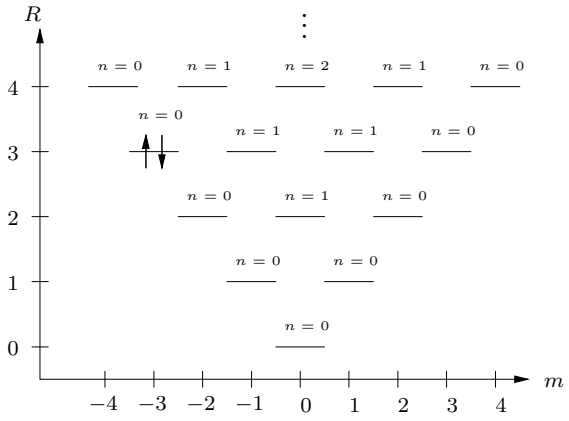

FIG. 1: Structure of single-particle orbitals of the two-dimensional harmonic oscillator. Angular momentum and shell number/energy on axes, and nodal quantum number n at each orbital. Orbital $n=0$, $m=-3$ in shell $R=3$ is occupied by two electrons for illustration.

of the projection of the angular momentum L_z. In $d=2$ dimensions we obtain the Fock-Darwin orbitals defined in polar coordinates by

$$\varphi_{n,m}(r,\theta) = \frac{1}{\sqrt{\pi}} e^{im\theta} r^{|m|} \tilde{L}_n^{|m|}(r^2) e^{-r^2/2}. \tag{7}$$

Here $\tilde{L}_n^k(x) = (-1)^n [n!/(n+|m|)!]^{1/2} L_n^k(x)$ is the normalized generalized Laguerre polynomial. The factor $(-1)^n$ is for convenience, see Appendix A 1. The harmonic oscillator energy is $2n+|m|+1$ and the eigenvalue of $L_z = -i\partial/\partial_\theta$ is m. All eigenfunctions with the same energy $2n+|m|+1=:R+1$ span a single-particle *shell*. The single-particle orbitals are illustrated in Fig. 1.

For a Slater determinant $|\Phi_{\alpha_1,\cdots,\alpha_N}\rangle$, we have

$$\sum_{i=1}^{N} H_0(i) |\Phi_{\alpha_1,\cdots,\alpha_N}\rangle = E^0_{\alpha_1,\cdots,\alpha_N} |\Phi_{\alpha_1,\cdots,\alpha_N}\rangle$$

with

$$E^0_{\alpha_1,\cdots,\alpha_N} := \sum_{i=1}^{N} (R_i+1),$$

where $R_i = 2n_i + |m_i|$, and

$$\sum_{i=1}^{N} L_z(i) |\Phi_{\alpha_1,\cdots,\alpha_N}\rangle = M |\Phi_{\alpha_1,\cdots,\alpha_N}\rangle,$$

where $M = \sum_{i=1}^{N} m_i$.

To complete our definition of $\mathscr{P}$, we let

$$\mathscr{B} = \mathscr{B}_R = \left\{ |\Phi_{\alpha_1,\cdots,\alpha_N}\rangle \ : \ \sum_{i=1}^{N} R_i \le R \right\}, \tag{8}$$

where R is called the energy cut, for obvious reasons. As $R \to \infty$, the whole Hilbert space is spanned, and the eigenpairs of PHP converge to those of H.

C. Configurational state functions and block diagonality

In order to reduce the complexity of the computations, we need to exploit symmetries of H. First of all, $[H,L_z]=0$, and it is obvious that also $[H,S_z]=0$, where the spin projection operator S_z is given by

$$S_z := \frac{1}{2} \sum_{a,\sigma} \sigma a^\dagger_{a,\sigma} a_{a,\sigma}.$$

The Slater determinants are eigenvectors of both L_z and S_z with eigenvalues M and $s_z = \sum_{i=1}^{N} \sigma_i/2$, respectively. We obtain a natural splitting of the model space $\mathscr{P}$ into subspaces with constant angular momentum M and spin projection s_z, viz,

$$\mathscr{P} = \bigoplus_{M,s_z} \mathscr{P}_{M,s_z}, \quad P = \sum_{M} \sum_{s_z} P_{M,s_z}.$$

The diagonalization of H can thus be done within each space $\mathscr{P}_{M,s_z}$ separately, amounting to diagonalizing individual blocks $P_{M,s_z} H P_{M,s_z}$.

The Hamiltonian (3) also commutes with total electron spin S^2, $[S^2,S_z]=0$, given by

$$S^2 := S_z^2 + \frac{1}{2}(S_+S_- + S_-S_+),$$

with

$$S_\pm := \sum_a a^\dagger_{a_\pm} a_{a_\mp},$$

so that a common basis for S_z and S^2 would lead to even smaller matrix blocks.

The eigenvalues of S^2 are on the form $s(s+1)$, where $0 \le 2s \le N$ is an odd (even) integer for odd (even) N. For a joint eigenfunction of S_z and S^2, called a configurational state function (CSF), $|s_z| \le s$. The Slater determinants are, however, not eigenfunctions of S^2, but such can be constructed by taking linear combinations of a small number Slater determinants. For details on this algorithm, see Ref. [9]. Suffice it to say here, that S^2 only couples Slater determinants with identical sets of doubly occupied orbitals (meaning that $\phi_{(a,+)}$ and $\phi_{(a,-)}$ are both occupied, as in Figure 1) and singly occupied orbitals (meaning that only one of $\phi_{(a,+)}$ and $\phi_{(a,-)}$ are occupied). It is easy to see that S^2 does not couple Slater determinants in $\mathscr{P}_{M,s_z}$ to another $\mathscr{P}_{M',s'_z}$. Thus, we obtain the splitting

$$\mathscr{P}_{M,s_z} = \bigoplus_{s} \mathscr{P}_{M,s_z,s}.$$

We stress that all the mentioned operators commute with each other, viz,

$$[H,\Omega_i] = [\Omega_i,\Omega_j] = 0,$$

with $\Omega_i \in \{L_z,S_z,S^2\}$. If a modified problem breaks, say, rotational symmetry, such that $[H,L_z] \neq 0$, we may still split the model space into to the eigenspaces of S_z and S^2.

D. Matrix elements of Coulomb interaction

The remaining ingredient in the FCI method is the Coulomb matrix elements u_{cd}^{ab} defined in Eqn. (5). These can be calculated by first expanding $L_n^k(x)$ in powers of x using

$$L_n^k(x) \equiv \sum_{m=0}^{n} (-1)^m \frac{(n+k)!}{(n-m)!(k+m)!m!} x^m,$$

and evaluating the resulting integral term-by-term by analytical methods [10]. The resulting expression is a seven-fold nested sum, which can be quite time-consuming, especially if a large number of Fock-Darwin orbitals occurs in the basis $\mathscr{B}$. Moreover, the terms are fractions of factorials with alternating signs, which is a potential source of loss of numerical precision.

We therefore opt for a more indirect approach, giving a procedure applicable to a wide range of potentials $U(r_{12})$ in addition to the Coulomb potential. Moreover, it can be generalized to arbitrary spatial dimensions d. The approach is based on directly transforming the product functions $\varphi_a(\vec{r}_1)\varphi_b(\vec{r}_2)$ to the centre-of-mass system, where the interaction $U(r_{12})$ only acts on the relative coordinate, and then transforming back to the lab system. This reduces the computational cost to a doubly nested sum, as well as the pre-computation of the centre-of-mass transformation and the relative coordinate interaction matrix. Both can be done exactly using Gaussian quadrature. The transformations to and from the centre of mass frame are unitary transformations, which are stable and will not magnify round-off errors.

In Appendix A we provide the details of the centre-of-mass transformation. One then obtains the following prescription for the interaction matrix elements u_{cd}^{ab}: Let $a = (\mu_1, \nu_1)$, $b = (\mu_2, \nu_2)$, $c = (\mu_3, \nu_3)$, and $d = (\mu_4, \nu_4)$ be the circular quantum number equivalents of the usual polar coordinate quantum numbers n_i and m_i. Due to conservation of angular momentum, we assume $m_1 + m_2 = m_3 + m_4$; otherwise, the matrix element $u_{cd}^{ab} = 0$. Define $M = \mu_1 + \mu_2$, $M' = \mu_3 + \mu_4$, $N = \nu_1 + \nu_2$, and $N' = \nu_3 + \nu_4$. Since u_{cd}^{ab} is linear in λ, we set $\lambda = 1$ without loss of generality. Now,

$$u_{cd}^{ab} = \sum_{p=p_0}^{M} T_{p,\mu_2}^{(M)} T_{p',\mu_4}^{(M')} \sum_{q=q_0}^{N} T_{q,\nu_2}^{(N)} T_{q',\nu_4}^{(N')} C_{n,n+s}^{|p-q|}, \qquad (9)$$

where $n = \min(p,q)$, $s = M' - M$, $p' = p + M' - M$, $q' = q + N' - N$. Moreover, $p_0 = \max(M' - M, 0)$ and $q_0 = \max(N' - N, 0)$.

Here, $T^{(N)}$ are centre-of-mass transformation coefficients defined in Appendix A, while the relative coordinate interaction matrix elements $C_{n,n'}^{|m|}$, $n, n' \geq 0$, are defined by

$$\begin{aligned} C_{n,n'}^{|m|} &:= \langle \varphi_{n,m}(r,\theta) | U(\sqrt{2}r) | \varphi_{n',m}(r,\theta) \rangle \\ &= 2 \int_0^\infty r^{2|m|} \tilde{L}_n^{|m|}(r^2) \tilde{L}_{n'}^{|m|}(r^2) U(\sqrt{2}r) e^{-r^2} r \mathrm{d}r. \end{aligned} \qquad (10)$$

Depending on $U(r_{12})$, the integral is best computed using generalized half-range Hermite quadrature (see Appendix B and Ref.[11]) or Gauss-Hermite quadrature. Weights and abscissa for quadratures are conveniently computed using the Golub-Welsch algorithm [12], which only depends on the ability to compute the coefficients of the three-term recursion relation for the polynomial class in question, as well as diagonalizing a symmetric tri-diagonal matrix.

Let $p(r)$ be a polynomial, and let $\alpha < 2$ and β be non-negative constants. Then

$$U(r_{12}) = r_{12}^{\alpha} p(r_{12}) e^{-\beta r_{12}^2} \qquad (11)$$

admit exact evaluations using generalized half-range Gauss-Hermite quadrature. The Coulomb potential, Gaussian potentials, and the parabolic interaction $-\lambda r_{12}^2/2$ of the analytically solvable model treated in Sec. IV C belong to this class of potentials.

In the case of $\alpha = 1$ and $p(r) = q(r^2)$ (i.e., an even polynomial), the integral is more convenient to evaluate using standard Gauss-Hermite quadrature. The Coulomb interaction falls into this class.

Of course, one may let $p(r)$ be a non-polynomial function as well and still obtain very good results, as long as $p(r)$ is well approximated with a polynomial, e.g., is smooth.

III. EFFECTIVE INTERACTIONS

A. Motivation

The FCI calculations converge relatively slowly as function of the model space parameter R [3], as the error ΔE in the eigenvalue behaves like $o(R^{-k})$ in general, where $k = O(1)$. This behaviour comes from the singular nature of the Coulomb interaction.

In Ref. [3], numerical results using an effective interaction were presented. This method is widely used in no-core shell model calculations in nuclear physics, where the nucleon-nucleon interaction is basically unknown but highly singular [4]. This so-called sub-cluster effective interaction scheme replaces the Coulomb interaction (or another interaction) $U(r_{ij}) = \lambda / r_{ij}$ with a renormalized interaction $\tilde{U}(i,j)$ obtained by a unitary transformation of the two-body Hamiltonian that decouples the model space $\mathscr{P}$ and its complement [13]. Therefore, the two-body problem becomes *exact* in a *finite* number of harmonic oscillator shells. Loosely speaking, the effective interaction incorporates information about the interaction's action *outside* the model space. In general, $\tilde{U}(i,j)$ is non-linear in λ and not a local potential.

Using the renormalized $\tilde{U}(i,j)$, the many-body system does not become exact, of course, but $\tilde{U}(i,j)$ will perform better than the bare interaction in this setting as well. To the author's knowledge, there exists no rigorous mathematical treatment with respect to this, but it has nevertheless enjoyed great success in the nuclear physics community [4, 14, 15], and our numerical experiments unambiguously demonstrate that the convergence of the FCI method is indeed improved drastically [3], especially for $N \leq 4$ particles. We stress that the cost of producing $\tilde{U}(i,j)$ is very small compared to the remaining calculations.

B. Unitary transformation of two-body Hamiltonian

We now describe the unitary transformation of the two-body Hamiltonian (i.e., Eqn. (1) or (3) with $N = 2$) that decouples $\mathscr{P}$ and its complement. This approach dates back as far as 1929, when Van Vleck introduced such a generic unitary transformation to de-couple the model space to first order in the interaction [16, 17].

Let P be given by Eqn. (6), and let $D = \dim(\mathscr{P})$. The idea is to find a unitary transformation $\mathscr{H} = Z^\dagger H Z$ of H such that

$$(1-P)\mathscr{H}P = 0,$$

i.e., $\mathscr{H}$ is block diagonal. This implies that H_{eff} defined by

$$H_{\text{eff}} := P\mathscr{H}P$$

has eigenvalues identical to D of those of the *full operator* H. Since D is finite, H_{eff} is called an effective Hamiltonian.

Selecting Z is equivalent to selecting a set of effective eigenpairs $\{(E_k, |\Psi_k^{\text{eff}}\rangle)\}_{k=1}^D$, where E_k is an eigenvalue of H and $\{|\Psi_k^{\text{eff}}\rangle\}_{k=1}^D \subset \mathscr{P}$ are the effective eigenvectors; an orthonormal basis for $\mathscr{P}$. It is clear that Z is not unique, since there are many ways to pick D eigenvalues of H, and for each such selection any unitary $D \times D$ matrix would yield an eigenvector set.

However, some choices are more natural than others, since the eigenvectors and eigenvalues are usually continuous functions of λ. We then select the D eigenvalues $E_k(\lambda)$ that develop adiabatically from $\lambda = 0$. For the corresponding effective eigenvectors $|\Psi_k^{\text{eff}}(\lambda)\rangle$, we choose the orthonormal set that minimizes the distance to the exact eigenvectors $\{|\Psi_k\rangle\}_{k=1}^D$, i.e.,

$$\{|\Psi_k^{\text{eff}}\rangle\}_{k=1}^D := \underset{\{|\Psi_k'\rangle\}_{k=1}^D}{\text{argmin}} \sum_{k=1}^D \||\Psi_k\rangle - |\Psi_k'\rangle\|^2, \qquad (12)$$

where the minimization is taken over orthonormal sets only. The effective eigenvectors also turn out to be continuous functions of λ, so H_{eff} will also be continuous.

Let U is the $D \times D$ matrix whose columns contain $P|\Psi_k\rangle$ in the chosen basis, and let V be the corresponding matrix containing $|\Psi_k^{\text{eff}}\rangle$. Clearly, V is unitary, while U only approximately so. Equation (12) can then be written

$$V := \underset{U'}{\text{argmin}}\ \text{trace}[(U-U')(U-U')^\dagger], \qquad (13)$$

where the minimum is taken over all unitary matrices. If U has singular value decomposition given by

$$U = X\Sigma Y^\dagger, \qquad (14)$$

the solution V is given by

$$V := XY^\dagger. \qquad (15)$$

If $E = \text{diag}(E_1, \cdots, E_D)$ is the diagonal matrix whose elements are the chosen eigenvalues, we have

$$H_{\text{eff}} = VEV^\dagger.$$

See Ref. [13] for a thorough discussion of the above prescription for H_{eff}.

Having computed the two-body H_{eff}, we define the effective interaction $\tilde{U}(1,2)$ by

$$\tilde{U}(1,2) := H_{\text{eff}} - P\sum_{i=1}^2 H_0(i)P,$$

which gives meaning *solely* in the model space. In second quantization,

$$\tilde{U}(1,2) := \frac{1}{2}\sum_{abcd}\sum_{\sigma\tau}\tilde{u}_{cd}^{ab}a_{a\sigma}^\dagger a_{b\tau}^\dagger a_{d\tau}a_{c\sigma},$$

and the N-body H_{eff} becomes (cf. Eqn. (1))

$$H_{\text{eff}} = \sum_{i=1}^N H_0(i) + \sum_{i<j}^N \tilde{U}(i,j),$$

with occupation number formalism form (cf. Eqn. (3))

$$H_{\text{eff}} = \sum_{a,b}\sum_{\sigma} h_b^a a_{a,\sigma}^\dagger a_{b,\sigma} + \frac{1}{2}\sum_{abcd}\sum_{\sigma\tau}\tilde{u}_{cd}^{ab}a_{a,\sigma}^\dagger a_{b,\tau}^\dagger a_{d,\tau}a_{c,\sigma}. \quad (16)$$

Now, H_{eff} is well-defined in the space of N-body Slater determinants where no pairs of occupied orbitals constitute a two-body state outside the two-particle model space, since then the matrix element $\tilde{u}_{cd}^{ab}$ would be undefined. A little thought shows us that if $\tilde{U}(1,2)$ was computed in a two-body energy cut space with parameter R, H_{eff} is well-defined on the many-body model space with the same cut R.

C. A comment concerning the choice of model space

The two-body problem is classically integrable, i.e., there exists $2d-1$ constants of motion Ω_i, such that their quantum mechanical observables commute with H and each other, viz,

$$[H, \Omega_i] = [\Omega_i, \Omega_j] = 0, \quad \text{for all } i, j.$$

Indeed, the centre-of-mass harmonic oscillator H_{C} defined in Eqn. (18) below and the corresponding centre-of-mass angular momentum provides two constants, while total angular momentum L_z provides a third.

Using the model space $\mathscr{P}$ defined by an energy cut, we have

$$[P, \Omega_i] = 0$$

as well, which is equivalent [13] to

$$[H_{\text{eff}}, \Omega_i] = 0, \qquad (17)$$

so that H_{eff} is integrable as well. In particular, $\tilde{U}(1,2)$ is block-diagonal with respect to Ω_i.

If we consider the commonly encountered model space $\mathscr{P}'$ defined by the Slater determinant basis $\mathscr{B}'$ given by

$$\mathscr{B}' := \{|\Phi_{\alpha_1,\cdots,\alpha_N}\rangle\ :\ \max(R_i) \le R\}$$

instead of Eqn. (8), we will have

$$[P', H_{\rm C}] \neq 0,$$

as is easily verified. Indeed, $\mathscr{P}'$ is not an invariant subspace of the centre-of-mass transformation T defined in Appendix A. Thus, $[H'_{\rm eff}, H_{\rm C}] \neq 0$, so that the centre-of-mass energy no longer is a constant of motion! The symmetry-breaking of the effective Hamiltonian in this case is problematic, since in the limit $\lambda \to 0$, the exact eigenfunctions that develop adiabatically are not all either in the model space or in the complement. The adiabatic continuation of the eigenpairs starting out in $\mathscr{P}$ is thus not well-defined.

We comment, that the model space $\mathscr{P}'$ is often used in both no-core shell model calculations and quantum dot calculations, but the effective interaction becomes, in fact, ill-behaved in this case.

D. Solution of the two-body problem

What remains for the effective interaction, is the computation of the exact eigenpairs $\{(E_k, |\Psi_k\rangle)\}_{k=1}^{D}$. We must also solve the problem of following eigenpairs adiabatically from $\lambda = 0$.

For the two-body Coulomb problem, analytical solutions are available only for very special values for λ [18]. These are useless for our purpose, so we must use numerical methods.

A direct application of the FCI method using Fock-Darwin orbitals with a large $R' > R$ will converge slowly, and there is no device in the method for following eigenvalues adiabatically. As the eigenvalues may cross, selecting, e.g., the lowest eigenvalues will not work in general.

For the two-body problem, the Pauli principle leads to a symmetric spatial wave function for the singlet $s = 0$ spin state, and an anti-symmetric wave function for the triplet $s = 1$ spin states. For the spatial part, we exploit the integrability of the system as follows. Define centre-of-mass coordinates by

$$\vec{R} := \frac{1}{\sqrt{2}}(\vec{r}_1 + \vec{r}_2)$$

and

$$\vec{r} := \frac{1}{\sqrt{2}}(\vec{r}_1 - \vec{r}_2).$$

Using these coordinates, the two-body Hamiltonian becomes

$$\begin{aligned} H &= H_0(\vec{R}) + \left[H_0(\vec{r}) + U(\sqrt{2}r;\lambda)\right] \\ &=: H_{\rm C} + H_{\rm rel} \end{aligned} \tag{18}$$

where $r_{12} = \sqrt{2}r := \sqrt{2}\|\vec{r}\|$. We have introduced the parameter λ explicitly in the potential in this equation. H is clearly separable, and the centre-of-mass coordinate Hamiltonian $H_{\rm C}$ is a trivial harmonic oscillator, while the relative coordinate Hamiltonian can be written as

$$H_{\rm rel} := -\frac{1}{2}\nabla^2 + \frac{1}{2}r^2 + U(\sqrt{2}r;\lambda),$$

where in polar coordinates $\vec{r} = (r\cos\theta, r\sin\theta)$ we have

$$\nabla^2 = \frac{1}{r}\frac{\partial}{\partial r} r \frac{\partial}{\partial r} + \frac{\partial^2}{\partial \theta^2}.$$

Applying separation of variables again, the eigenfunctions of $H_{\rm rel}$ can be written

$$\psi_{n,m}(\vec{r}) := \frac{e^{im\theta}}{\sqrt{2\pi}} u_{n,m}(r)$$

where n is the nodal quantum number. $u_{n,m}(r)$ satisfies

$$K_{|m|} u_{n,m}(r) = \mu_{n,m} u_{n,m}(r) \tag{19}$$

where

$$K_{|m|} := -\frac{1}{2r}\frac{\partial}{\partial r} r \frac{\partial}{\partial r} + \frac{m^2}{2r^2} + \frac{1}{2}r^2 + U(\sqrt{2}r;\lambda). \tag{20}$$

Equation (19) is an eigenvalue problem in the Hilbert space $L^2([0,\infty), r\mathrm{d}r)$, where the measure $r\mathrm{d}r$ is induced by the polar coordinate transformation. Although it is natural to try and solve the radial problem using Fock-Darwin orbitals, this will converge slowly. The solution to this problem is to use a radial basis of generalized half-range Hermite functions [11]. In Appendix B this is laid out in some detail.

Equation (19) is a one-dimensional equation, so there will be no degeneracy in the eigenvalues $\mu_{m,n}$ for fixed m. In particular, the eigenvalues as function of the interaction strength λ will not cross, and will be continuous functions of λ. We thus have $\mu_{m,n} < \mu_{m,n+1}$ for all n, where n is the nodal quantum number.

At $\lambda = 0$ we regain the harmonic oscillator eigenvalues $2n + |m| + 1$. Correspondingly, the eigenfunctions $\psi_{m,n}(r,\theta)$ approaches the Fock-Darwin orbitals $\varphi_{m,n}(r,\theta)$, i.e., the harmonic oscillator eigenfunctions. For the radial part,

$$\lim_{\lambda=0} u_{m,n}(r) = g_n^{|m|}(r) := \sqrt{2} r^{|m|} \tilde{L}_n^{|m|}(r^2) e^{-r^2/2}.$$

Reintroducing spin, the full eigenfunctions $\Psi = \Psi_{n_1,m_1,n_2,m_2}$ are on the form

$$\Psi(x_1, x_2) = \varphi_{n_1,m_1}(\vec{R}) \frac{e^{im_2\theta}}{\sqrt{2\pi}} u_{n_2,m_2}(r) \chi_{s,s_z},$$

where $s = 0$ for odd m_2, and $s = 1$ for even m_2, and $|s_z| \leq s$ is an integer.

Let $R_i = 2n_i + |m_i|$ be the shell numbers for the centre-of-mass coordinate and relative coordinate, respectively. The eigenvalue $E = E_{n_1,m_1,n_2,m_2}$ is

$$E = R_1 + 1 + \mu_{n_2,m_2},$$

with limit

$$E \underset{\lambda\to 0}{\longrightarrow} R_1 + R_2 + 2,$$

which is the harmonic oscillator eigenvalue.

As the centre-of-mass coordinate transformation conserves harmonic oscillator energy, at $\lambda = 0$, the eigenfunctions that

are in the model space are exactly those obeying $R_1 + R_2 \leq R$. Turning on the interaction adiabatically, the eigenpairs we must choose for the effective Hamiltonian at a given λ are exactly those with $R_1 + R_2 \leq R$.

The model-space projection $P\Psi$ needed in Eqns. (12) and (13) is now given by

$$P\Psi(x_1, x_2) = \varphi_{n_1,m_1}(\vec{R}) \frac{e^{im_2\theta}}{\sqrt{2\pi}} \left[\tilde{P}^{|m_2|}_{R-R_1} u_{n_2,m_2}(r) \right] \chi_{s,s_z},$$

where

$$\tilde{P}^{|m|}_R := \sum_{n=0}^{\bar{n}} |g^{|m|}_n\rangle\langle g^{|m|}_n|, \quad \bar{n} = \left\lfloor \frac{R-|m|}{2} \right\rfloor, \qquad (21)$$

where $\lfloor x \rfloor$ is the integer part of x. This operator thus projects onto the $\bar{n}+1$ first radial basis functions with given $|m|$.

Due to Eqn. (17), the unitary operator Z can be decomposed into its action on blocks defined by tuples of n_1, m_1 and m_2 [13]. The minimization (12) can then be applied on block-per-block basis as well. Each sub-problem is equivalent to the calculation of an effective Hamiltonian K_{eff} of the radial problem for a given m_2 and $\bar{n}$.

To this end, let $\bar{n}$ and $m = m_2$ be given. Let U be the $(\bar{n}+1) \times (\bar{n}+1)$ matrix whose elements are given by

$$U_{n,k} = \langle g^{|m|}_n | u_{m,n} \rangle, \quad 0 \leq n,k \leq \bar{n},$$

i.e., the model space projections of the exact eigenvectors with the lowest eigenvalues. Let $U = X\Sigma Y^\dagger$ be the singular value decomposition, and let $V = XY^\dagger$. Then,

$$K_{\text{eff}} = V \,\text{diag}(E_0, \cdots, E_{\bar{n}}) V^\dagger$$

and

$$\tilde{C}^{\bar{n},|m|} := K_{\text{eff}} - \text{diag}(|m|+1, 2+|m|+1, \cdots, 2\bar{n}+|m|+1)$$

is the (n_1, m_1, m_2)-block of the effective interaction. If we return to Eqn. (9), the effective interaction matrix elements $\tilde{u}^{ab}_{cd}$ are now given by replacing the matrix elements $C^{|p-q|}_{n,n+s}$ by the matrix elements $\tilde{C}^{\bar{n},|p-q|}_{n,n+s}$, where

$$\bar{n} = \left\lfloor \frac{R - R_1 - |m|}{2} \right\rfloor, \quad R_1 = N + M - (p+q),$$

where N, M, p and q are defined immediately after Eqn. (9).

IV. CODE ORGANIZATION AND USE

A. Overview

The main program is called QDOT, and processes a textual configuration file with problem parameters before proceeding with the diagonalization of the Hamiltonian. Eventually, it writes the resulting data to a MATLAB/GNU OCTAVE compatible script for further processing.

As a C++ library as well as stand-alone application, OPENFCI is organized in several namespaces, which logically separate independent units. There are three main namespaces: `manybody`, `gauss`, and `quantumdot`. Put simply, `manybody` provides generic tools for many-body calculations, such as occupation number formalism, Slater determinants and CSFs, while `gauss` provides tools for orthogonal polynomials and Gaussian quadrature. These namespaces are independent of each other, and are in no way dependent on the particular quantum dot model. On the other hand, `quantumdot` synthesizes elements from the two former into a quantum dot FCI library. In QDOT, the main work is thus processing of the configuration file.

Two other namespaces are also defined, being `simple_sparse` and `simple_dense`, which are, respectively, simple implementations of sparse and dense matrices suitable for our needs. We will not go into details in the present article.

It should be clear that extending and customizing QDOT is a relatively easy task. The application QDOT is provided as a tool with a minimum of functionality, and the interested will almost certainly desire to further develop this small application.

In order to help with getting started on such tasks, some stand-alone demonstration applications are provided, all based on the core classes and functions. These include an interaction matrix element tabulator TABULATE, and a simple program PAIRING for studying the well-known pairing Hamiltonian [19], which we will not discuss further here. Finally, there is a small interactive console-based Slater determinant demonstration program SLATER_DEMO as well. These applications will also serve as indicators of the flexibility of OPENFCI.

OPENFCI does not yet support parallel computation on clusters of computers, using for example the Message Passing Interface [20]. Future versions will almost certainly be parallelized, but the present version in fact competes with parallel implementations of the standard FCI method with respect to convergence due to the effective interaction implemented, see Sec. IV C. The simple structure of OPENFCI also allows users with less resources to compile and run the code.

B. Core functionality

The `manybody` namespace currently contains four main classes: `Slater`, `CsfMachine`, `NChooseKBitset`, and `MatrixMachine`. These will probably form the backbone of any manybody computation with OPENFCI.

The class `Slater` provides Slater determinants, creation and annihilation operators, and so on. It is based on the standard template library's (STL) `bitset` class, which provides generic bit set manipulations. The class `NChooseKBitset` provides means for generating sets of k objects out of n possible represented as bit-patterns, i.e., bit patterns corresponding to Slater determinants in the basis $\mathscr{B}$ or $\mathscr{B}'$. This results in a STL `vector<Slater>` object, which represent Slater determinant bases in OPENFCI.

The class `CsfMachine` is a tool for converting a basis of Slater determinants into a basis of configurational state functions. These are represented as `vector<csf_block>` objects, where `csf_block` is a `struct` containing a few CSFs associated with the same set of Slater determinants [9].

A CSF basis is again input for the class `MatrixMachine`, which is a template class, and generates a sparse matrix PAP of an operator A, where P projects onto the basis. It also handles bases of pure Slater determinants as they are trivially dealt with in the CSF framework. The template parameter to `MatrixMachine` is a class that should provide the matrix elements h^{α}_{β}, $u^{\alpha\beta}_{\gamma\delta}$, etc, of the generic operator given by

$$A = \sum_{\alpha\beta} h^{\alpha}_{\beta} a^{\dagger}_{\alpha} a_{\beta} + \frac{1}{2} \sum_{\alpha\beta\gamma\delta} u^{\alpha\beta}_{\gamma\delta} a^{\dagger}_{\alpha} a^{\dagger}_{\beta} a_{\delta} a_{\gamma} + \frac{1}{3!} \sum_{\alpha\beta\cdots} v^{\alpha\beta\gamma}_{\delta\epsilon\zeta} a^{\dagger}_{\alpha} a^{\dagger}_{\beta} a^{\dagger}_{\gamma} a_{\zeta} a_{\epsilon} a_{\delta}.$$

Notice, that the indices are generic orbitals, and not assumed to be on the form (a,σ) as in Eqn. (3).

Currently, only one-, two-, and three-body operators are implemented. The reason is, that the matrix elements are *not* computed by directly applying the sum of creation- and annihilation operators to Slater determinants, since this approach, however natural, is very inefficient. Instead, we apply Wick's theorem directly [8] on the matrix elements known to be not identically zero.

In the `gauss` namespace, several functions are defined which computes sequences of orthogonal polynomials via recurrence relations and weights and abscissa for Gaussian quadratures based on these. The latter is done using the Golub-Welsh algorithm, which only depends on being able to compute the coefficients of the recurrence relation [12]. The most important functions are perhaps `computeLaguerrePolys()` and `computeGenHalfGaussHermite()`, which computes a sequence of generalized Laguerre polynomials evaluated at a given set of points and quadrature rules for generalized half-range Hermite functions, respectively.

Finally, the `quantumdot` namespace defines classes and functions that combined define the quantum dot problem. The class `RadialPotential` encapsulates potentials on the form (11). It also computes effective interaction blocks $\tilde{C}^{\bar{n},|m|}$. The class `QdotHilbertSpace` provides means for generating the bases $\mathscr{B}$ and $\mathscr{B}'$, utilizing conservation of angular momentum, using a fast, custom made algorithm independent of `NChooseKBitset`. The class `QdotFci` sews everything together and is basically a complete solver for the FCI method with effective interactions.

C. Sample runs

A basic configuration file for QDOT is shown in Fig. 2. Varying the parameters `lambda`, `R`, `S` and the number of particles `A` [23], and running QDOT each time, we produce a table of ground state energies, shown in Table I. By changing the parameter `use_veff` we turn on and off the effective interaction. The corresponding effective interaction ground states are also shown in the table. Notice, that with the effective interaction we obtain the same precision as the bare interaction, but with much smaller model spaces. This indicates that OPENFCI can produce results that in fact compete with parallel implementations of the standard FCI method, even in its present serial form.

```
# ** Simple configuration file for qdot **

# -- model space parameters --
A = 4      # number of particles
M = 0      # angular momentum
S = 0      # total spin * 2
R = 15     # cut of model space

# -- interaction parameters --
lambda = 1.0   # interaction strength

# pot_p = -0.5 0      # uncomment
# pot_p_iseven = yes  # these lines
# pot_alpha = 0       # for Johnson &
# pot_beta = 0        # Payne model

# -- computational parameters --
use_energy_cut = yes
nev = 50                # no. eigenpairs
use_veff = no
matlab_output = results.m
```

FIG. 2: Simple configuration file for QDOT

TABLE I: Some ground state eigenvalues produced by QDOT for $N = 3,4$ electrons with $\lambda = 2$. Both the bare and the effective interaction are used

	$N=3$, $M=0$, $s=\frac{1}{2}$		$N=4$, $M=s=0$	
R	E_0	$E_{0,\text{eff}}$	E_0	$E_{0,\text{eff}}$
6	9.02370	8.96523	13.98824	13.88832
10	8.97698	8.95555	13.86113	13.83280
14	8.96800	8.95465	13.84491	13.82848
18	8.96411	8.95444	13.83923	13.82761
22	8.96191	8.95435	13.83626	13.82730
26	8.96049	8.95430		
30	8.95950	8.95428		

In Table II we compare the ground state energies reported in Ref. [9] with the alternative model space $\mathscr{P}'$ to the corresponding values produced by QDOT, also using $\mathscr{P}'$. This Table also appears in Ref. [3], and serves as a check of the validity of the calculations.

By uncommenting the lines following the definition of `lambda`, we override the default Coulomb interaction, and produce a configuration file for the analytically solvable model given by Johnson and Payne [7], where the Coulomb

TABLE II: Comparison of current code and Ref. [9], taken from Ref. [3]

				$R=5$		$R=6$		$R=7$	
N	λ	M	$2s$	Current	Ref. 9	Current	Ref. 9	Current	Ref. 9
2	1	0	0	3.013626		3.011020		3.009236	
	2	0	0	3.733598	3.7338	3.731057	3.7312	3.729324	3.7295
		1	2	4.143592	4.1437	4.142946	4.1431	4.142581	4.1427
3	2	1	1	8.175035	8.1755	8.169913		8.166708	8.1671
	4	1	1	11.04480	11.046	11.04338		11.04254	11.043
		0	3	11.05428	11.055	11.05325		11.05262	11.053
4	6	0	0	23.68944	23.691	23.65559		23.64832	23.650
		2	4	23.86769	23.870	23.80796		23.80373	23.805
5	2	0	5	21.15093	21.15	21.13414	21.13	21.12992	21.13
	4	0	5	29.43528	29.44	29.30898	29.31	29.30251	29.30

interaction is replaced by the parabolic interaction

$$U(r_{12}) = -\frac{1}{2}\lambda r_{12}^2.$$

If λ is sufficiently small, all the eigenvalues of this model are on the form

$$E_{j,k} = 1 + j + (k+N-1)\sqrt{1-N\lambda}, \quad j,k \geq 0. \tag{22}$$

Since the potential is smooth, the eigenfunctions are all smooth, implying exponential convergence with respect to R [3]. We therefore expect very accurate eigenvalues even with moderate R. In Table III we show the first eigenvalues along with the error computed for $N=4$ electrons with $\lambda = 1/8$. The computations are done in the $M = s = s_z = 0$ model space with $R = 10$ and $R = 15$. Some duplicates exist, and they are included for illustration purposes. It is evident, that the eigenvalues become very accurate with increasing R; a clear indication of the correctness of the implementation.

TABLE III: Results from diagonalizing the Johnson and Payne model. Many digits are included due to comparison with exact results and high precision

$R=10$		$R=15$	
E	ΔE	E	ΔE
4.535550207816	$1.63\cdot10^{-5}$	4.535533958447	$5.25\cdot10^{-8}$
5.950417930316	$6.70\cdot10^{-4}$	5.949751427847	$3.96\cdot10^{-6}$
5.950417930316	$6.70\cdot10^{-4}$	5.949751427847	$3.96\cdot10^{-6}$
5.950417930316	$6.70\cdot10^{-4}$	5.949751427847	$3.96\cdot10^{-6}$
5.951592166603	$1.84\cdot10^{-3}$	5.949760599290	$1.31\cdot10^{-5}$
6.243059891817	$4.19\cdot10^{-4}$	6.242642740293	$2.05\cdot10^{-6}$
6.243059891817	$4.19\cdot10^{-4}$	6.242642740293	$2.05\cdot10^{-6}$
6.535776573577	$2.43\cdot10^{-4}$	6.535534873729	$9.68\cdot10^{-7}$
6.535776573577	$2.43\cdot10^{-4}$	6.535534873729	$9.68\cdot10^{-7}$
6.535776573577	$2.43\cdot10^{-4}$	6.535534873729	$9.68\cdot10^{-7}$
7.375904323762	$1.19\cdot10^{-2}$	7.364103882564	$1.43\cdot10^{-4}$
7.375904323762	$1.19\cdot10^{-2}$	7.364103882564	$1.43\cdot10^{-4}$
7.375904323762	$1.19\cdot10^{-2}$	7.364103882564	$1.43\cdot10^{-4}$
7.375904323762	$1.19\cdot10^{-2}$	7.364103882564	$1.43\cdot10^{-4}$
7.375904323762	$1.19\cdot10^{-2}$	7.364103882564	$1.43\cdot10^{-4}$
7.393706556283	$2.97\cdot10^{-2}$	7.364440927813	$4.80\cdot10^{-4}$
7.393706556283	$2.97\cdot10^{-2}$	7.364440927813	$4.80\cdot10^{-4}$
7.393706556283	$2.97\cdot10^{-2}$	7.364440927813	$4.80\cdot10^{-4}$
7.410720999386	$4.68\cdot10^{-2}$	7.364876152101	$9.15\cdot10^{-4}$
7.665921446569	$9.07\cdot10^{-3}$	7.656945606956	$9.14\cdot10^{-5}$

V. CONCLUSION AND OUTLOOK

We have presented OPENFCI, an open source full configuration interaction implementation for quantum dots and similar systems. OPENFCI also implements a renormalized effective interaction widely used in nuclear no-core shell model calculations, and we demonstrated that such interactions are indeed useful in the quantum dot calculations as well.

OPENFCI is easy to extend and adapt. Possible applications are computations on systems with more general symmetry-breaking geometries and in $d = 3$ spatial dimensions. Also, a generalization of the CSF part of the code to handle isobaric spin would allow us to handle nuclear systems.

There is one more symmetry of the Hamiltonian H that can be exploited, namely that of conservation of centre-of-mass motion, which would further reduce the block sizes of the matrices. We exploited this symmetry for the effective interaction, but it is a fact that it is a symmetry for the full Hamiltonian as well. Using the energy cut model space $\mathscr{P}$ we may take care of this symmetry in a way similar to the CSF treatment [21].

As mentioned, we have not parallelized the code at the time of writing, but it is not difficult to do so. A future version will almost certainly provide parallelized executables, for example using the Message Passing Interface [20].

APPENDIX A: CENTRE OF MASS TRANSFORMATION

1. Cartesian coordinates

In this appendix, we derive the centre-of-mass (COM) transformation utilized in Eqn. (9) for the interaction matrix elements u_{cd}^{ab}.

The one-dimensional harmonic oscillator (HO) Hamiltonian $(p_x^2 + x^2)/2$ is easily diagonalized to yield eigenfunctions

on the form

$$\begin{aligned}\phi_n(x) &= (2^n n!\sqrt{\pi})^{-1/2} H_n(x) e^{-x^2/2} \\ &= (n!)^{-1/2} A_x^n \phi_0(x), \end{aligned} \tag{A1}$$

where $A_x := (x - ip_x)/\sqrt{2}$ is the raising operator in the x-coordinate, and where $\phi_0(x) = \pi^{-1/4}\exp(-x^2/2)$. The eigenvalues are $n+1/2$.

Using separation of variables, the two-dimensional HO H_0 in x_1 and x_2 is found to have eigenfunctions on the form $\Phi_{n_1,n_2}(x_1,x_2) := \phi_{n_1}(x_1)\phi_{n_2}(x_2)$ and eigenvalues n_1+n_2+1. Define the raising operators $A_{x_i} := (x_i - ip_{x_i})/\sqrt{2}$, so that

$$\Phi_{n_1,n_2}(\vec{x}) := (n_1!n_2!)^{-1/2} A_{x_1}^{n_1} A_{x_2}^{n_2} \Phi_{0,0}(\vec{x}), \tag{A2}$$

where the non-degenerate ground state is given by

$$\Phi_{0,0}(x_1,x_2) = \frac{1}{\sqrt{\pi}} e^{-(x_1^2+x_2^2)/2}. \tag{A3}$$

Note that this can equally well describe two (distinguishable and spinless) particles in one dimension.

To this end, we introduce normalized COM frame coordinates by

$$\begin{bmatrix}\xi_1 \\ \xi_2\end{bmatrix} = \frac{1}{\sqrt{2}}\begin{bmatrix}1 & 1 \\ 1 & -1\end{bmatrix}\begin{bmatrix}x_1 \\ x_2\end{bmatrix} =: F\begin{bmatrix}x_1 \\ x_2\end{bmatrix} \tag{A4}$$

The matrix F is symmetric and orthogonal, i.e., $F^TF = F^2 = 1$, transforming a set of Cartesian coordinates into another. The operator H_0 is invariant under this transformation, so the eigenfunctions have the same form with respect to these coordinates, viz,

$$\begin{aligned}\Phi'_{n_1,n_2}(\xi_1,\xi_2) &:= \phi_{n_1}(\xi_1)\phi_{n_2}(\xi_2) \\ &= (n_1!n_2!)^{-1/2} A_{\xi_1}^{n_1} A_{\xi_2}^{n_2} \Phi'_{0,0}, \end{aligned} \tag{A5}$$

where $A_{\xi_i} = (\xi_i - ip'_i)/\sqrt{2}$ are the raising operators with respect to the COM coordinates, and p'_i are the corresponding momentum components.

Define the operator T by

$$T\psi(x_1,x_2) := \psi(\xi_1,\xi_2) = \psi\left(\frac{x_1+x_2}{\sqrt{2}}, \frac{x_1-x_2}{\sqrt{2}}\right), \tag{A6}$$

so that

$$T\Phi_{n_1,n_2} := \Phi'_{n_1,n_2}. \tag{A7}$$

Since T maps eigenfunctions in the two frames onto each other, T must be a unitary operator, and the invariance of H_0 under the coordinate transformation is the same as $[H_0,T]=0$, i.e., that energy is conserved. This in turn means that T is block diagonal with respect to each shell $R = n_1+n_2$, viz,

$$\begin{aligned}T\Phi_{R-n_2,n_2} &= \sum_{n=0}^{R} \langle \Phi_{R-n,n} | \Phi'_{R-n_2,n_2}\rangle \Phi_{R-n,n} \\ &=: \sum_{n=0}^{R} T^{(R)}_{n_2,n} \Phi_{R-n,n}, \end{aligned} \tag{A8}$$

where $T^{(R)}$ is the $(R+1)\times(R+1)$ transformation matrix within shell R. It is real, symmetric, and orthogonal. Numerically, the matrix elements are conveniently computed using two-dimensional Gauss-Hermite quadrature of sufficiently high order, producing exact matrix elements.

In a two-dimensional setting, the two-particle harmonic oscillator becomes a 4-dimensional oscillator. Let $\vec{r}_i = (x_i,y_i)$, $i=1,2$, be the particles' coordinates, and let $a=(m_1,n_2)$ and $b=(m_2,n_2)$ to compress the notation a little. An eigenfunction is now on the form

$$\begin{aligned}\Psi_{a,b}(\vec{r}_1,\vec{r}_2) &:= \Phi_a(\vec{r}_1)\Phi_b(\vec{r}_2) \\ &= C A_{x_1}^{m_1} A_{y_1}^{n_1} A_{x_2}^{m_2} A_{y_2}^{n_2} \Psi_{0,0}(\vec{r}_1,\vec{r}_2) \end{aligned} \tag{A9}$$

where $C = (m_1!n_1!m_2!n_2!)^{-1/2}$.

The COM coordinate transformation now acts in the x and y directions separately, viz, F acts on x_i and y_i to yield the COM coordinates ξ_i and η_i: $[\xi_1,\xi_2]^T = F[x_1,x_2]^T$ and $[\eta_1,\eta_2]^T = F[y_1,y_2]^T$. The induced operator T again conserves energy. Let $M = m_1+m_2$ and $N = n_1+n_2$. It is readily verifiable that the COM frame transformation becomes

$$\begin{aligned} T\Psi_{M-m_2,N-n_2,m_2,n_2} &:= \Psi'_{M-m_2,N-n_2,m_2,n_2} \\ &= \sum_{p=0}^{M} T^{(M)}_{m_2,p} \sum_{q=0}^{N} T^{(N)}_{n_2,p} \Psi_{M-p,N-q,p,q}. \end{aligned} \tag{A10}$$

Note that the shell number is $R = N+M$, which is conserved by T.

2. Centre of mass transformation for Fock-Darwin orbitals

Consider a Fock-Darwin orbital $\varphi_{n,m}(\vec{r})$ in shell $R = 2n+|m|$ with energy $R+1$. It is straightforward but somewhat tedious to show that these can be written in terms of co-called circular raising operators B_+ and B_- [22] defined by

$$\begin{bmatrix}B_+ \\ B_-\end{bmatrix} := \frac{1}{\sqrt{2}}\begin{bmatrix}1 & i \\ 1 & -i\end{bmatrix}\begin{bmatrix}A_x \\ A_y\end{bmatrix}. \tag{A11}$$

Letting $\mu = n+\max(0,m)$ and $\nu = n+\max(0,-m)$ (which gives $\mu,\nu \geq 0$) one obtains

$$\varphi_{n,m}(\vec{r}) = (\mu!\nu!)^{-1/2} B_+^{\mu} B_-^{\nu} \Phi_{0,0}(\vec{r}), \tag{A12}$$

which should be compared with Eqn. (A2). Moreover, $R = \mu+\nu$ and $m = \mu-\nu$, giving energy and angular momentum, respectively. We comment that this is the reason for the non-standard factor $(-1)^n$ in the normalization of the Fock-Darwin orbitals in Eqn. (7).

Let a two-particle HO state be given by

$$\begin{aligned}\tilde{\Psi}_{\mu_1,\nu_1,\mu_2,\nu_2} &:= \varphi_{n_1,m_1}(\vec{r}_1)\varphi_{n_2,m_2}(\vec{r}_2), \\ &= C B_{1+}^{\mu_1} B_{1-}^{\nu_1} B_{2+}^{\mu_2} B_{2-}^{\nu_2} \Psi_{0,0}(\vec{r}_1,\vec{r}_2), \end{aligned} \tag{A13}$$

where $\mu_i = n_i+\max(0,m_i)$ and $\nu_i = n_i+\max(0,-m_i)$, and where $C = (\mu_1!\nu_1!\mu_2!\nu_2!)^{-1/2}$. We will now prove that, in fact, when applying the centre-of-mass transformation to

Eqn. (A13), we obtain an expression on the same form as Eqn. (A10) viz,

$$\begin{aligned} T\tilde{\Psi}_{M-\mu_2,N-\nu_2,\mu_2,\nu_2} &:= \tilde{\Psi}'_{M-\mu_2,N-\nu_2,\mu_2,\nu_2} \\ &= \sum_{p=0}^{M} T^{(M)}_{\mu_2,p} \sum_{q=0}^{N} T^{(N)}_{\nu_2,q} \tilde{\Psi}_{M-p,N-q,p,q}, \end{aligned} \tag{A14}$$

where $M := \mu_1 + \mu_2$ and $N := \nu_1 + \nu_2$.

To this end, we return to the raising operators A_{ξ_i} and A_{η_i}, and express them in terms of A_{x_i} and A_{y_i}. By using Eqn. (A4), we obtain

$$\begin{bmatrix} A_{\xi_1} \\ A_{\xi_2} \end{bmatrix} = F \begin{bmatrix} A_{x_1} \\ A_{x_2} \end{bmatrix}, \tag{A15}$$

and similarly for A_{η_i} in terms of A_{y_i}. In terms of the raising operators, the COM transformation becomes

$$\begin{aligned} \Psi'_{m_1,n_1,m_2,n_2} &= C\,(A_{x_1} + A_{x_2})^{m_1}\,(A_{y_1} + A_{y_2})^{n_1} \\ &\times\ (A_{x_1} - A_{x_2})^{m_2}\,(A_{y_1} - A_{y_2})^{n_2}\,\Psi_{0,0}, \end{aligned} \tag{A16}$$

where

$$C = (2^{n_1+n_2+m_1+m_2} n_1! n_2! m_1! m_2!)^{-1/2}, \tag{A17}$$

and we have used Eqn. (A9), but in the analogous COM case. Expanding the powers using the binomial formula (and the fact that the raising operators commute), we obtain a linear combination of the individual eigenfunctions, which must be identical to Eqn. (A10).

Let the COM circular ladder operators be defined by

$$\begin{bmatrix} B'_{j+} \\ B'_{j-} \end{bmatrix} := \frac{1}{\sqrt{2}} \begin{bmatrix} 1 & i \\ 1 & -i \end{bmatrix} \begin{bmatrix} A_{\xi_j} \\ A_{\eta_j} \end{bmatrix}. \tag{A18}$$

Using Eqn. (A15), we obtain that the circular raising operators transform *in the same way* as the Cartesian operators when going to the COM frame, i.e.,

$$\begin{bmatrix} B'_{1+} \\ B'_{2+} \end{bmatrix} = F \begin{bmatrix} B_{1+} \\ B_{2+} \end{bmatrix}, \tag{A19}$$

and similarly for B'_{i-} and terms of B_{i-}. Using Eqn. (A13) in the COM case, we obtain

$$\begin{aligned} \tilde{\Psi}'_{\mu_1,\nu_1,\mu_2,\nu_2} &= C\,(B_{1+} + B_{2+})^{\mu_1}\,(B_{1-} + B_{2-})^{\nu_1} \\ &\times\ (B_{1+} - B_{2+})^{\mu_2}\,(B_{1-} - B_{2-})^{\nu_2}\,\Psi_{0,0}, \end{aligned} \tag{A20}$$

with

$$C = (2^{\mu_1+\nu_1+\mu_2+\nu_2} \mu_1! \nu_1! \mu_2! \nu_2!)^{-1/2}. \tag{A21}$$

Eqn. (A20) is on the same form as Eqn. (A16). Again, by expanding the powers using the binomial formula (and that the raising operators commute), we obtain a linear combination with coefficients identical to those of the expansion of Eqn. (A16). It then follows that Eqn. (A14) holds.

APPENDIX B: NUMERICAL TREATMENT OF RADIAL PROBLEM

We now briefly discuss the numerical method used for solving the radial problem (19), i.e., the eigenvalue problem for the operator $K_{|m|}$ defined in Eqn. (20). This is an eigenproblem in the Hilbert space $L^2([0,\infty), r\mathrm{d}r)$, where the measure $r\mathrm{d}r$ is induced by the polar coordinate transformation. The inner product on this space is thus given by

$$\langle f|g\rangle = \int_0^\infty f(r) g(r) r\mathrm{d}r. \tag{B1}$$

Let the Fock-Darwin orbitals be given by

$$\varphi_{n,m}(r,\theta) = \frac{e^{im\theta}}{\sqrt{2\pi}} g_n^{|m|}(r), \tag{B2}$$

with radial part

$$g_n^{|m|}(r) := \sqrt{2}\tilde{L}_n^{|m|}(r^2) r^{|m|} \exp(-r^2/2) \tag{B3}$$

Thus,

$$\langle g_n^{|m|} | g_{n'}^{|m|} \rangle = \delta_{n,n'},$$

and these functions form an orthonormal sequence in $L^2([0,\infty), r\mathrm{d}r)$ for fixed $|m|$.

In the electronic case, $U(\sqrt{2}r) = \lambda/\sqrt{2}r$ has a singularity at $r = 0$ which gives rise to a cusp in the eigenfunction $u_{m,n}(r)$ at $r = 0$, or in one of its derivatives. Away from $r = 0$, the eigenfunction is smooth. These considerations are also true for more general potentials smooth for $r > 0$.

Diagonalizing the matrix of K with respect to the truncated basis $\{g_n^{|m|}(r)\}_{n=0}^{\bar{n}}$ will give eigenpairs converging slowly with respect to increasing $\bar{n}$ due to the non-smoothness of $u_{n,m}(r)$ at $r = 0$. This is easily seen for the $m = 0$ case and $\lambda = 1$, which has the exact ground state

$$u_{0,0}(r) = \left(r + \frac{1}{\sqrt{2}}\right) e^{-r^2/2},$$

a polynomial of odd degree multiplied by a Gaussian. The cusp at $r = 0$ is evident. However,

$$g_n^0(r) = \sqrt{2}\tilde{L}_n(r^2) e^{-r^2/2},$$

which are all *even* polynomials. It is clear, that $\bar{n}$ must be large to resolve the cusp of $u_{0,0}(r)$.

The eigenproblem is best solved using a basis of generalized half-range Hermite functions $f_j(r)$ [11], which will resolve the cusp nicely. These functions are defined by

$$f_j(r) := P_j(r) \exp(-r^2/2),$$

where $P_j(r)$ are the orthonormal polynomials defined by Gram-Schmidt orthogonalization of the monomials r^k with respect to the weight function $r\exp(-r^2)$. Thus,

$$\langle f_j | f_{j'} \rangle = \int_0^\infty f_j(r) f_{j'}(r) r\mathrm{d}r = \delta_{j,j'}.$$

The fundamental difference between $f_j(r)$ and $g_n^{|m|}(r)$ is that the latter contains *only* even (odd) powers of r for even (odd) $|m|$. Both sets constitute orthonormal bases, but $f_j(r)$ will in general have better approximation properties.

Moreover, since $\deg(r^{|m|}L_n^{|m|}(r^2)) = 2n+|m|$,

$$g_n^{|m|}(r) = \sum_{j=0}^{2n+|m|} \langle f_j | g_n^{|m|} \rangle f_j(r) \tag{B4}$$

gives the Fock-Darwin orbitals as a *finite* linear combination of the generalized half-range Hermite functions, while the converse is not possible.

Computing the matrix of K with respect to $\{f_j(r)\}_{j=0}^{\bar{j}}$ and diagonalizing will give eigenpairs converging exponentially fast with respect to increasing $\bar{j}$. The resulting eigenfunctions' expansion in $g_n^{|m|}$ are readily computed using Eqn. (B4), whose coefficients $\langle f_j | g_n^{|m|} \rangle$ can be computed numerically exactly using Gaussian quadrature induced by $P_J(r)$, for J sufficiently large.

The basis size $\bar{j}$ to use in the diagonalization depends on how many eigenfunctions $\bar{n}$ we desire. We adjust $\bar{j}$ semi-empirically, noting that $2\bar{n}+|m|$ is sufficient to resolve $g_{\bar{n}}^{|m|}$, and assuming that the exact eigenfunctions are dominated by the latter. We then add a fixed number j_0 to get $\bar{j} = 2\bar{n}+|m|+j_0$, and numerical experiments confirm that this produces eigenvalues that indeed have converged within desired precision.

ACKNOWLEDGMENTS

The author wishes to thank Prof. M. Hjorth-Jensen (CMA) for helpful discussions, suggestions and feedback. This work was financed by CMA through the Norwegian Research Council.

[1] S. M. Reimann and M. Manninen, Rev. Mod. Phys **74**, 1283 (2002).
[2] The code can be downloaded at: `http://folk.uio.no/simenkva/openfci.shtml`.
[3] S. Kvaal (2008), submitted to Phys. Rev. B., arXiv:0808.2145.
[4] P. Navrátil, J. Vary, and B. Barrett, Phys. Rev. C **62**, 054311 (2000).
[5] See `http://www.gnu.org/`.
[6] See `http://www.doxygen.org/`.
[7] N. F. Johnson and M. C. Payne, Phys. Rev. Lett. **67**, 1157 (1991).
[8] S. Raimes, *Many-Electron Theory* (North-Holland, 1972).
[9] M. Rontani, C. Cavazzoni, D. Belucci, and G. Goldoni, J. Chem. Phys. **124**, 124102 (2006).
[10] E. Anisimovas and A. Matulis, Journal of Physics: Condensed Matter **10**, 601 (1998).
[11] J. S. Ball, SIAM Journal on Numerical Analysis **40**, 2311 (2003).
[12] G. H. Golub and J. H. Welsch, Math. Comp. **23**, 221 (1969), ISSN 00255718.
[13] S. Kvaal (2008), to appear in Phys. Rev. C, arXiv:0808.1832.
[14] M. Hjorth-Jensen, T. Kuo, and E. Osnes, Phys. Rep. **261**, 125 (1995).
[15] B. R. Barrett, I. Stetcu, P. Navrátil, and J. P. Vary, Journal of Physics A: Mathematical and General **39**, 9983 (2006).
[16] J. Van Vleck, Phys. Rev. **33**, 467 (1929).
[17] Kemble, *The Fundamental Principles of Quantum Mechanics with Elementary Applications* (McGraw Hill, 1937).
[18] M. Taut, Phys. Rev. A **48**, 3561 (1993).
[19] R. Richardson and N. Sherman, Nucl. Phys. **52**, 221 (1964).
[20] See `http://www-unix.mcs.anl.gov/mpi/` for a description of the Message Passing Interface standard.
[21] A. Wensauer, M. Korkusinski, and P. Hawrylak, Solid State Communications **130**, 115 (2004).
[22] R. Mota, V. D. Granados, A. Queijiro, and J. Garcia, J. Phys. A: Math. Gen. **36**, 2979 (2002).
[23] In nuclear physics, it is common to denote by A the number of particles, i.e., the atomic number. The choice of the variable name was chosen also partly because N is used frequently for other purposes in the code.